TEMPORAL CONTRAST ANALYSIS IN HUMAN VISION

ANDREW SIDWELL

Nine experiments are reported which investigate the mechanisms mediating the perception of temporal contrast, the change of luminance over time, by the human visual system. A distinction is made between linear systems, whose performance may be appropriately characterised in the frequency domain, and nonlinear systems which are sensitive to the temporal structure of visual stimuli. Of particular interest is the role played by systems which are selectively sensitive to relatively slow, nonperiodic luminance changes in the perception of both periodic and nonperiodic temporal contrast.

Using a trapezoidal waveform in which amplitude, frequency, and luminance gradient may be varied independently, it is first shown that the visual system is sensitive to the slope of a temporal profile. An adaptation technique is then used to show that waveform - specific threshold elevation occurs at low flicker frequencies, but not above about 5 Hz. The pattern of results suggests that separate channels exist for fast and slow luminance transitions, irrespective of their periodicity, and that the 'slow' system is subdivided into brightening and darkening channels.

In the final two experiments the fast and slow systems are studied in detail by probing the internal representations of step and ramp stimuli, using a masking technique. The step response is consistent with a system whose output is the second derivative of the smoothed input function. The same system can also account for the measured ramp response. This latter finding is likely to be an artifact of the measurement technique, using a 'fast' pulse stimulus. Polarity - specific interactions are observed which indicate polarity selectivity at the level of the 2nd derivative, or the filter output.

The experimental findings are integrated within a model of the complete temporal contrast system. While both the structure and the parameters of the fast system are well specified, further work remains on the characteristics of the slow system. The place of temporal contrast analysis within a larger model of movement perception is discussed.

TEMPORAL CONTRAST ANALYSIS IN HUMAN VISION

Andrew Sidwell

Thesis submitted for the degree of Doctor of Philosophy

University of Durham

Department of Psychology

1983

CONTENTS

FIGURES AND TABLES

STATEMENT OF COPYRIGHT

DECLARATION

I hereby declare that the work in this thesis is entirely my own, and that no part has been previously submitted for a degree in this or any other university.

Andrew Sidwell

June 1983

ACKNOWLEDGEMENTS

The work reported in this thesis was made possible by the kind provision of research facilities by my supervisor, Professor Michael Morgan, and by the financial support of a postgraduate research studentship from the Science and Engineering Research Council. I should also like to thank Professor Mark Haggard and Dr Quentin Summerfield of the MRC Institute of Hearing Research for the use of facilities during the later stages of preparation.

I am grateful to all the members of staff and research students in the Psychology Department at Durham, for enabling my time there to be both pleasant and productive. Special mention is due to Mrs Cathy Thompson, for original inspiration and later assistance in the field of computing; to Dr John Findlay, for many helpful discussions on the theory and practice of visual psychophysics; to Mr Malcolm Rolling, for untiring patience and technical assistance in the production of some of the graphics; and to Dr Laurence Harris, for many insightful comments on an earlier draft.

I am deeply indebted to the five experimental subjects whose observations provided the data reported in this thesis: Julia Addington-Hall, Susan Chivers, Trevor Crawford, Annie Humphreys, and Elizabeth Maylor. I should particularly like to thank Dr Humphreys, for continuing to provide help and support in many ways when it was neither profitable nor popular to do so.

Finally, I wish to thank Dr Barbara Payman for her unfailing encouragement and support during the writing of this thesis. I hope that its submission may provide some small reward for her patience.

For B.C.P.

CHAPTER 1

INTRODUCTION

'Temporal contrast' means a change in luminance over time. The term is used to emphasise the close parallels that exist with spatial contrast: changes of luminance over space. Changes of luminance in time may be divided into periodic variations (flicker) and nonperiodic variations (often called transients) such as flashes. Flicker and flashes are relatively uncommon in the natural environment: these stimuli have been used primarily as tools to study the temporal properties of the visual system, rather than being of intrinsic interest.

Most flicker research is aimed at a description of the temporal transfer properties of the visual system under various conditions. From this research theoretical models may be developed to mimic the observed behaviour. Conventionally the description is in terms of the limiting conditions for the perception of flicker. In early studies flicker was used to measure the temporal resolution of the visual system; more recently attention has turned to the attenuation of signals during processing. The relatively recent interest in the responses to transient stimuli is aimed at determining whether the temporal characteristics revealed by such stimuli are compatible with those established using periodic stimuli.

This introductory chapter is devoted largely to a survey of the historical development of research into temporal contrast phenomena. Beyond the most fundamental studies, the material has been selected for its

relevance to the main themes of the experiments reported later in the thesis. Several comprehensive reviews already exist in the literature. The traditional flicker research up to the advent of systems analysis is reviewed by Landis (1954b), and a more critical synthesis of the same work is provided by Pieron (1961). The historical development of flicker research to 1963 is reviewed by Brown (1965), and studies and models based on a linear systems approach are reviewed by Kelly (1972). Perhaps the most complete recent review of both psychophysical and physiological research is provided by van de Grind et al (1973). An annotated bibliography of research on temporal transients, covering the period from 1711 to 1969, is available by Hargroves and Hargroves (1971).

This review is organised according to the distinction made in the literature between the effects of periodic and nonperiodic stimuli. Section 1.1 presents the main findings and theoretical models concerned with flicker, covering the period 1740 to the present day. The review of transient stimuli in Section 1.2 is largely restricted to studies which have considered the relationship between these and periodic stimuli. Over the last 15 years the field of flicker research has become dominated by the study of spatiotemporal interactions, that is the relationship between spatial and temporal contrast. In this area, unlike much of the earlier work using uniform fields, the detection of flicker is of interest per se, since a moving patterned stimulus may be considered to produce purely temporal change at a single spatial point. Section 1.3 contains a review of the main findings on spatiotemporal interactions. This completes the historical survey of flicker research and puts the present studies in perspective. Although the work described in this thesis uses only uniform fields, the results are intended to be interpreted within the context of spatiotemporal contrast. The motivation behind the concentration on purely temporal contrast is explained

in Section 1.4, together with a brief guide to the present studies.

1.1 Flicker

1.1.1 Definitions

A summary of the main notation and abbreviations to be used throughout the thesis can be found in the Appendix.

Flicker may be defined as the repetitive change of light intensity between two levels. [The term 'intermittence', used in many early flicker studies, refers to squarewave modulation with a minimum light intensity of zero.] Flicker is completely specified by four parameters:

1. frequency. The rate of repetition, normally expressed in cycles per second or Hertz (Hz).

2. mean luminance. The time average level of the flicker waveform (L_{mean}). Also referred to as the adaptation or Talbot level (see next section for a formal statement of the Talbot - Plateau law).

3. amplitude. The difference between peak and mean luminance ($L_{max} - L_{mean} = \Delta L$). More recently amplitude has sometimes been specified in terms of modulation (m), a dimensionless measure expressing amplitude as a proportion of mean luminance. Modulation became particularly important once flicker technology

allowed the generation of stimuli with $L_{min} > 0$. With a symmetrical waveform, modulation reaches a maximum of 1 when $L_{min} = 0$. The term percentage modulation is often used, defined as m x 100. Modulations of greater than 1 or 100% may be obtained with asymmetrical waveforms, where $(L_{max} - L_{mean}) > (L_{mean} - L_{min})$. The term temporal contrast is synonymous with modulation. It is used to emphasise the analogy with spatial contrast or modulation.

4. waveform. This variable defines the temporal distribution of light intensity, or the form of the transition between the two extreme luminance levels. The only standardised form of expression is the Fourier transform, which provides the coefficients of the sinewave series which summate to produce the waveform. However this is only used in literature employing a linear systems approach to flicker detection. More commonly the waveform is referred to by its temporal profile, such as sawtooth, triangular, or square wave. In the traditional flicker literature, where only square or rectangular waveforms were commonly used, the proportion of the total cycle occupied by the light phase was often manipulated. This measure is known variously as the pulse - to - cycle fraction (PCF), the light - time fraction, and (confusingly) the light - dark ratio (LDR) (Landis, 1954b).

In addition to these parameters defining the flicker waveform, the complete description of a flicker stimulus must include a specification of three spatial parameters: size, surround luminance, and retinal location.

1.1.2 1740 - 1952 : Critical flicker frequency and intermittence

1.1.2.1 Fusion : the Talbot - Plateau law. Perhaps the first scientific investigation into flicker perception was reported by Segner (1740), who observed that squarewave flicker could not be seen above a certain frequency. This critical flicker frequency (CFF), or flicker fusion frequency (FFF), represents the temporal frequency threshold for 100% modulated flicker, and became the dominant measure of flicker sensitivity for over two centuries. The Talbot - Plateau law, stated originally by Talbot (1834) and reformulated more precisely by Plateau (1835), holds that a light flickering at a frequency above the CFF will appear equal in brightness to a steady light having the same mean luminance. The importance of this law, which remains essentially unchallenged today, lies in the relationship between the site of the neural mechanism determining the fusion percept and any nonlinearities in the visual system. As pointed out by Ives (1922a) and later by deLange (1952, 1954), if the logarithmic transformation between intensity and brightness (Weber - Fechner law) took place before the filter element determining fusion threshold, then fused flicker would appear less bright than a steady light of the same mean intensity. Thus any nonlinear element must follow the site of fusion. Furthermore such an element may be assumed to be essentially linear at fusion since its input covers only a small range, having been greatly attenuated by the filter.

1.1.2.2 Luminance : the Ferry - Porter law. If other factors are held constant, CFF increases with mean luminance. Charpentier (1887) proposed that CFF was a square function of luminance, and Pieron (1922) suggested that a power function with an exponent of less than 0.5 applied. The now

generally accepted logarithmic relationship was first stated by Baader (1891):

$$CFF = k \cdot \log L_{mean} + c \qquad \text{Equation 1.01}$$

where k (in Hz / logL unit) and c (in Hz) are parametric constants. This linear function between CFF and log luminance became known as the Ferry - Porter law after its formulation by Ferry (1892), based on data from only a 1 log unit luminance range. Porter (1902) measured CFF over a range of almost 5 log units, and showed that the data could be fitted by two straight lines with different coefficients in the photopic and scotopic ranges. His figures were essentially confirmed by Hecht and Verrijp (1933), who showed that linearity breaks down above about 500 td, where CFF reaches a peak. These authors also showed that the slope of the photopic function more closely matches that of the scotopic range with increasing eccentricity, indicating an identification of the two curve segments with rods and cones. Hecht (1933) interpreted the different slope coefficients as reflecting the time constants of the photochemical systems underlying flicker perception. At fusion the phasic changes in pigment concentration become too small to detect, and the point at which this occurs depends on the tonic pigment level, which is proportional to mean luminance.

Hecht's interpretation of the CFF vs luminance function was challenged by Crozier and Wolf and their co-workers, and this dispute resulted in a large number of studies published between 1933 and 1944, reviewed by Landis (1954a). The fact that the two-limbed linear function breaks down at both very high and very low luminance levels led to the proposal (Crozier, 1936) that the underlying function was a combination of two sigmoidal integrated probability curves. These curves result directly from

the statistical properties of the entire visual system, both retinal and central, whereby a given stimulation level will raise a given proportion of neural units above their excitation threshold, itself determined probabilistically. Fusion occurs when the average effect of a light flash becomes indiscriminable from its aftereffect.

1.1.2.3 Phase relations. The conflicting models of Hecht and Crozier make different predictions about the effect on CFF of varying the luminance distribution within the cycle of intermittence, and an extensive literature on the effects of varying the pulse - to - cycle fraction developed during this period; see Pieron (1965) for a comprehensive review.

If it is assumed that the two antagonistic processes of accumulation and decomposition of photopigment in Hecht's model have equivalent time courses, then CFF will be highest when the light and dark phases are of equal duration (PCF = 0.5). CFF will decrease symmetrically with higher and lower PCFs, since the total cycle duration would need to increase to compensate for the relatively shorter phase. This prediction is expressed in the law established by Porter (1902) after a series of meticulous and elegant experiments:

$$CFF = k \cdot \log[PCF\ (1 - PCF)] + c \qquad \text{Equation 1.02}$$

where k and c are constants. Brightness, or Talbot level, varies with PCF since the absolute length of the light phase changes. Porter recognised this problem, but was not able to compensate by varying flash intensity. Ives (1922a) kept L_{mean} approximately constant by varying stimulus intensity inversely with PCF, and confirmed Porter's law for photopic but not

scotopic levels, where CFF is independent of intensity. With L_{mean} held constant, the CFF of the scotopic system decreases almost linearly with increasing log PCF:

$$CFF = c - k \cdot \log PCF \qquad \text{Equation 1.03}$$

Pieron (1928) suggested that the difference between the linear scotopic function and the U-shaped photopic function when PCF < 0.5 was related to the absolute duration of the dark phase. As PCF decreases the absolute duration of the dark phase increases, causing a reduction in 'luminous efficiency'. This in turn causes CFF to decrease, in opposition to the trend of increasing CFF with decreasing PCF (Equation 1.03). Since the absolute length of the dark phase is dependent not only on PCF but also on frequency, the dependent variable, the antagonistic factors do not exactly cancel out, and the U-shaped function is not perfectly symmetrical. Pieron (1961) showed that, if constant CFF is assumed, then critical dark time is a linear function of PCF. From this he concluded that flicker fusion was determined by the duration of the dark phase, or 'intermittence'.

The relationship embodied in Equation 1.03 is often unclear in the many studies which followed the pioneering work of Porter and Ives, as the covarying parameters of frequency, L_{mean}, and PCF were manipulated. The proliferation of apparently conflicting findings led Landis (1954b) in an untypically perceptive moment to conclude:

> "From this survey of the (PCF) effect the confusion is evident and other than attributing the difficulties to the interaction of variables and the lack of independence of cps and (PCF) no clarification can be offered. ..... If (PCF) is a real problem it is certain that no-one has offered the beginning of a solution." (p274)

Landis was apparently unaware of the paper published by deLange in 1952

which suggested for the first time that the methods of systems analysis may help to account for many flicker phenomena within a unified theoretical framework. Moreover it is ironic that the review from which Landis's remarks are taken was published only one month before deLange's second paper (1954) containing a more detailed account of the theory and its application to the findings of Porter, Ives, and Hecht.

1.1.2.4 Waveform. Before undertaking a review of the impact of systems analysis on flicker research it is appropriate to consider here the few studies carried out prior to 1952 which did not use the traditional intermittent stimulus, since these provide a useful and often interesting precursor to the later work.

In 1907 Kennelly and Whiting reported a remarkable series of experiments which anticipated much of the later flicker work, but whose significance remains largely unrecognised. Of particular interest are the experiments in which modulation depth was varied, independently of L_{mean}. CFF vs L_{mean} curves were obtained at 4 modulation depths, from which Kennelly and Whiting concluded that

$$\begin{aligned} CFF &= k \cdot \log(m \cdot L_{mean}) + c \\ &= k \cdot \log\Delta L + c \end{aligned} \qquad \text{Equation 1.04}$$

where c and k are constants and m = modulation, as defined in Section 1.1.1. This amounts to a reformulation of the traditional Ferry - Porter law (Equation 1.01), as Kennelly and Whiting point out:

> "The (CFF) does not depend upon the mean illumination of the target ..... It depends on the maximum and minimum cyclic illuminations." (p337)

This conclusion was later reached independently by Kelly (1961a).

After measuring the frequency threshold of rectangular-wave flicker at different PCFs Kennelly and Whiting concluded that CFF was independent of flicker waveform, and determined solely by amplitude. Although this inference does not appear to follow from the experiments carried out, it did stimulate Luckiesh (1914) to make the first measurements of flicker thresholds using non-rectangular waveforms. CFF was measured for trapezoidal, triangular, and squarewave flicker, all with the same L_{max}, L_{min}, and L_{mean}. Luckiesh found that CFF increased with the slope of the waveform, so that maximum CFF was obtained with squarewave flicker. He concluded, contrary to Kennelly and Whiting, that CFF was dependent on waveform, although did not go on to make a quantitative estimate of the relationship.

Luckiesh's observations were greatly extended by Ives (1922a), who measured thresholds for triangular, sawtooth, squarewave, and, for the first time, sinewave flicker [1]. Using an optical system which allowed amplitude to be varied independently of L_{mean}, Ives obtained measurements of CFF vs L_{mean}, waveform, and amplitude which were well in advance of contemporary flicker research. His two main conclusions were:

1. waveform. Ives supported Luckiesh's conclusion that CFF is

---

[1] Kelly (1972) claimed that the first published measurements of sinewave modulation sensitivity were made by Dow (1907), using a grease spot flicker photometer. In fact, Dow's photometer produced a conventional squarewave stimulus, the amplitude of which was not variable. Dow's measurements were concerned with the deviation in mean luminance which could occur at the fusion frequency before flicker becomes visible, rather than with modulation depth. However, the resulting curves do bear some similarity to later modulation threshold curves.

dependent on flicker waveform, but not that it is specifically determined by the temporal luminance profile. He found that CFF for sawtooth flicker was lower than for sinewave flicker, and furthermore that it was unaffected by the direction of the sawtooth. He concluded that CFF was determined by "some feature of the shape which is unaltered by direction", and went on to suggest that this feature was the Fourier fundamental.

2. amplitude. Ives essentially supported Kennelly and Whiting's observation that CFF varied with log amplitude (Equation 1.04). However, he extended the relation to cover different waveforms by proposing that the crucial parameter was not the amplitude of the waveform itself but that of its Fourier fundamental.

This latter relation was found to hold for all stimuli except low frequency sinewaves. Ives observed that the threshold amplitude vs frequency curve for these stimuli was non-monotonic, showing a modulation minimum occurring at about 5 Hz. Unfortunately this phenomenon, along with the rest of Ives's work, remained virtually ignored by flicker researchers for 30 years until rediscovered by deLange (1952), except for some comments by Cobb (1934). In 1954 Landis commented: "It is surprising that no-one has followed up the implications of (Luckiesh and Ives's) results." (Landis, 1954b: p270).

1.1.3 1952 - 1982 : Systems analysis; empirical results

In 1952 Harold deLange, an electrical engineer working for Philips in the Netherlands, published the first of six papers to appear over the next 9

years which did 'follow up' Ives's results. Previously the phenomenon of flicker fusion had been explained by the 'filling in' of the dark phases, and the stimulus had been considered purely as a time function of luminance. DeLange recognised that the inability of the visual system to follow rapid modulations had much in common with the characteristics of a low-pass electrical filter, and decided to apply the descriptive techniques of systems analysis, already an established technique in electrical and mechanical engineering, to the temporal behaviour of the visual system. In order to test the validity of such an approach he also constructed an electrical analogue to simulate the processes involved.

The modulation (m) of a waveform can be varied by changing either its amplitude or its mean level. The modulation (m) of a waveform is almost always changed as it passes through a physical system, the degree of attenuation or gain being frequency - dependent. The function of modulation change vs frequency (the modulation transfer function: MTF) provides a complete description of a system's performance. The MTF, or attenuation characteristic (AC), shows the efficiency with which a system passes sinusoidal modulation over a range of frequencies, by plotting the ratio of input amplitude to output amplitude. It is conventionally measured by applying a signal of known amplitude to the input and measuring the output signal. It is of course not possible to measure the output in the visual system directly; instead it is assumed that the output at threshold has a constant amplitude (ΔL_c), and so the input required to produce this level is measured. The power of systems analysis, in view of the confusion prevailing at the time over the effects on CFF of waveform variations, lies in its ability to predict the response to any arbitrary input, once its sinewave Fourier components are known. The three requirements for this analysis are:

a) the MTF (sinewave response function) is known,

b) the system is linear, ie it obeys the principle of algebraic summation of inputs, and

c) the output at threshold is constant and independent of frequency.

Comparing three flicker waveforms deLange (1952, 1954) showed that CFF at high frequencies was independent of the time function of the stimulus, and determined solely by the modulation of the Fourier fundamental (m_f), as concluded by Ives (1922a). The power of this analysis is underlined by the fact that the curve extends up to the 200% modulation point (the maximum obtainable with a rectangular waveform), even though the fundamental in this case is not physically realisable. The dependence of CFF on fundamental frequency implies that the visual system operates as a linear system, at least for frequencies at or above fusion and under the conditions used (2° diameter foveal field, surround at L_{mean}). However, the response becomes increasingly nonlinear at low frequencies [2], and threshold is no longer predictable from the fundamental alone. DeLange (1952) therefore tried to measure the MTF directly, using trapezoidal flicker to approximate a sinewave, and showed that the low frequency region of the curve asymptotes at m = 1.35% (Figure 1.01). DeLange assumed that no attenuation occurs at very low frequencies, and suggested that this figure represents the critical modulation necessary for the

---

[2] The change in approach from the time to the frequency domain was accompanied by the adoption of the engineering convention of plotting modulation as a function of frequency. For technical reasons, however, deLange (1952, 1954) continued to measure frequency as the dependent variable and to refer to the frequency threshold (CFF). This accounts for his assumption that the visual system is nonlinear at low modulations, whereas it is now accepted that the nonlinearity appears at low frequencies. Later deLange (1958, 1961) used a combination of fixed frequency and fixed modulation conditions, in order to keep the dependent variable as orthogonal to the threshold curve as possible.

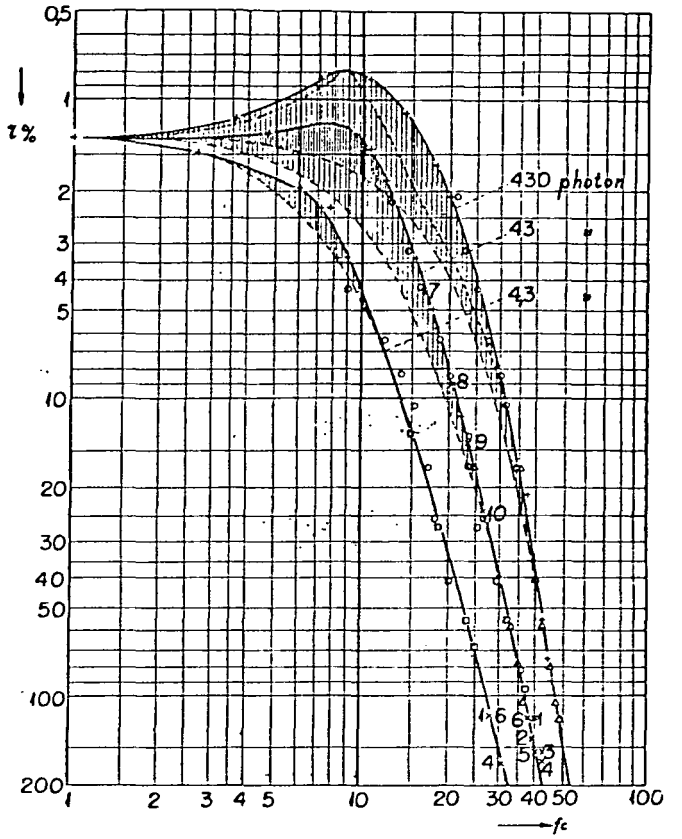

Figure 1.01 : The first published modulation sensitivity curves for flicker, measured at 3 adaptation levels (photon = troland), taken from deLange (1952). The different plotting symbols refer to different waveforms, showing that threshold is determined by the Fourier fundamental. The dashed curves represent the response of a simple low - pass filter. The shaded area between the dashed and solid lines was interpreted by deLange as a resonance effect. The dotted curve is calculated from an electrical analogue with feedback - induced resonance (see Section 1.1.4).

threshold mechanism to register a signal. In other words, at threshold an arbitrary periodic stimulus appears at the site of the fusion mechanism as a sinewave of 1.35% modulation. The increment threshold for successive (temporal) contrast that this represents is comparable to the Weber - Fechner fraction for simultaneous (spatial) contrast using a similar stimulus (Stiles, 1929).

DeLange (1954) suggested that the nonlinearity at low frequencies was due to the contribution of higher harmonics which are too low to be attenuated by the rapid high - frequency cut-off. In his last published paper (deLange, 1961) this is explained in more detail, taking into account the nature of the nonlinear threshold element. With harmonics passing unattenuated, or even amplified, through the initial filter a non-sinusoidal waveform is presented to the decision mechanism (Figure 1.02), which responds if luminance deviates from L_{mean} by more than a critical proportion in either direction. DeLange showed that low frequency thresholds of the two types of rectangular modulation shown in Figure 1.02 are predictable from his model of the initial filter stage.

Mean luminance (Ferry - Porter law). DeLange (1952) found that at low luminance levels (4.3 td) a monotonic relationship exists between amplitude and fusion frequency. As luminance increases the curve shifts towards higher frequencies and increases in slope, obeying Porter's law relating CFF and luminance (Equation 1.02). The coefficient of intercept (c) increases linearly with log modulation. In addition the curve becomes increasingly non-monotonic, developing a peak at about 10 Hz whose size increases with luminance. DeLange produced this peak in his electrical analogue by adding to the basic low-pass filter a resonance - inducing feedback loop with a fixed delay of about 12 ms, citing physiological

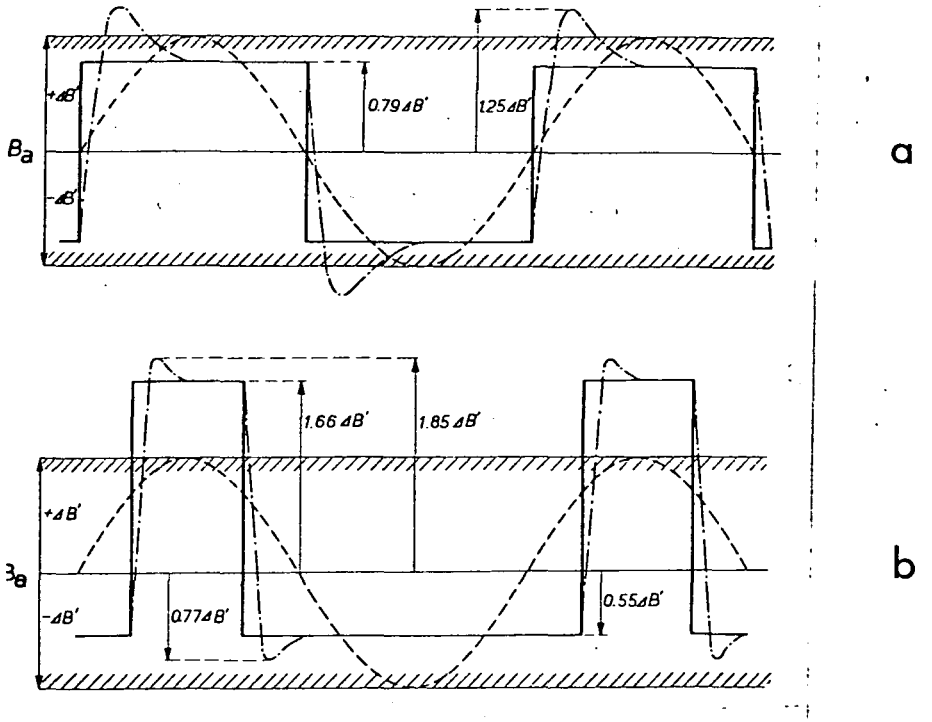

Figure 1.02 : DeLange's (1961) explanation for the observation that at low frequencies the threshold for non-sinusoidal waveforms is not predictable from the Fourier fundamental alone. The solid curves represent two input waveforms with the same fundamental, marked as a dashed line. The threshold mechanism operates whenever its input variation exceeds the shaded line. At low luminances harmonics pass unattenuated through the filter, and the detector receives an undistorted signal (solid line). Thus the threshold for waveform (a) is higher than the sinewave threshold, but the threshold for waveform (b) is lower. At high luminances relative high frequency sensitivity increases, and the filter introduces linear distortion (dot - dash line). Under these conditions the threshold for both forms of squarewave is lower than that for sinewaves.

evidence of such loops in retinal structures.

Originally deLange (1952, 1954) found that the low frequency (LF) asymptote was independent of luminance, and represented the absolute threshold of temporal contrast. Improved measuring techniques and a greater luminance range later revealed (deLange, 1958) that the LF sections are displaced vertically as a linear function of log L_{mean}.

In 1961 D.H. Kelly published the first of a series of papers which further developed deLange's theory of flicker processing, by coincidence appearing immediately after deLange's final paper in the same issue of the Journal of the Optical Society of America. Kelly (1961a) repeated deLange's measurements using a large flicker field (65° diameter, vignetted to a dark surround), in order to establish the linearity of the high frequency (HF) response. In a truly linear system the response to the AC signal component should be independent of the DC mean level. However, deLange's MTF curves were shifted with mean luminance, or DC level. Kelly (1961a) showed that the functions at different adaptation levels converged on a common HF asymptote when plotted in terms of absolute amplitude (ΔL) (Figure 1.03a). At the same time the curves reach a common LF asymptote when plotted as relative amplitude (m), as deLange had shown (Figure 1.03b). [Kelly was unable to replicate deLange's (1958) finding that the absolute threshold varied with L_{mean}, except at very low (scotopic) levels.] In other words, threshold is independent of adaptation level at high frequencies (linear behaviour), but approximately proportional to it at low frequencies (Weber - Fechner behaviour). At intermediate frequencies the curve shifts smoothly from one type to the other. Replotting his data as frequency vs L_{mean}, Kelly (1961a) went on to show that the traditional formulation of the Ferry - Porter law was valid only over a

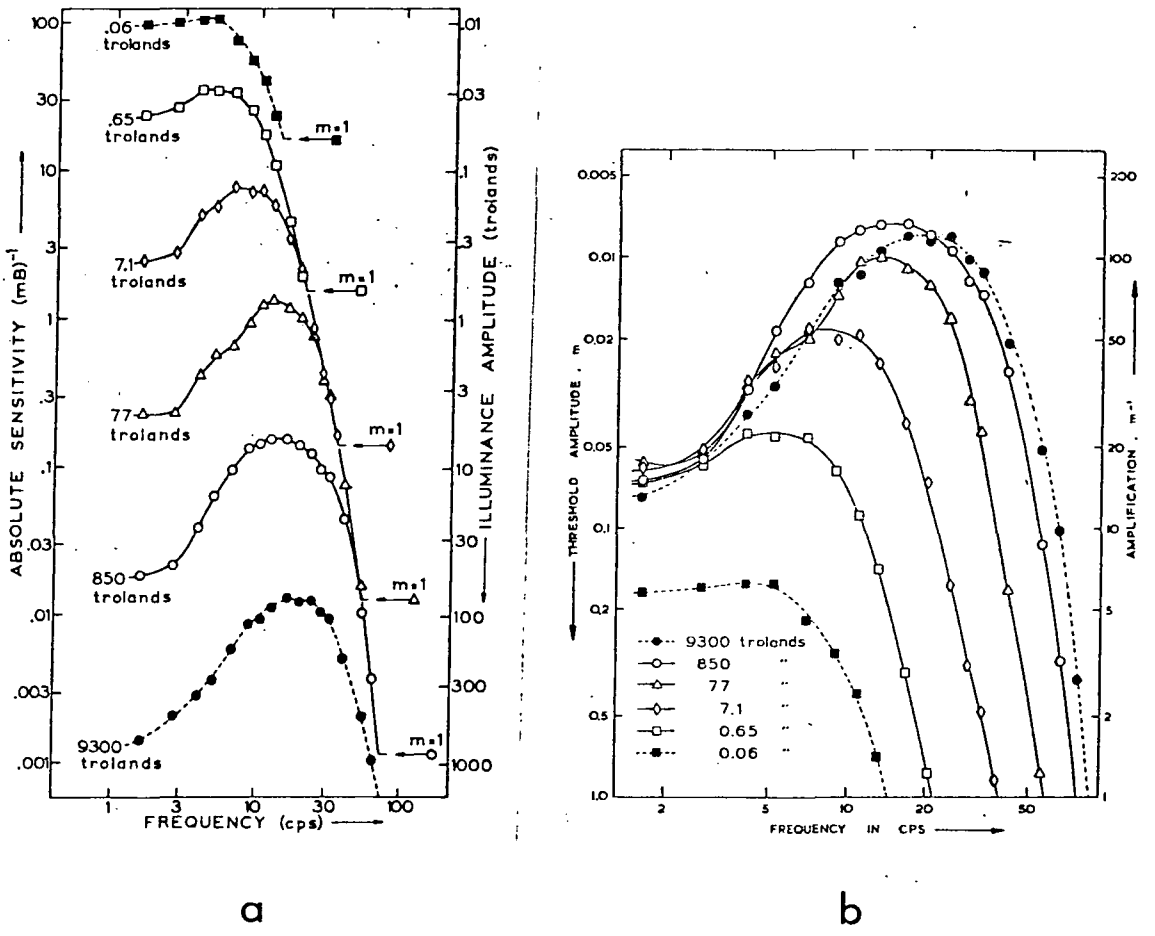

Figure 1.03 : (a) Absolute amplitude sensitivity vs frequency at 6 adaptation levels. When plotted this way, all the curves converge onto a common asymptote which is independent of Lmean.
(b) Relative amplitude sensitivity vs frequency. All the curves converge onto a low frequency asymptote, independent of Lmean. At intermediate frequencies the system shifts smoothly from (b) (Weber - law behaviour) to (a) (linear response).
[Taken from Kelly (1961a: 425 and 426).]

restricted range, which became smaller with decreasing modulation. Figure 1.03 shows that CFF is an approximately linear function of log absolute amplitude, rather than of log L_{mean} as the Ferry - Porter law states. As mentioned in Section 1.1.2 above, this relationship was originally reported by Kennelly and Whiting (1907), in a paper of which Kelly was apparently unaware. The original erroneous formulation arose from early studies in which L_{mean} always covaried with amplitude, since technical limitations meant that L_{min} was fixed. If absolute amplitude is held constant, CFF actually decreases when L_{mean} is increased, since relative modulation than decreases (Kelly, 1964).

1.1.4 Theoretical models

A review of the development of models of flicker processing and detection systems need not include pre - systems analysis theories: although early empirical data are still relevant early theories are not so durable, since linear models are generally simpler and more inclusive. Since the threshold for an arbitrary waveform is predictable from the thresholds of its sinusoidal Fourier components, the aim of any flicker model must be to account for the sinewave MTF. The models of Hecht, Crozier, and Pieron do not satisfy this criterion. The following review will concentrate on major theoretical developments, rather than provide an exhaustive summary. A recent comprehensive review of theoretical models which also examines possible physiological substrates is available by van de Grind et al (1973).

Almost all flicker models of the last 30 years fit the general 3-stage form outlined in Figure 1.04. Light energy is transduced into a form which is an analogue of intensity. This signal passes through a filter, characterised

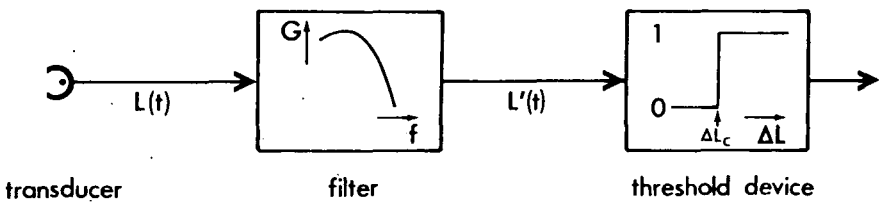

Figure 1.04 : General model of flicker processing. Light energy is transduced by the photoreceptors into an analog of the time function of luminance, L(t). After passing through a filter with frequency - dependent gain the signal is distorted [L(t)]. The final stage is a nonlinear threshold device which responds "seen" if the input deviation ΔL exceeds the criterion level ΔLc.

by the deLange curve or temporal MTF. The filter output passes to a nonlinear detector whose state changes if the input fluctuations exceed a fixed value. Relatively little work has been done until recently on the mechanics of the detector stage, beyond assuming that a deviation from the mean level of $>\pm\Delta L_c$ gives rise to a percept of flicker. The remainder of this section will therefore be devoted to possible mechanisms of the filter stage.

1. Cascaded - filter models. The main features of the deLange curve which any proposed filter must account for are a) linear high frequency behaviour, b) the luminance - dependent sensitivity peak, and c) nonlinear Weber law behaviour at low frequencies. DeLange (1952, 1961) noted the similarity of the HF roll-off to the attenuation of a simple low-pass filter consisting of a cascade of RC (resistor - capacitor) integrator circuits. The gain (G) of a series of N such circuits is given by:

$$G(f) = (1 + (2\ fRC)^2)^{N/2} \qquad \text{Equation 1.05}$$

where f is frequency. This function converges onto a HF asymptote, the slope of which (in log-log co-ordinates) is equal to N, the number of RC stages. A good approximation to the data of Figure 1.01 is obtained if increasing mean luminance has the effect of both increasing N and decreasing the time - constant (RC). The midrange peak was interpreted by deLange as a resonance phenomenon, and may be produced either by including inductive elements in the circuit, or by a feedback network. DeLange (1952) chose the latter on physiological grounds, and confirmed this in his second model (deLange, 1961) by showing that a bandpass filter would require capacitances as large as 250 uF and inductances as large as

1 H to approximate the observed curves. DeLange considered that such values were unreasonable in a physiological system.

All attempts to model the temporal MTF as a linear system encounter the problem of accounting for the low frequency nonlinearity, where gain is dependent on adaptation level (Kelly, 1961a). Several models have thus postulated a two - stage system incorporating a linear low-pass filter similar to deLange's and a nonlinear filter to simulate Weber law behaviour. The most influential model of the second mechanism was proposed by Fuortes and Hodgkin (1964) from work on Limulus receptor potentials. The Fuortes - Hodgkin model is based on a cascade of 10 RC integrators in which the R provides a leak to ground whose value is determined by feedback from the system's output (Figure 1.05a). R decreases as a log function of adaptation level, thereby shortening the time - constant RC and reducing the gain predicted by Equation 1.05. Leak resistances are varied by the same amount in each stage, and are determined by output rather than input to account for observed delays in the response to steps and flashes by the Limulus photoreceptors. The model produces a reasonable fit to observed transient responses over 3.5 decades of intensity, although the predicted response is more oscillatory (ie the bandpass peak is too narrowly tuned). [Marimont (1965) suggested that this was due to too great a delay in the feedback loop, and further improved the fit by taking the feedback from the penultimate stage (Figure 1.05a).] The Fuortes - Hodgkin model was developed to account for the time course of responses to transient stimuli (20 ms flashes), and was extended by Pinter (1966) to steady - state stimuli (sinusoidal flicker). Pinter showed that the qualitative fit was reasonable above about 1 Hz, although the amplitude of the peak was less than predicted, according with Fuortes and Hodgkin's predicted oscillations. As frequency is reduced below 1 Hz, however, the model fails to account

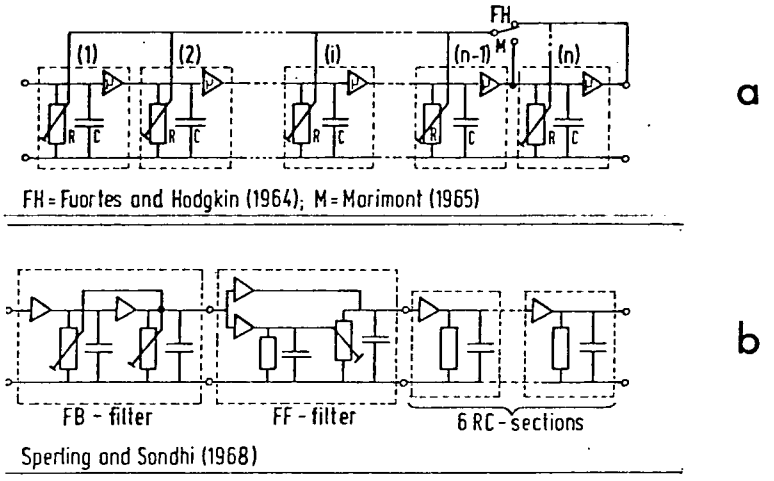

Figure 1.05 : Two cascaded - filter models of flicker detection incorporating adapting networks to account for low frequency nonlinearity. [Taken from van de Grind et al (1973 : 535)]
(a) Fuortes and Hodgkin (1964). 10 leaky integrators whose time - constant (R) is determined by feedback from the system output. Marimont (1965) improved the fit to the observed data by taking the feedback from the penultimate stage.
(b) Sperling and Sondhi (1968). A development of the Fuortes - Hodgkin model, claimed to incorporate a less complex feedback network. See text for details.

for the decreasing gain and increasing phase lead, and Pinter proposed an additional 'linear lead network' following the filter to explain this very low frequency behaviour.

The complexity of the extensive feedback network in the Fuortes - Hodgkin model was questioned by Sperling and Sondhi (1968), who proposed that the same transfer characteristics may be obtained by 9 cascaded RC elements organised into 3 systems (Figure 1.05b). The first filter consists of two Fuortes - Hodgkin feedback - controlled RC stages acting to compress the dynamic range. The second stage is an RC filter whose leak resistance is controlled by the input level (feedforward control) with a fixed delay in the control loop. This filter has the interesting property that it mimics Weber law behaviour without an explicit logarithmic response anywhere in the system, by dividing the current input by the time - average of recent inputs (this idea had been earlier described by Barlow, 1965). The third section contains 6 cascaded RC filters with fixed values. The model produces a reasonable approximation to the measured human deLange curve over 4 log units of intensity, but like the original Fuortes - Hodgkin model tends to overestimate both peak and low - frequency sensitivity.

2. Diffusion models. A second major line of theoretical thought, quite distinct from the electrical analogue models initiated by deLange, is based on known neuronal diffusion characteristics. This basis alone may be considered to bestow greater prima facie physiological validity. Any cascaded integrator model assumes that the gain curve asymptotes to a high frequency linear function in log-log co-ordinates, the slope of which equals the number of RC sections. However, as Kelly (1969) pointed out, the

Ferry - Porter law (as restated by Kelly, 1961a) requires that CFF vary inversely with log amplitude, ie sensitivity is an exponential function of frequency, and hence has an accelerating slope in log-log co-ordinates. This may be seen by careful inspection of the curves in Figure 1.03. In fact Kelly (1969) proved that a model exhibiting true Ferry - Porter behaviour is not physically realisable, and showed that the HF sensitivity lies between that predicted by the Ferry - Porter law:

$$G(f) = e^{-k/f} \qquad \text{Equation 1.06}$$

and that predicted from cascaded integrators (Equation 1.05). In contrast to either of these theoretical functions, Kelly (1969, 1971) showed that the high frequency asymptote was best fitted by an exponential square-root function:

$$G(f) = k \cdot \exp(-f^{0.5}) \qquad \text{Equation 1.07}$$

This function is thought to be due to diffusion processes within the photoreceptors, and is very similar to the theoretical response function derived from a diffusion equation by Ives (1922b). Ives's diffusion model remained virtually ignored until Kelly's rediscovery, although Veringa (1961, 1970) independently derived a very similar formulation.

Such a diffusion process thus provides the best fit so far for the linear HF response curve, and Kelly's complete model (1971) incorporates it as one element of a two-stage single channel model, with a nonlinear neural network accounting for the adaptive LF behaviour. [Note that this, Kelly's second model, differs fundamentally from his first model (Kelly, 1961b), which proposed that the LF response is due to a linear filtering stage in the

photoreceptors, followed by a nonlinear neural pulse - encoding stage providing the low-pass behaviour at high frequencies.] The gains of two series filters combine multiplicatively, so that the response of the LF system alone is obtained by dividing the overall response by that of the HF diffusion stage. This results in a high-pass sigmoidal function whose slope and LF asymptote vary with adaptation level. Kelly's model of this stage consists of a network of RC integrators each with inhibitory feedback, with both the gain and the number of stages dependent on DC level. A sophisticated mathematical analysis was used to restrict the number of possible candidate networks, and one network which satisfied most of the requirements was described. This type of network has a bandpass characteristic, but the HF part of the response may be ignored since these frequencies are eliminated by the low-pass diffusion stage. The Kelly model is to date the simplest, most completely specified model accounting for both transient and periodic stimuli, and is of particular interest in that it was developed as part of a larger model incorporating spatiotemporal interactions. The effect of spatial factors is discussed in Section 1.3.

1.2 Transients

Temporal contrast, or the change in luminance over time, may be divided into periodic changes, the work on which was reviewed in Section 1.1, and nonperiodic changes. This latter class, sometimes called transients, include stimuli such as steps (increments and decrements), flashes, paired flashes, etc. The studies mentioned in this section are largely restricted to those which have considered the relationship between the way in which the

visual system processes and analyses these stimuli and the mechanisms for the detection of flicker. Any complete model of temporal contrast analysis must be able to account for both types of input. The detection of transients is considered in the experiments described in Chapters 6, 7, and 8.

1.2.1 Single flashes

The basic principle of temporal integration by the human visual system is embodied in Bloch's Law (Bloch, 1885). This states that as the duration (t) of a flash increases from zero its amplitude at threshold (ΔL_c) decreases so that the total energy ($\Delta L \cdot t$) remains constant up to the critical duration (t_c). As duration increases further ΔL_c is constant and independent of t. The classical observations of the relation between critical duration and adaptation level, which many subsequent theorists have used, are those of Graham and Kemp (1938), Keller (1941), and Herrick (1956). Graham and Kemp found that t_c decreases almost linearly with increasing log luminance. Keller repeated the experiment under very similar conditions, and concluded that the slightly curved function was best described as a power function with a small negative exponent:

$$t_c = k \cdot L_{mean}^{-p} \qquad \text{Equation 1.08}$$

Herrick again repeated the experiments, this time using a negative flash (luminance decrement), with essentially the same results.

Critical duration, as a measure of temporal integration, is clearly related to critical flicker frequency, which may be considered as a measure of temporal resolution. Pieron (1965) pointed out similarities in the mean

luminance functions of each, and Matin (1968) compared directly the flash data referred to above with the flicker thresholds of Lloyd and Landis (1960), measured under similar conditions. Over a range of 5 log units of luminance the two measures corresponded extremely closely. In other words, flicker appears fused when the period between the onset of successive flashes is less than the integration period of a single flash. However, Lloyd and Landis, who were continuing to investigate the effects of pulse - to - cycle time almost 10 years after the introduction of systems analysis, believed that CFF varied with log L_{mean}, rather than with modulation amplitude (Kelly, 1961a; Levinson and Harmon, 1961). Matin (1968) continued this erroneous belief, thus the validity of his analysis is doubtful for conditions other than those in which modulation and L_{mean} covary.

Matin (1968) went on to modify the detection stage of the Fuortes and Hodgkin (1964) model of flicker response in order to account for the observed relationships between transient and flicker data. He concluded that the neural response at threshold has a constant absolute amplitude rather than a constant ratio to the tonic level. Sperling and Sondhi (1968), in their development of the Fuortes - Hodgkin model, derived estimates of the time constants of the various filter elements from flash thresholds. When applied to sinusoidal flicker the estimated parameters provide a good fit to the HF portion of the empirical curve, but consistently overestimate low - frequency sensitivity.

A more comprehensive attempt to integrate transient phenomena within the framework of linear systems theory has been made by Roufs (1966, 1972a), who compared responses to flashes and flicker with respect to two common measures: a) sensitivity, and b) inertia (temporal integration). He found that sensitivity to flashes (F) is an almost constant proportion of the

sensitivity to flicker (S), defined as the point of peak sensitivity on the deLange curve. S/F = 2.5 over a 5 log unit range of luminance. Similarly critical duration (t_c) varies reciprocally with half - power frequency (f_h) (the frequency at which sensitivity has dropped to half its peak value) over a similar range: $f_h \cdot t_c = 0.5$. These simple quantitative relationships suggest that both periodic and transient variations are passed through the same filter and detected by the same threshold mechanism, greatly simplifying theoretical modelling. In particular it allows the analysis of both stimuli to be combined within the framework of linear systems theory.

Roufs's (1972b) model consists of a linear filter followed by a simple peak detector with a fixed criterion level (Figure 1.06b). If the filter output exceeds the criterion deviation from a fixed reference level, the detector makes a positive response. This model allows quantitative estimates to be made of the system's response to an arbitrary input, in terms of 'threshold units'. This basic model was later amended (Roufs, 1974a) to account for observed thresholds of incremental and decremental flashes, the modification allowing the detection mechanism to respond to a deviation which is approximately equally large in either direction. This change was achieved at the cost of accounting for the detection of low - frequency sinusoids, where peak - trough detection should take place. Finally, (Roufs, 1974b), probability summation was introduced to explain the lowering of the threshold for multiple flashes at long interflash intervals.

An alternative model of the detection system which has been contrasted with that of Roufs was proposed by Rashbass (1970), based on thresholds for pairs of flashes separated by a variable interval. The Rashbass model (Figure 1.06a) consists of an initial linear filter, followed by a mechanism which squares (and therefore rectifies) the signal. The

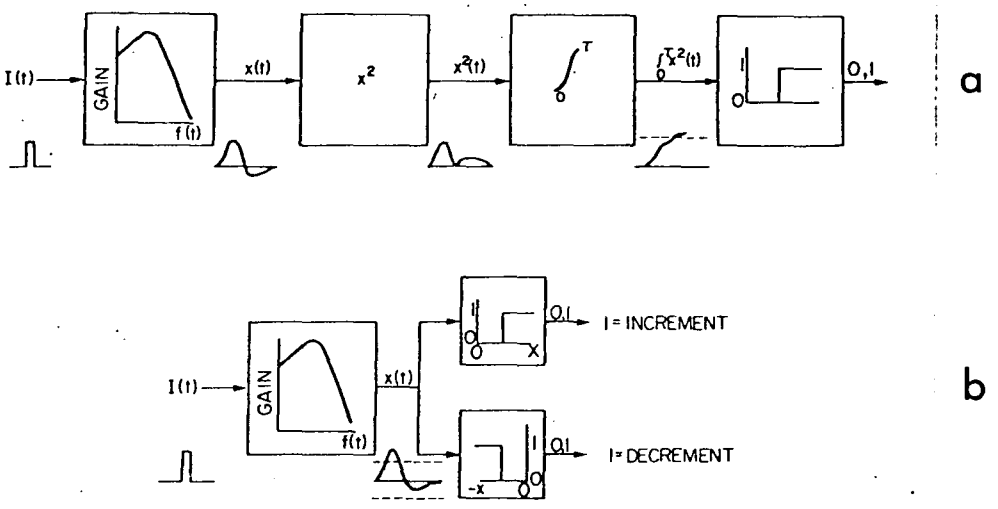

Figure 1.06 : Two models of the detection of transients. [Taken from Krauskopf (1980: 672)]
(a) Rashbass (1970). The initial filter stage is followed by a squaring element which rectifies the signal before it passes through a perfect integrator. The final detector responds if the integrated signal exceeds the recent average by more than the criterion level.
(b) Roufs (1974a). The quasi - linear filter stage is followed immediately by a detection mechanism which responds if the instantaneous signal deviates from the mean by more than the criterion level in either direction.

rectified signal passes through a perfect integrator with a time constant of about 200 ms, whose output is tested to see if it has risen above a criterion level. In statistical terms the mechanism computes a running measure of the signal variance, and responds if this changes within the integration period from the average level. It is thus insensitive to intrinsic noise arising from the filter. The two models make different predictions about the interaction between two flashes occurring sufficiently close to interact within the filter. As the ratio of the amplitudes of the two stimuli changes, Rashbass predicts a smooth change from detection of one to detection of the other. Roufs, on the other hand, by measuring the absolute instantaneous value of the filter output, predicts a fairly sharp perceptual discontinuity. The empirical evidence (Rashbass, 1970; Roufs, 1974a) displays no such discontinuities, and Rashbass (1976) reconciles the difference by pointing out that the slope of the psychometric function for a single flash increases with the number of available detectors (n). In the Rashbass model n = 2, whereas the Roufs model requires that n = infinity, which Rashbass considers physiologically untenable.

A more fundamental difference between the two models lies in the treatment of incremental and decremental flashes. In the Roufs model information about flash polarity is preserved up to the detection stage, whereas in the Rashbass model this information is lost during rectification by the squaring element. Krauskopf (1980) tried to discriminate between the models by independently varying the threshold for positive and negative steps. Prolonged adaptation to flicker with a sawtooth waveform produced elevation of the threshold for steps in the same direction as the fast phase of the sawtooth, but had much less effect on steps in the opposite direction. These differential effects suggest not only that polarity information is still available at the detection stage, and hence that the

signal is unrectified, but also that the detectors themselves are polarity - sensitive. The Roufs model is unspecific about this aspect of the detection stage, although Krauskopf's interpretation is not incompatible with the model (Roufs, personal communication).

1.2.2 The shape of the impulse response

Experiments using only single transient stimuli are restricted to making statements about only one dimension of the impulse response - its maximum amplitude. However, since the visual system does not have an infinite bandwidth, the temporal form of any stimulus will be changed by the system. Any higher processes of detection and analysis have then to deal with this modified signal. It therefore becomes of interest to extend the study of transient stimuli into two dimensions, amplitude and time, to investigate the form of the internal response. The conventional techniques for this involve the use of two or more stimuli separated by a variable interval.

The first study of the interaction of two flashes was carried out by Granit and Davis (1931). They plotted the response to a subthreshold flash of fixed amplitude and duration by measuring the threshold duration for a second flash, as a function of the interflash interval. Their results were interpreted as showing that the response falls exponentially to a plateau until the critical duration, then falls approximately linearly to reach a baseline level after approximately 130 ms. Stiles and Crawford (1934) used a 100 ms test flash occurring before, during, and after a 1 second negative flash of fixed amplitude, and found that threshold for the test flash was raised both immediately before and after the 1 second flash. Crawford (1946)

reported essentially the same effect using a 10 ms test flash superimposed on a 52 ms positive flash, interpreting the apparent retroactive interference as the 'overtaking' of the weak test flash by the strong stimulus flash. The Crawford technique has also been used to probe positive (Boynton and Kandel, 1957) and negative (Baker, 1953) steps. These studies found that a very great threshold elevation peak occurs at or near an incremental step, and a somewhat smaller peak occurs at a decremental step. The size of the peak increases with mean luminance. Threshold elevation was thought to be a reflection of the burst of transient neural activity produced by the step.

More recently attention has turned to the specification of the time course of the response to transient stimuli. The response to a delta function input, ie an impulse of effectively zero duration, may be predicted by taking the Fourier transform of the gain function [G(f)] of the system. [The gain function contains both amplitude and phase information, in contrast to the simple amplitude information of the MTF.] Kelly (1961b) showed that his hypothetical gain function, derived from flicker sensitivity data, produced an impulse response which was monophasic at low luminances, but became faster and increasingly biphasic as luminance increased (Figure 1.07a). This hypothetical internal response may be thought of as analogous to neuronal firing rate at some point in the system: after a stimulus flash the rate first increases (excitation), then decreases to reach a level lower than the initial spontaneous rate (inhibition) before returning to the baseline level. As adaptation level increases the sinewave MTF becomes an increasingly bandpass characteristic (deLange, 1952). This effect is thus associated with an increasingly negative phase of the impulse response. However the initial positive phase of the response remains dominant even at the highest levels tested, with important consequences for models based on peak detection of response deviations. Kelly (1961b) went on to make

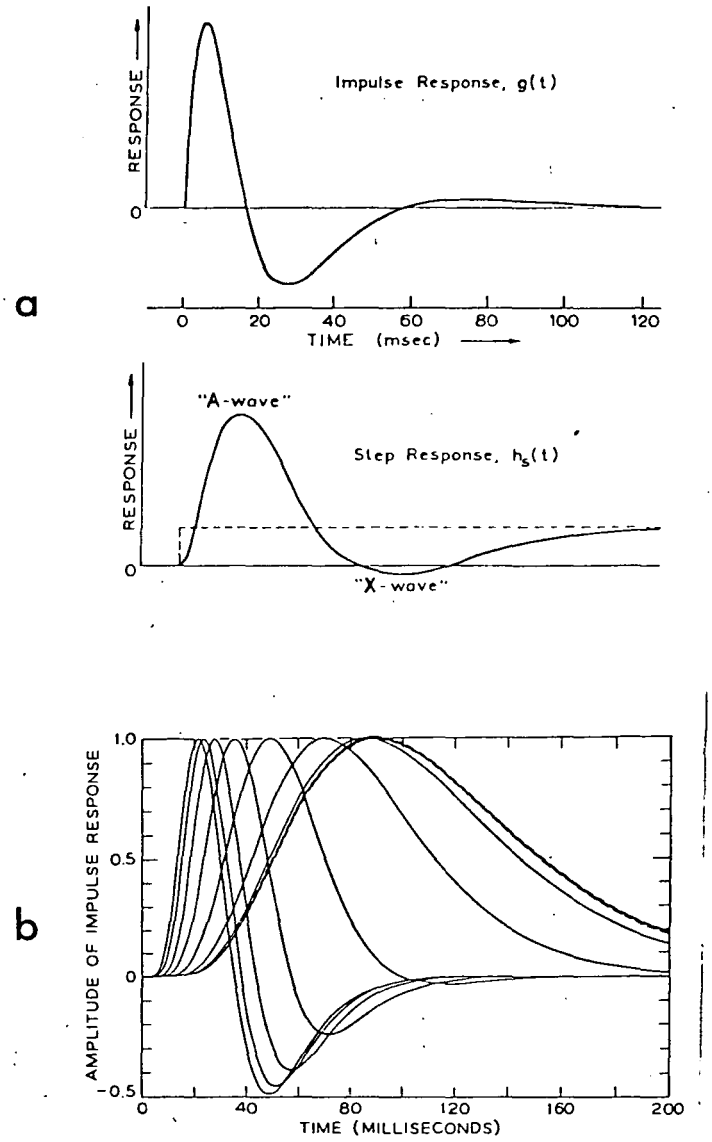

Figure 1.07 : Hypothetical impulse responses calculated from two models of flicker responses.
(a) Kelly (1961b). The impulse response at high mean luminance showing a marked negative (inhibitory) phase. The step response is the time - integral of the pulse response.
(b) Sperling and Sondhi (1968). The impulse response as a function of mean adaptation level. The response is monophasic at low luminances, where the temporal MTF approximates a simple low-pass filter. As Lmean is increased, the deLange function displays increasingly bandpass behaviour, with a relative loss of low frequency sensitivity. This results in a faster and more oscillatory transient response.

quantitative estimates of the magnitude of his transient responses, but took no account of stochastic effects which would have increased the detection probability of a periodic signal relative to a single stimulus. Roufs (1972a) suggests that this may reduce apparent thresholds by a factor of two. This should therefore be applied as a scaling factor to an uncorrected impulse response. Sperling and Sondhi (1968) used their model of flicker responses to derive a similar hypothetical response function (Figure 1.07b). This function has become a standard for the evaluation of other models. Blackwell (1963) used the amplitude threshold of a pair of flashes to measure temporal summation as a function of interflash interval. He found that summation was complete at short intervals, whereas at very long intervals summation was no greater than expected probabilistically, and the flashes were seen separately. Between these two extremes summation did not follow a simple monotonic transition, but reached a dip somewhat lower than the final level. That is, the flashes were inhibiting each other at certain intervals. This finding is consistent with a biphasic impulse response, and was investigated more thoroughly by Ikeda (1965), using pairs of opposite polarity flashes (doublets) with a variable amplitude ratio to measure the negative phase. These doublets give a summation function which is the inverse of that obtained with same - polarity pairs, suggesting both that the internal response is biphasic and that the responses to positive and negative flashes are mirror - symmetrical. Ikeda also confirmed Blackwell's observation that as adaptation level is reduced the response becomes more extended and the inhibition becomes weaker, as the change in the sinewave MTF would predict.

Plotting simple twin - flash thresholds against flash interval, Roufs (1973) found that the point at which threshold reaches a maximum corresponds to the critical duration for a single flash. He also showed that

the threshold characteristic in the range where the stimuli interact within the filter is predictable from his model derived to explain flicker thresholds (Roufs, 1972b; see above). In predicting the impulse response from the deLange curve phase information is also necessary: Roufs assumes that the filter has the characteristics of a minimum phase - shift system (Bode, 1945).

Unlike Kelly (1961b) and Sperling and Sondhi (1968), whose hypothetical impulse responses were derived from deLange curves, Roufs (1973) suggested that the luminance level does not qualitatively affect the form of the threshold function, but acts only quantitatively on the scaling parameters determining time - course and sensitivity. This was investigated more thoroughly by the use of opposite - polarity flash pairs (doublets) to probe the negative phase of the response (Roufs, 1974a). The size of the negative phase is related to relative low - frequency sensitivity. Relative sensitivity is specified by the shape of the deLange function, which is dependent at low frequencies on luminance level. If the form of the impulse response is independent of luminance level, it follows that it must be determined by that part of the deLange curve which is invariant with L_{mean}, ie the high frequency section. This implies that the complete deLange curve does not represent the response of a single system, but rather that the high and low frequency ends are determined by at least two separate, and parallel systems. This is a critical point for the application of systems analysis, which assumes that the internal detection threshold is independent of frequency. Parallel systems with different, though overlapping, frequency ranges complicate the interpretation of the sinewave sensitivity function.

The doublet threshold function shows the same invariance with

adaptation level (over more than 3 log units) as that for same - polarity twin flashes (Roufs, 1974a). Roufs also compared the measured threshold function with that predicted from deLange functions measured under identical conditions. At high luminances (3400 td) the two coincide well, but at low levels (2 td) the empirical function is more oscillatory than predicted. Roufs then went on to measure single flash thresholds over a large range of durations, using procedures designed to minimise variability as much as possible. These very careful measurements revealed a shallow threshold minimum in the region of the critical duration, in contrast to the conventional Bloch's Law finding of two converging asymptotes. The form of this function was again independent of luminance level. These two lines of evidence suggest that the response to transient stimuli is less affected by the low frequency content of the signal than systems analysis, using the deLange curve, would predict. To account for this observation, Roufs proposed that the deLange curve represents the envelope of two filters: a symmetrical bandpass filter centred on the peak frequency, dealing with transients and HF flicker, and a parallel system dealing with relatively slow luminance changes (Figure 1.08). These systems he termed respectively the 'agitation' and 'swell' systems, referring to the perceptual experiences which each gives rise to.

It is possible to derive a predicted impulse response analytically from the sinewave threshold curve, with appropriate assumptions about phase transfer. In order to carry out the procedure in reverse, however, it is necessary to measure the impulse response empirically. Ideally a pulse of zero duration and infinite amplitude should be used, since this has a frequency spectrum extending to infinity. This is fortunately not necessary since the visual system, like all physical systems, has a limited bandwidth. It is sufficient to use a pulse whose duration is short compared to the time

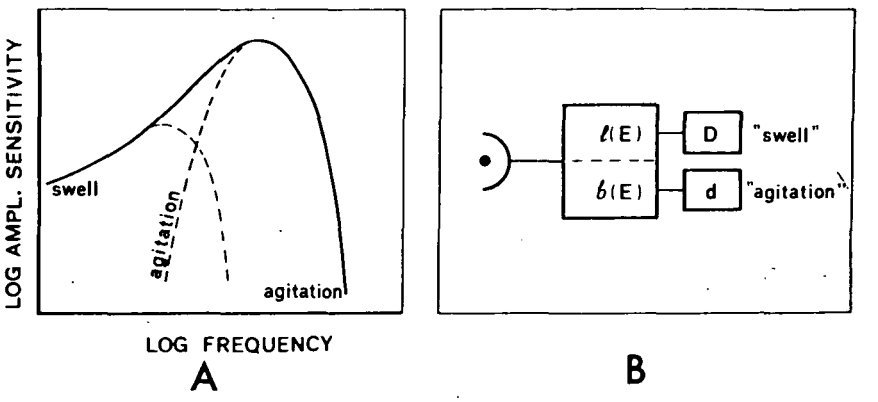

Figure 1.08 : (a) The deLange function may be considered as than envelope of the sensitivity functions of two systems: a bandpass filter centred on the peak frequency and a nonlinear low-pass filter. (b) Hypothetical block diagram of the relationship between the two filters, showing their parallel arrangement.
[Taken from Roufs and Pellegrino van Stuyvenburg, 1976]

constants of the system, ie one whose frequency spectrum extends beyond that of the system being measured. In order to measure the internal response to transients, Roufs and Blommaert (1975, 1981) developed a sophisticated psychophysical technique based on the threshold for two flashes with a fixed amplitude ratio. Taking great care to minimise the effect of drifts in sensitivity, because of the extremely small effects involved, they measured responses to both pulses and steps at a single adaptation level. Responses to increments and decrements were mirror - symmetrical, and equal to the derivative of the step response. More importantly, the Fourier transform of the measured impulse response confirmed the hypothetical bandpass filter response. However, because measurements were only obtained at one luminance level, no evidence is available on the question of whether the response is independent of mean luminance, as the model predicts.

Roufs has concentrated on specifying the characteristics of the linear, high - frequency system in his model. The system thought to be responsive to slow, possibly non-periodic luminance changes remains unspecified. The experiments in Chapters 7 and 8 attempt to provide further insight into the analysis and detection of these non-abrupt transients.

1.3 Spatiotemporal interactions

So far the characteristics of the visual system have been considered only in relation to purely temporal aspects of the stimulus. However, the temporal contrast threshold is dependent on at least two spatial parameters:

area (or size) and spatial structure. Although all the experiments described in the thesis used uniform fields a brief review of the main findings on spatiotemporal interactions is provided here since almost all flicker research in the last 20 years has been carried out in this area. In addition, this area is relevant to the relationship between temporal contrast analysis and movement analysis, discussed in more detail in the final chapter.

Delange's seminal observations were all obtained with the spatial pattern shown in Figure 1.09a. The first report of the effect of spatial variables on the temporal MTF was made by Kelly (1959), who compared deLange's pattern with the patterns in Figures 1.10b and c. Kelly showed that a large, effectively edgeless field caused a marked loss of sensitivity to low frequencies, compared to the function obtained with deLange's small, sharp - edged field. In order to bring the study of both spatial and temporal contrast within linear systems theory, Kelly (1960) proposed that spatiotemporal contrast thresholds should be measured using patterns with a circularly symmetric sinusoidal luminance function, the contrast of which decreases with eccentricity and is varied sinusoidally in time (Figure 1.09d). Spatial sinusoids had been used routinely for the study of optical systems since first being proposed by Duffieux (1946), and the spatial MTF of the human visual system was first measured by Schade (1956). Kelly (1960) argued that the traditional one-dimensional grating, in which luminance is constant in the orientation orthogonal to that of the modulation, provides a poor stimulus for fixation and ignores the rough isotropism of retinal structure. Although Kelly's specific proposal has not been widely adopted (but see Kelly, 1966), the use of temporally modulated sinewave gratings became a major growth area in visual psychophysics over the next 20 years.

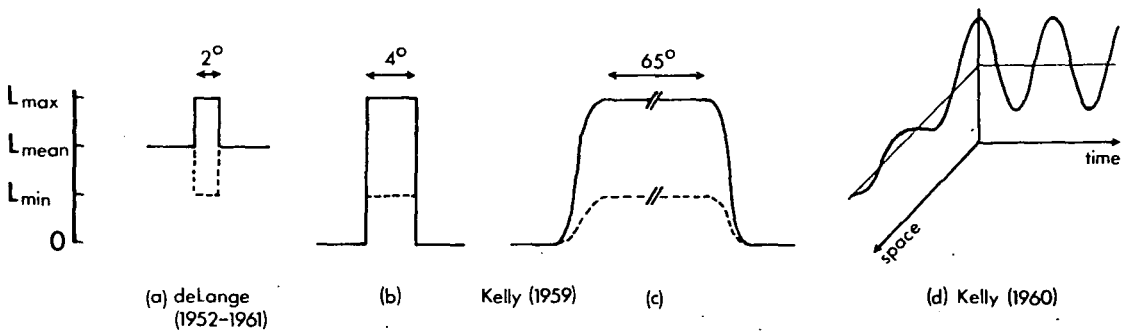

Figure 1.09 : Comparison of the spatial luminance profiles of the flicker stimuli of deLange and Kelly. (a) DeLange's 2 deg foveal field with surround at mean luminance. (b) and (c) Kelly compared a small sharp - edged field with a large, edgeless field, showing that edges enhance LF sensitivity. (d) Kelly suggested using a radially symmetric pattern in which luminance varies sinusoidally in both time and space for the systematic investigation of spatiotemporal interactions.

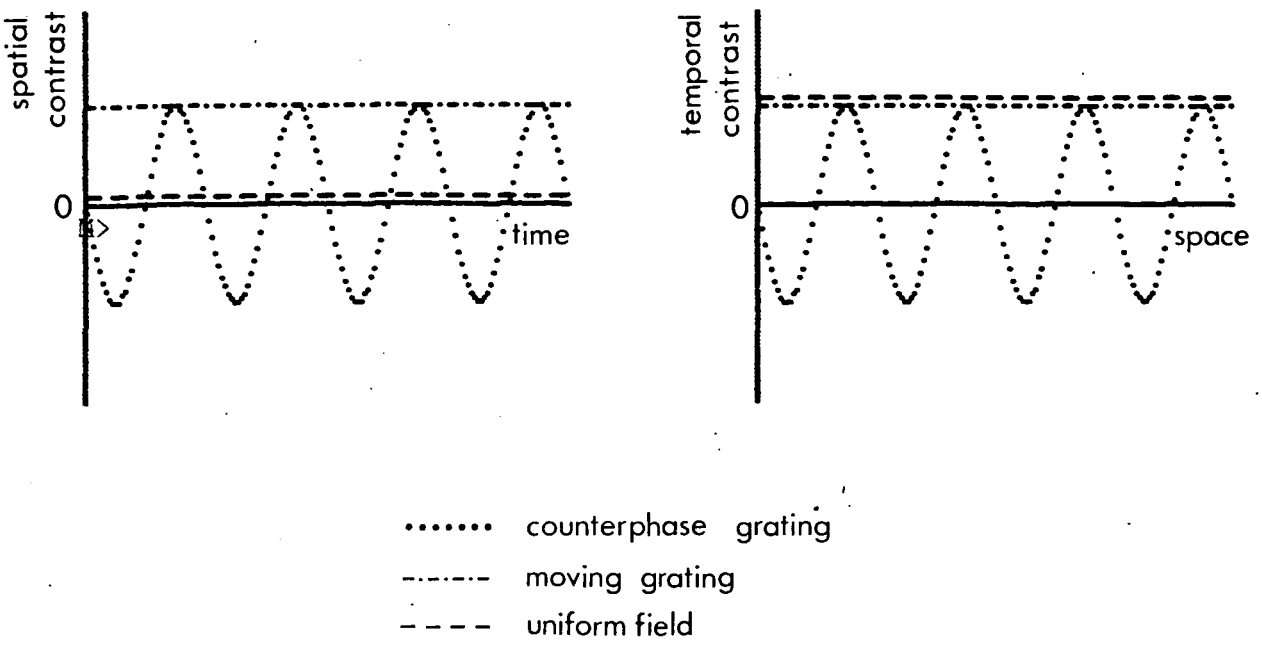

Figure 1.10 : The variation of spatial contrast over time and temporal contrast over space in 3 types of spatiotemporal modulation.

In this type of stimulus the spatial luminance function is multiplied by the temporal function to produce a standing wave, or counterphase grating:

$$L(s,t) = L(s) \cdot L(t) = \cos f_s s \cdot \cos f_t t \qquad \text{Equation 1.09}$$

where f_s = spatial frequency and f_t = temporal frequency. Thus spatial contrast varies over time and temporal contrast varies over space (Figure 1.10). This makes it difficult to compare results obtained with grating stimuli with those using uniform fields (which have spatially constant temporal contrast). To overcome this problem some studies have used moving gratings, or travelling waves, described by the expression:

$$L(s,t) = \cos(f_s s + f_t t) \qquad \text{Equation 1.10}$$

Here each spatial position is flickered by the same amount. The two stimuli (phase-reversing and drifting gratings) are trigonometrically related by

$$2 \cdot \cos f_s s \cdot \cos f_t t = \cos(f_s s + f_t t) + \cos(f_s s - f_t t) \qquad \text{Equation 1.11}$$

In other words a counterphase grating may be regarded as the sum of two travelling waves of half amplitude, moving in opposite directions at the same speed.

If there were no spatiotemporal interaction in the visual system, then spatial and temporal responses would be separable as in Equation 1.09. That is, flicker sensitivity would be independent of spatial structure, and spatial contrast sensitivity would be independent of flicker frequency.

However, the first measurements of spatiotemporal contrast thresholds, by Robson (1966), showed that the combined threshold cannot be obtained by multiplying the two simple functions. At high temporal frequencies increasing spatial modulation has the effect of displacing the deLange curve downwards. At low temporal frequencies, however, increasing spatial frequency acts to increase sensitivity and eliminate the nonlinearity of the uniform - field deLange curve. This process is almost complete by 4 cycles$\cdot$deg^{-1}, and is consistent with Kelly's (1959) observation that low frequency flicker thresholds are lower with a large edgeless field (containing no high spatial frequencies) than with a small sharp - edged field (rich in high spatial frequency components). Interestingly, an exactly analogous effect is obtained when the effect of temporal modulation on spatial sensitivity is measured. Kelly (1966) plotted a complete spatiotemporal threshold surface for a wide range of frequency combinations, using his circular sinewave gratings, showing the same reciprocal interactions.

Using travelling wave stimuli van Nes et al (1967) measured thresholds that were qualitatively similar to those of Robson and Kelly, confirming their formal equivalence with modulation at a point. However, the first quantitative comparisons were not reported until eight years later, when Levinson and Sekuler (1975) compared sensitivity to drifting and flickering stimuli under identical conditions. They found that motion thresholds are consistently lower than flicker thresholds and suggested that, at least over a limited range of spatial frequencies, the two thresholds differ by a factor of two. This was interpreted as evidence of independent, direction - selective movement mechanisms (Equation 1.11). Kelly (1979b) measured threshold surfaces for flickering and drifting gratings over the entire visible spatiotemporal frequency range, using stimuli stabilised by a sophisticated eye-tracking system (Kelly, 1979a), and confirmed that the surfaces differed

by a factor of two. Although the spatial MTF changes shape as a function of temporal frequency, and vice versa, constant - velocity curves, representing a profile of the threshold surface taken at 45° to the frequency axes, all have an identical bandpass form above about 0.1 deg·s^{-1}. The gain at any given velocity and spatial frequency is obtained by two scaling factors: f_{max} gives the location (in spatial frequency), and S_{max} the height (in sensitivity units) of the peak of the bandpass function.

$$G(f,v) = S_{max} \cdot v \cdot f^2 \cdot e^{(-2f/f_{max})} \qquad \text{Equation 1.12}$$

where f = spatial frequency. The two constants were obtained by trial and error curve fitting as

$$S_{max} = 7.3[\log(v/3)]^3 + 6.1$$
$$f_{max} = 45.9 \,/\, (v + 2)$$

Equation 1.12 is consistent with the exponential square - root function of the diffusion model of flicker thresholds (Equation 1.07), being related by a 45° rotation in the frequency domain.

An elegant demonstration of the role of natural fixational eye movements in spatial vision is provided by the close matching of the unstabilised contrast sensitivity function (Kelly, 1979b) by the stabilised constant - velocity curve for 0.15 deg·s^{-1}, corresponding to the modal velocity of spontaneous drift movements. Hence threshold functions measured in unstabilised conditions do not lie parallel to the spatial frequency axis, as is commonly assumed, but at 45° to it. The complete theoretical spatiotemporal surface from Equation 1.12 is shown in Figure 1.11, together with a contour map of the same surface. This shows that the surface is nearly symmetrical about the 2 deg·s^{-1} diagonal, and it is

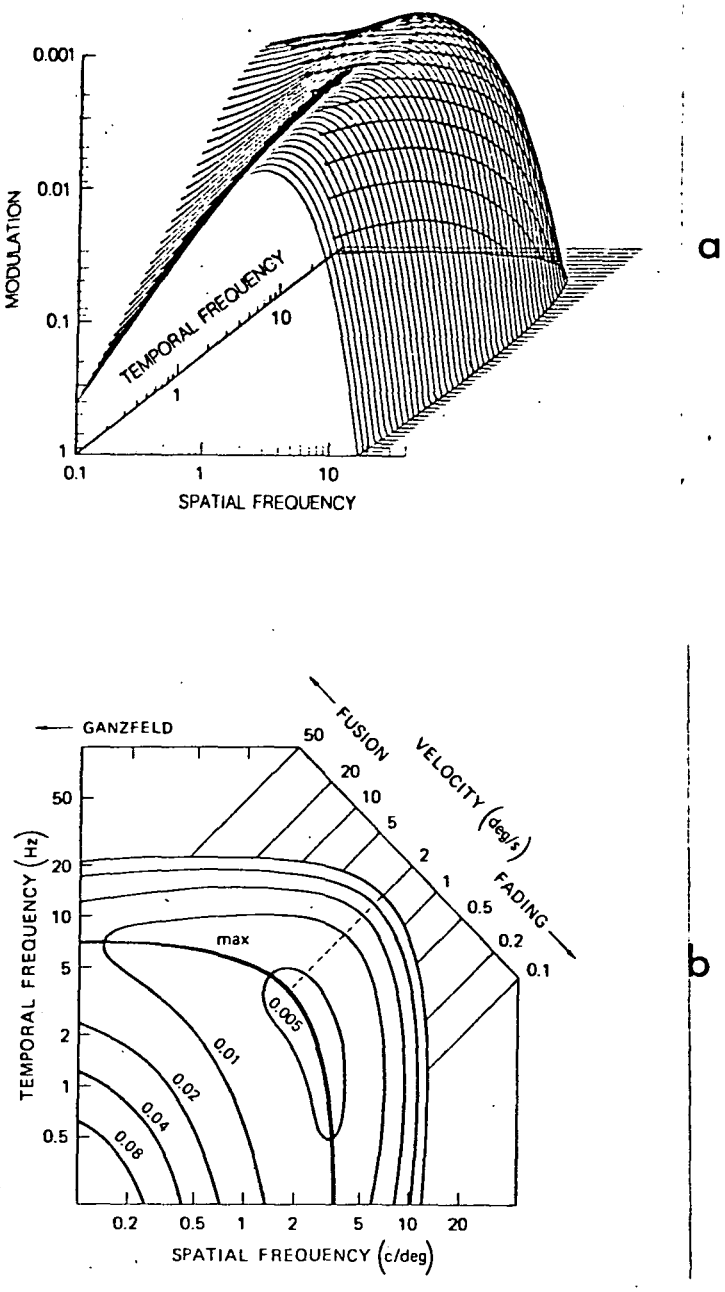

Figure 1.11 : (a) The spatiotemporal modulation threshold surface obtained by Kelly (1979b), using retinally stabilised moving gratings. The 3-dimensional function is derived from an analytical approximation to the empirical data.
(b) A contour map of the same surface. The heavy line marked 'max' represents the peak sensitivity at each velocity. Note that the surface is approximately symmetrical about the (dashed) diagonal marking 2 deg/sec.

possible that true symmetry would be obtained with more accurate stabilisation, having the effect of reducing the nominal velocities by a constant amount.

A theoretical model of the mechanisms underlying the threshold surface has also been developed. Burbeck and Kelly (1980) argue that their surface may be considered as the convolution of two independent or 'separable' mechanisms, one with a spatial response which is independent of temporal modulation, the other with a temporal response independent of spatial frequency. Each of these is further subdivided into two independent mechanisms: the 'excitatory' and 'inhibitory' systems, making four independent systems in all. The final surface represents the difference between the surfaces of the excitatory and inhibitory systems. These each exhibit approximately low-pass behaviour within each frequency domain, with the inhibitory system having a more rapid high frequency cut-off than the excitatory system. Thus, at sufficiently high frequencies, the excitatory system operates alone and the system as a whole displays simple low-pass behaviour. At lower frequencies the inhibitory system becomes progressively more sensitive and the compound response surface shows a dip. This elegant model of spatiotemporal interaction was developed to fit an analytical description of sensitivity to large, stabilised, sinewave gratings drifting at a constant velocity. It is not intended as a model of a physiological system, although Burbeck and Kelly note that the antagonistic interaction between excitatory and inhibitory systems has similarities to the centre - surround organisation of some receptive fields. Further developments of the model are necessary to include such parameters as adaptation level, stimulus size, eccentricity, and directional selectivity. However, at present the Burbeck - Kelly model represents the single most simple and complete theory of spatiotemporal interaction.

1.4 Present studies

Almost all studies on periodic or transient temporal modulations have been concerned with the analysis of the temporal behaviour of the visual system at a purely descriptive rather than at an explanatory level. The aim of the theoretical models derived from such studies is to give a description of as wide a set of data as possible, without claiming physiological relevance. Time - varying stimuli are used as methods of investigation, rather than being of intrinsic interest. This thesis attempts to reveal some of the processes underlying the analysis and detection of temporal contrast. Many of the techniques and concepts used have been developed over the past 15 years to study the processing of spatial contrast, and it is to underline the many parallels with the temporal domain, both methodological and conceptual, that the term 'temporal contrast' has been adopted. In spatial vision the introduction of systems analysis as a descriptive technique by Schade (1956) was followed 12 years later by its application in a model of spatial analysis (Campbell and Robson, 1968). Since that time the concepts of spatial frequency analysis have played a dominant role in visual psychophysics. Although the description of temporal response in systems analysis terms came earlier (deLange, 1952), this has not been followed by the development of explanatory models of temporal contrast analysis. This lack is one of the primary motivations behind the work contained in this thesis.

Purely time - varying stimuli are relatively rare in the natural environment. The investigation of temporal contrast should be seen within the context of spatiotemporal interactions, for example moving stimuli. A pattern moving across the retina will produce luminance changes over time

at each point. The problem of movement perception may thus be considered as the problem of organising the many localised temporal modulations into a global percept. The first stage of such a process is clearly the analysis of purely temporal changes, and the present studies are designed to investigate this stage.

The experimental work of the thesis is organised broadly into two groups of three chapters. The first group, Chapters 3 to 5, is concerned with the processing of periodic stimuli. In particular, it has recently been suggested that low spatial frequencies may be analysed into spatial luminance gradients, rather than into frequency components. McCann et al (1974) studied the visibility of single spatial luminance gradients superimposed on a uniform field, and found that thresholds were determined by contrast ($L_{max} - L_{min}$, measured in $cd \cdot m^{-2}$) and independent of gradient (contrast per unit of space: $cd \cdot m^{-2} \cdot deg^{-1}$). They were unable to account for the common finding (eg Campbell and Robson, 1968) that contrast sensitivity decreases at low spatial frequencies, rather than remaining constant as their findings on gradient detection would predict. However, this study failed to control for stimulus size, and Hoekstra et al (1974) showed that contrast sensitivity is independent of spatial frequency if grating width is adjusted so that the number of cycles remains constant. Returning to single spatial luminance gradients, van den Brink and Keemink (1976) showed that thresholds varied with stimulus size, so that contrast / width remains constant. In other words, gradient thresholds are determined by luminance gradient and not luminance contrast. They went on to suggest (van der Wildt, Keemink, and van den Brink, 1976) that a sinewave grating may be considered as a series of zones of linear gradients, equivalent to a single wide gradient field. They found that the entire contrast sensitivity function is predictable from the detection thresholds of linear gradients. A similar

conclusion was reached by Campbell, Johnstone, and Ross (1981; Ross and Johnstone, 1980) from a study of detection thresholds for gratings with a trapezoidal luminance profile. They found that doubling the ramp width in the trapezoid doubles the threshold amplitude, so that the gradient at threshold remains constant. With ramp widths less than 0.5°, however, threshold is independent of ramp width and equal to that of a squarewave grating (having a ramp width of zero). They suggested that the complete contrast sensitivity function is the envelope of the response curves of two mechanisms: one detecting luminance gradients across a field 0.5° wide, sensitive to low frequency sinewaves; the second, sensitive above about 1 cycle·deg^{-1}, comprising an array of frequency tuned channels (Campbell and Robson, 1968). It is interesting to note the similarities between this recent model of spatial analysis and the Roufs (1974a) model of 'swell' and 'agitation' channels for temporal analysis. The experiments in Chapters 3 to 5 are linked by the idea that the operation of a system detecting temporal luminance gradients may account for the various differences between high and low frequency flicker.

In the second group of chapters, 6 to 8, the detection of temporal transients is investigated. The techniques developed by Roufs to follow the internal responses to steps and pulses are extended to the analysis of nonabrupt transients, or luminance gradients. Roufs (1974a) has shown that steps and pulses are mediated by a linear bandpass filter corresponding to the high frequency portion of the deLange function. It seems likely that the second channel of the Roufs model (Figure 1.08) mediates the detection of nonabrupt transients. In the final chapter, Chapter 9, a theoretical model of the temporal contrast system is proposed, and its possible place in a model of spatiotemporal analysis is discussed.

CHAPTER 2

GENERAL METHODS

2.1 Subjects

In order to establish a pool of experienced psychophysical subjects, as well as to minimise the effect of individual differences, it was originally intended to use the same group of four subjects in all experiments. These observers - AS, APH, EAM, and SMC - were all postgraduate research students in the Psychology Department at Durham University. All four were used in Experiments 3.1, 3.2, and 4.1. SMC left the subject pool after Experiment 4.1 and was replaced by subject TJC, another research student, for Experiment 5.1. Only the three other subjects took part in Experiment 5.2. In Experiment 6.1 EAM was replaced by subject MJM, an experienced psychophysical observer. The lengthy and intensive nature of the experiments in Chapters 7 and 8 required that subjects be paid for their work, and for this reason only one other subject apart from the author was used: this was APH in Experiments 7.1 and 7.2 and a new subject, JMAH, in Experiment 8.1.

All subjects except the author were emmetropic and unaware of the hypotheses being tested. The author is an anastigmatic myope corrected by -1.5 D in each eye.

2.2 Apparatus

The visual display in all of the experiments consisted of a CRT display monitor, provided with high frequency rasters to both X and Y inputs to generate a uniform field. The luminance of this field was varied by a computer - generated voltage signal applied to the Z amplifier.

A Tektronix 602 display monitor (P31 phosphor) was used in Experiments 3.1 to 6.1 inclusive. The screen subtended 6.88° horizontal by 5.32° vertical at 91.5 cm from the subject, and was surrounded by an angled hood painted matt white and measuring 20.74° by 18.56°. The output luminance of the 602 is linear with Z amplifier input over the range 36 to 208 $cd \cdot m^{-2}$, with a mean luminance of 122 $cd \cdot m^{-2}$.

A Tektronix 603 storage monitor (P31 phosphor) was used for the experiments in Chapters 7 and 8. The screen was masked with black card to give a circular black field 5° in diameter at 114.6 cm from the subject. The output of the 603 is linear over the range 1.99 to 11.49 $cd \cdot m^{-2}$, with a mean luminance of 6.74 $cd \cdot m^{-2}$.

The vertical raster in all experiments was a 1.2 MHz sawtooth waveform, provided by a function generator (Feedback Instruments, model TWG 501). The horizontal raster was taken from the sweep output of a Telequipment D83 oscilloscope, with a frequency (frame rate) between 50 Hz and 5 kHz. Details of the frame rate used in each experiment are given in the separate Apparatus sections.

The luminance functions were generated by a Computer Automation LSI 2/20 minicomputer, digitised at the same frequency as the horizontal raster. The functions were applied to the Z input of the display monitor

through a digital - analogue converter (Cambridge Electronic Design, model 502 interface), having 9 bit resolution over the amplifier's linear range. The Z amplifier update was synchronised by the computer with the triggering of the display sweep, so that the screen maintained a constant luminance during each frame.

The effect of digitisation on the spectral content of a periodic function is to create sidebands at $\pm$ the fundamental frequency around the sampling frequency (and its harmonics). The lowest frequency sidebands will thus occur with the highest flicker frequency and the lowest sampling frequency. With the 50 Hz frame rate used in Experiment 4.1, a digitised 16 Hz sinewave will contain frequency components at $50 \pm 16 = 34$ and 66 Hz with an amplitude 0.47 times that of the fundamental. The 34 Hz sideband is 1.7 log units below threshold when the fundamental is at threshold, calculated from the theoretical threshold function of Levinson and Harmon (1961), making the digitised waveform indiscriminable from a true sinewave.

The computer also controlled trial presentations, signalled the various phases of the experiment to the subject via red LEDs mounted on the response box and the display surround, and recorded and analysed responses. The screen was viewed binocularly in all experiments, either through natural pupils or through 3mm diameter artificial pupils ($1 \text{ cd} \cdot \text{m}^{-2} = 7.07$ td). The testing room was in complete darkness except for the display screen. Fixation was maintained at all times upon a black spot in the centre of the screen, with the head supported by a chinrest.

The Apparatus sections of each Experiment give details of specific variations to this general design, including factors such as frame rate, response apparatus, and viewing conditions.

CHAPTER 3

IS FLICKER ANALYSED BY LUMINANCE GRADIENTS OR FREQUENCY?

3.1 Introduction

The fundamental theme of this and the following two Chapters is the distinction between flicker frequency and the rate of change of luminance. The rate of change is the slope of the flicker waveform, and will often be referred to as luminance velocity (by analogy with the spatial domain), measured in $cd \cdot m^{-2} \cdot s^{-1}$. In conventional flicker waveforms the effects of flicker frequency and luminance velocity are confounded. It is therefore interesting to ask how far the effects of frequency change are attributable to change in slope.

The possible importance of such a distinction lies in the many differences which have emerged in the visual system's response to high and low frequency flicker. Roufs (1974a) concluded that the deLange curve constituted the envelope of the response functions of two parallel systems: a bandpass filter sensitive to high frequency (HF) flicker and abrupt transients, and a low-pass filter sensitive to low frequency (LF) sinewaves. This distinction at a theoretical level parallels the many empirical differences in HF and LF threshold behaviour, reviewed in Section 1.1.3. In essence, HF thresholds are predictable from a linear systems model, but the system becomes increasingly nonlinear as frequency is reduced and threshold

becomes dependent on mean luminance. In addition, spatial variables such as size and spectral composition affect only low frequency sensitivity. These differences, together with the LF nonlinearity, suggest that systems analysis may not provide the most appropriate characterisation of low frequency behaviour.

As a first step towards a qualitative analysis of flicker processes it was decided to investigate the possibility that the low frequency system is sensitive not to the frequency of the flicker signal but to the rate of luminance change within the waveform. That is, whether the appropriate level of analysis lies in the temporal rather than the frequency domain.

In a conventional flicker stimulus the luminance velocity, ie the slope of the waveform, varies as a function of both frequency and amplitude. Since it was decided to adopt the convention of measuring flicker sensitivity using amplitude as the dependent variable, the two experiments described in this chapter both use a novel flicker stimulus designed to dissociate slope and amplitude. The essentials of the technique, explained in Figure 3.01, lie in taking a basic triangular waveform, chosen to contain only one velocity component in each direction, and progressively clipping the peaks until the threshold amplitude is reached. In this way the gradient of the slope is maintained, although its duration decreases. Experiment 3.1 uses the clipped trapezoidal waveform at a number of adaptation levels. The established result with sinewave flicker (Kelly, 1961a) is that mean luminance affects LF but not HF thresholds. It is therefore interesting to ask whether the same pattern is obtained when the waveform maintains a ramp at low frequencies, and thus to obtain information about the luminance - dependent performance of any system sensitive to the ramp component. In addition, as will be shown in Section 3.2.2, the conditions

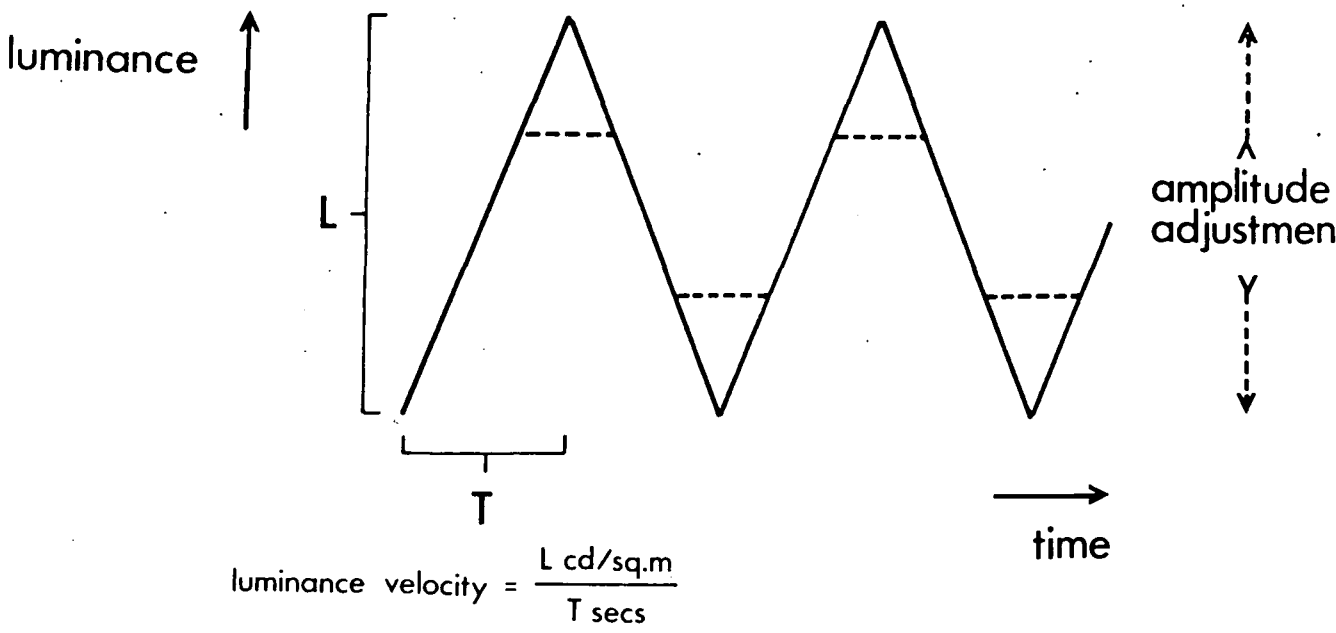

Figure 3.01 : The flicker waveform used in Experiments 3.1 and 3.2. The triangular function has a constant rate of change of luminance, or 'luminance velocity', measured in $cd.m^{-2}.sec^{-1}$. Amplitude is varied by clipping the peaks, so that both fundamental frequency and luminance velocity remain unchanged.

chosen allow a preliminary comparison between waveforms with similar slope but different frequency.

The second experiment in the chapter looks at this latter factor in a more systematic way. If low frequency flicker is detected on the basis of its temporal profile, we would expect threshold to vary as a function of luminance velocity, but be independent of frequency. On the other hand, if the system is primarily interested in the frequency content of the stimulus, the opposite pattern of results should emerge, with sensitivity dependent on fundamental frequency but independent of velocity. As pointed out above, conventional flicker studies are unable to discriminate between these possibilities since velocity covaries with the dependent variable. Experiment 3.2 answers this question by measuring flicker thresholds with a matrix of frequency and velocity conditions.

3.2 Experiment 3.1

3.2.1 Apparatus

The general details of the visual display are given in Chapter 2. The frame rate of the display was 5 kHz. Modulation depth was controlled by the subject via an adjustable voltage source, read through the interface's A-D converter. The computer also controlled trial presentations and recorded and analysed threshold estimates. Subjects viewed the screen binocularly through 3 mm diameter artificial pupils (1 $cd \cdot m^{-2}$ = 7.07 td) (Figure 3.02). Adaptation level was varied by placing neutral density filters

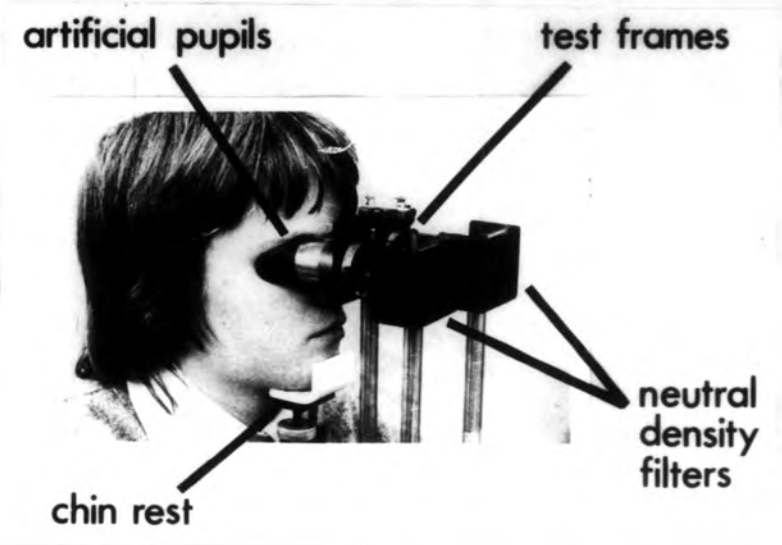

Figure 3.02 : The viewing apparatus for Experiment 3.1. The binocular artificial pupils are fully adjustable to allow both images to be centred on the foveae. Test frames mounted in front allow the appropriate optical corrections to be made for subjects who normally wear glasses. Adaptation level was varied by means of neutral density filters. Since the testing room was in darkness except for the display screen, additional shielding was necessary to eliminate unwanted reflected light - this has been removed in the photo to show the apparatus more clearly.

in front of each eye, together with additional shielding to avoid reflected light reaching the subject. A pair of test frames mounted in front of the artificial pupils allowed optical correction to be provided for those subjects who required it.

3.2.2 Design and Procedure

Thresholds were measured over 4 octaves of frequency from 1 to 16 Hz, at 1/3 octave intervals. The unfiltered screen plus neutral density filters of 1, 2, 3, and 4 log units absorption gave 5 adaptation levels from 0.0862 to 862 td. The peak - peak amplitude of the unclipped triangular waveforms, measured at the screen, was kept constant at 173 $cd \cdot m^{-2}$, with the result that the slope of the waveform varied with both frequency and adaptation condition. As frequency increases the duration of each half-cycle decreases, increasing the slope. As filter absorption increases, the amplitude of the stimulus decreases, decreasing the slope. Although it was not the purpose of this experiment to control luminance velocity, the actual velocities used (in $td \cdot s^{-1}$) are shown in Table 3.01. It may be seen that each waveform has roughly the same slope as that of the waveform 1 log unit darker and 3.33 octaves higher in frequency. This correspondence therefore produces some preliminary data on the effects of velocity independent of frequency, studied more systematically in the second experiment.

Each session consisted of 5 minutes adaptation to the mean luminance of the display, then the 13 frequency conditions were presented and flicker thresholds obtained by the method of adjustment. Each trial consisted of 5 seconds of no flicker, followed by a period of up to 10 seconds during

Frequency	Mean luminance (td) 862	86.2	8.62	0.862	0.0862
1.00	2449.2	244.9	24.5	2.4	0.2
1.23	3085.8	308.6	30.9	3.1	0.3
1.59	3887.9	388.8	38.9	3.9	0.4
2.00	4898.4	489.8	49.0	4.9	0.5
2.52	6171.6	617.2	61.7	6.2	0.6
3.17	7775.7	777.6	77.8	7.8	0.8
4.00	9796.8	979.7	98.0	9.8	1.0
5.04	12343.2	1234.3	123.4	12.3	1.2
6.35	15551.4	1555.1	155.5	15.6	1.6
8.00	19593.6	1959.4	195.9	19.6	2.0
10.08	24686.4	2468.6	246.9	24.7	2.5
12.70	31102.0	3110.3	311.0	31.1	3.1
16.00	39187.1	3918.7	391.9	39.2	3.9

Table 3.01 : Slope of waveform (in td.sec^{-1}) in each condition of Experiment 3.1. The conditions marked have approximately the same luminance velocity but different temporal frequency.

which the subject varied the amplitude of flicker by means of an adjustment knob until flicker was at threshold. Each threshold estimate was signalled by pressing a button, which immediately initiated the next trial. If a threshold failed to be set within 10 seconds the trial was repeated. In the first half of the session the conditions were presented in order of increasing frequency, with the subjects instructed to reduce amplitude from maximum until flicker was just undetectable. After the 13th condition the subject was allowed to rest before repeating the conditions in reverse order, this time increasing amplitude from zero until flicker was just detectable. Five threshold estimates were made in each half for each condition, thus the final threshold is the mean of ten estimates. Each session contained only a single adaptation condition, with the conditions carried out in order of decreasing mean luminance. The order of conditions was the same for all four subjects.

3.2.3 Results

Threshold amplitude (ΔL_c) for clipped triangular flicker as a function of frequency is plotted in Figures 3.03 (individual subjects) and 3.04a (group mean). A simple pattern of results emerges which is similar for all subjects: below a certain critical frequency threshold is independent of frequency, and varies only with adaptation level. Log threshold is a linear function of log luminance, with a slope of less than 1 :

$$\Delta L_c = L_{mean}^{0.82} / 23.88 \qquad \text{Equation 3.01}$$

This function is a very good fit to the data from 1 to 5.04 Hz, accounting for over 98% of the variance across all subjects. The critical frequency, or

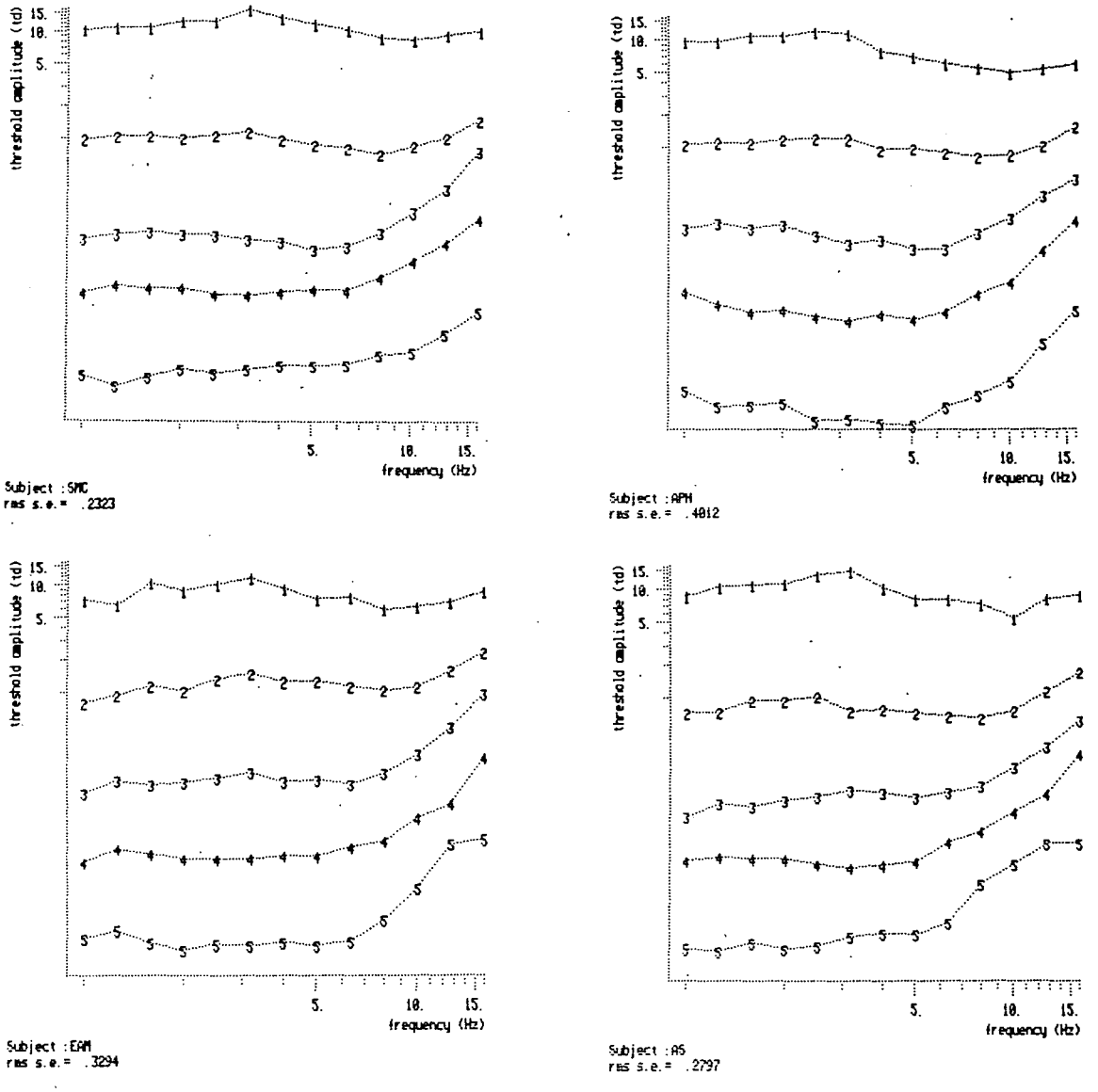

mean luminance (td)

1·····1	862
2·····2	86.2
3·····3	8.62
4·····4	0.862
5·····5	0.0862

Figure 3.03 : Threshold amplitude as a function of frequency in the five adaptation level conditions of Experiment 3.1. The graphs show the data from each of the four subjects. Error bars have been omitted for the sake of clarity, but the mean standard error is shown under each graph. Note that the amplitude plotted is that of the waveform itself, not of the fundamental.

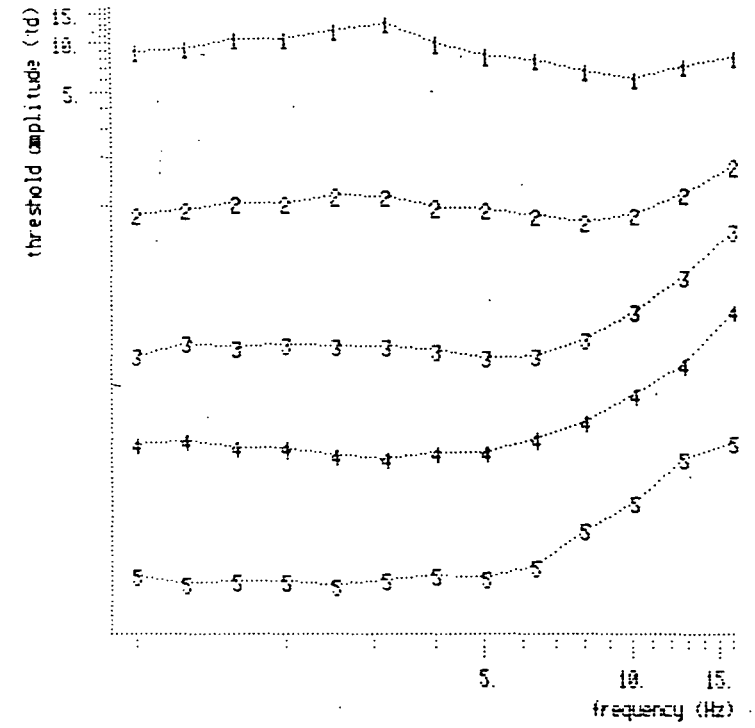

a

mean luminance (td)

1·····1	862
2·····2	86.2
3·····3	8.62
4·····4	0.862
5·····5	0.0862

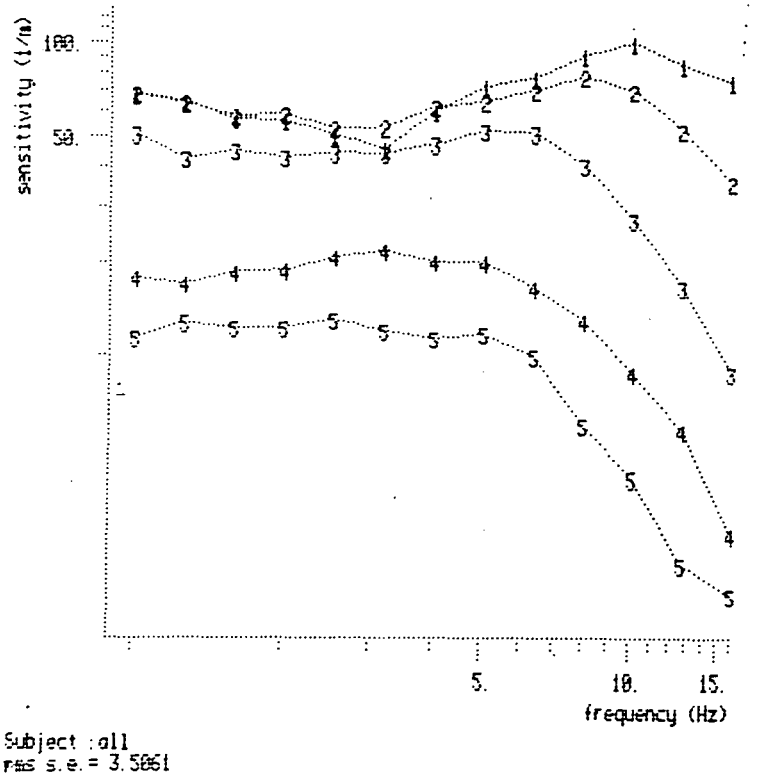

b

Figure 3.04 : (a) Mean threshold amplitude curves for trapezoidal flicker at five adaptation levels (average of four subjects).
(b) The same data replotted as sensitivity (the reciprocal of modulation). Modulation is a dimensionless measure expressing amplitude as a proportion of mean level.

inflection point, appears to increase with adaptation level. Above this point threshold increases with frequency, and the curves show signs of convergence. Without data from higher frequencies it is not possible to determine whether the functions are actually converging, ie show positive acceleration, or whether threshold is a simple linear function of frequency. However, an analysis of variance (Table 3.02) shows not only the expected main effects but also a highly significant interaction, indicating a change in form of the function with L_{mean}. The main purpose of this experiment is a comparison between trapezoidal flicker, in which the slope of the waveform is maintained as amplitude is reduced, and conventional sinewave flicker, in which luminance velocity decreases with amplitude. To facilitate this comparison, the data were replotted in terms of sensitivity (the reciprocal of threshold modulation). This is shown in Figures 3.04b (mean data) and 3.05 (individual subjects). Plotted in this way, the data show many of the features of the sinewave MTFs reported by deLange (1958, Figures 5 and 6) and Kelly (1961a, reproduced in Figure 1.03). Quantitative differences in the present data may be attributable to uncontrolled factors such as stimulus size and surround, and differences in psychophysical procedure. At high adaptation levels (curve 1) the functions display a sensitivity peak, which becomes less marked and moves to lower frequencies as luminance is decreased. Between 1 and 5 Hz sensitivity is independent of frequency, and down to 8.62 td appears also to be independent of L_{mean}. At lower levels low frequency sensitivity is reduced. DeLange (1958) suggested that the final value of the LF asymptote is a function of L_{mean} at all levels, whereas Kelly (1961a) claimed that this effect is only obtained at scotopic levels.

The apparent differences between the thresholds plotted in absolute (Figure 3.04a) and relative (Figure 3.04b) terms deserve further comment.

	Source	df	F	p
main effects	1.Frequency	12,36	38.1578	<0.00001
	2.Mean luminance	4,12	958.6737	<0.00001
interactions	1 x 2	48,144	21.8800	<0.00001

Table 3.02 : Analysis of variance on the amplitude threshold data in Figure 3.03.

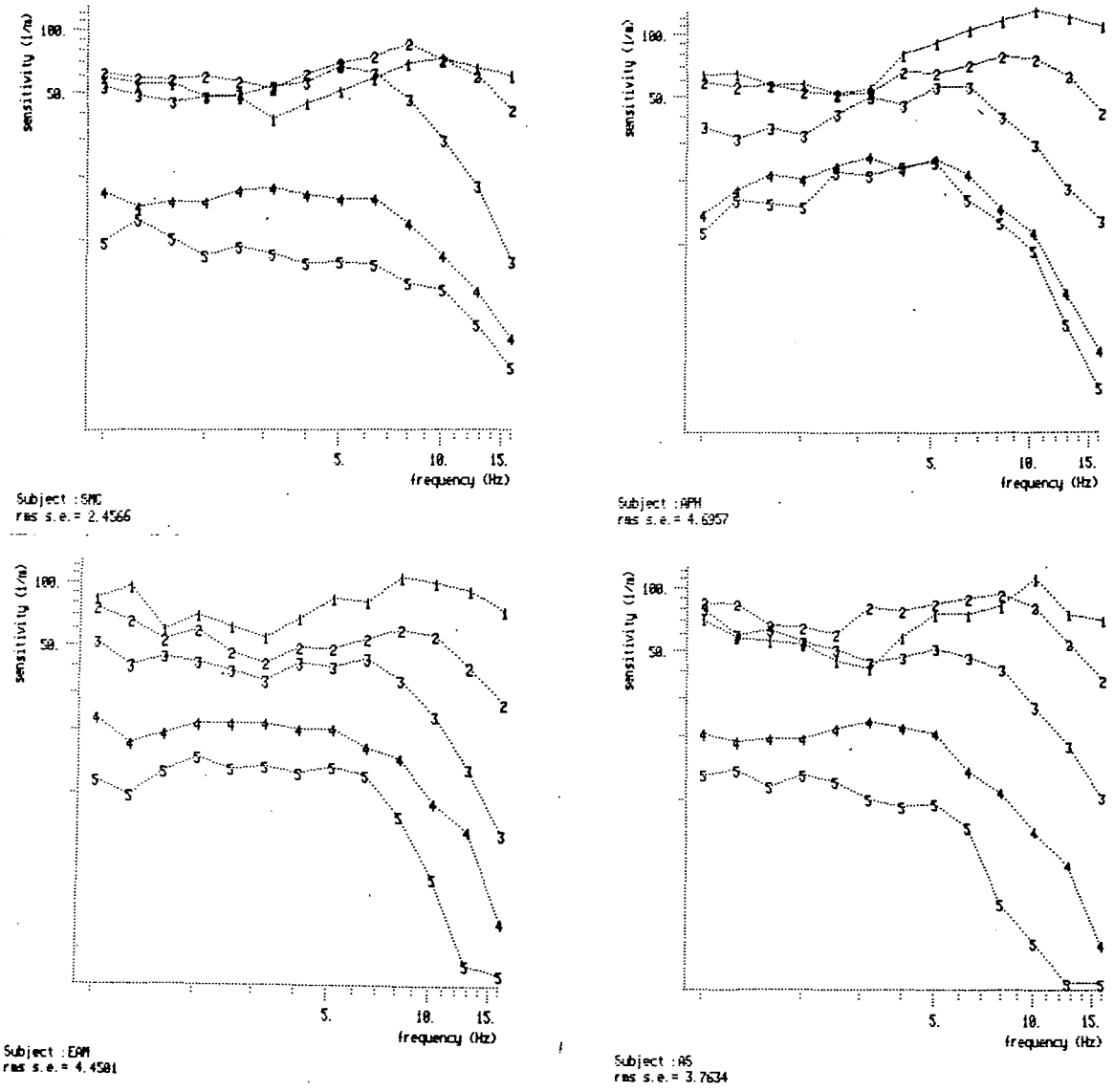

mean luminance (td)	
1·····1	862
2·····2	86.2
3·····3	8.62
4·····4	0.862
5·····5	0.0862

Figure 3.05 : The individual amplitude threshold data of Figure 3.03 replotted in terms of sensitivity.

The five levels of L_{mean} are separated by 1 log unit of luminance. If the five threshold curves in Figure 3.04a were also separated by 1 log unit, that is if the exponent of the right-hand term in Equation 3.01 were equal to 1, then the sensitivity curves in Figure 3.04b would lie on top of one another. Since the log L_{mean} vs log ΔL_c function has a slope of <1, the sensitivity curves tend to be displaced downwards (a slope of >1 would result in upward displacement). L_{mean} and ΔL_c are extremely highly correlated up to 5 Hz, with no systematic deviations. This suggests that the apparent discrepancy between the two figures is an artifact of the graphical representation: logarithmic scaling tends to minimise differences at high levels. Although the consequences of this effect are opposite on the two graphs they are not equal, by virtue of the fact that there are more data points at high levels in Figure 3.04b. The strong conclusion drawn from numerical analysis is that the curves in Figure 3.04a are displaced vertically at low frequencies by 0.82 log units; similarly the curves in Figure 3.04b are displaced by 1 - 0.82 = 0.18 log units.

This observation is contrary to Kelly's (1961a) findings for sinewave flicker, but in agreement with deLange (1958). At low frequencies, and thus also at low velocities, thresholds are not completely independent of adaptation level. The slight dependence on mean luminance is robust and holds over 4 log units, accounting for over 98% of the variance. However, the same analysis shows that threshold is independent of frequency, and thus of luminance velocity, up to 5 Hz. This finding is underlined by the fact that there is no correspondence between thresholds for stimuli of different frequency but similar slope, identified in Table 3.01. Since it is unlikely that a system sensitive to the ramp component is equally sensitive to such a wide range of gradients, the overall conclusion must be that the stimuli used in this experiment are not detected at threshold on the basis of

their slopes. As amplitude is reduced the ramp becomes shorter in duration, and at some point will fall within the temporal window of the gradient detection system. [Cf the minimum gradient width of 0.5° required by the Campbell, Johnstone, and Ross (1981) spatial luminance gradient system, mentioned in Chapter 1.] It seems likely that ramps shorter than the critical duration will be detected instead by a system sensitive to steps and other fast transients. In the next experiment velocity and frequency are independently varied so as to investigate more thoroughly the possible influences of velocity.

3.3 Experiment 3.2

3.3.1 Apparatus

The CRT display was the same as that described for the last experiment in Section 3.2.1. Since the same adaptation level (122 $cd \cdot m^{-2}$) was used throughout the experiment, artificial pupils were not used.

3.3.2 Design and Procedure

Flicker thresholds were measured over a 4 octave range of both frequency and velocity, at 1/2 octave intervals. Thus the nine frequencies, from 1 to 16 Hz, and nine velocities, from 279 to 4471 $cd \cdot m^{-2} \cdot s^{-1}$, form a matrix of 81 flicker conditions. The 5 kHz frame and digitisation rate was the fastest obtainable with the display program, and was chosen to ensure

the most accurate reproduction of the highest velocity. In this condition the ramp is output in steps of just under 0.9 $cd \cdot m^{-2}$. For just over half the conditions, ie the low frequency / high velocity conditions, the amplitude of the basic triangular waveform was greater than the luminance range of the oscilloscope, so that the waveform was clipped to the maximum obtainable amplitude (173 $cd \cdot m^{-2}$ peak-peak) before being presented to the subject.

The structure of both individual trials and the complete session were essentially the same as in Experiment 3.1. 10 conditions from the condition matrix were presented in each session (11 conditions in the last session). Each of the four subjects started the condition matrix from a different corner and progressed through the conditions in a different order.

3.3.3 Results

Flicker sensitivity (the reciprocal of threshold modulation) vs frequency curves in all nine velocity conditions are plotted in Figures 3.06 (individual subjects) and 3.07a (mean across subjects). All the curves have the general form of the sensitivity function of condition 1 in Figure 3.04b, the highest luminance condition of Experiment 3.1. The nine velocity conditions are plotted together, showing that velocity appears to have little systematic effect on threshold. However, an analysis of variance performed on the data (Table 3.03) shows significant main effects of both frequency and velocity, together with a highly significant interaction. This interaction is largely due to the 16 Hz condition, which is unusual in showing a simple monotonic ordering of threshold with velocity. While this effect is interesting, it is untypical of the rest of the data, and since we are

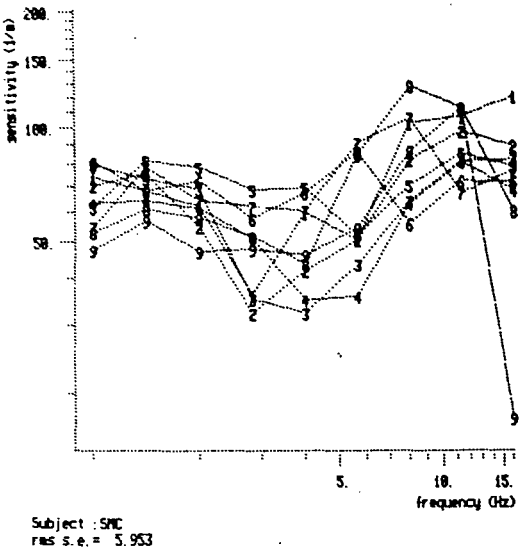

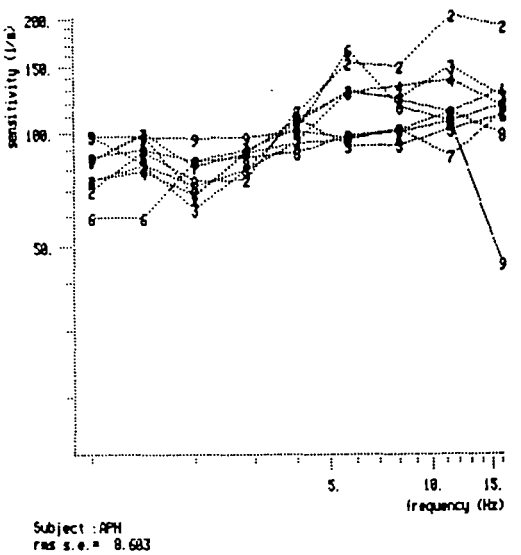

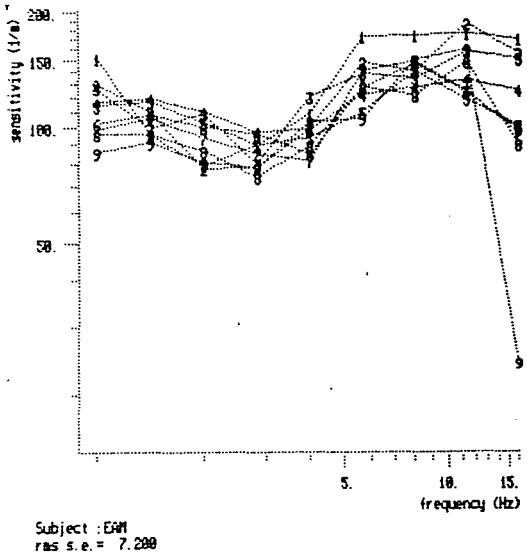

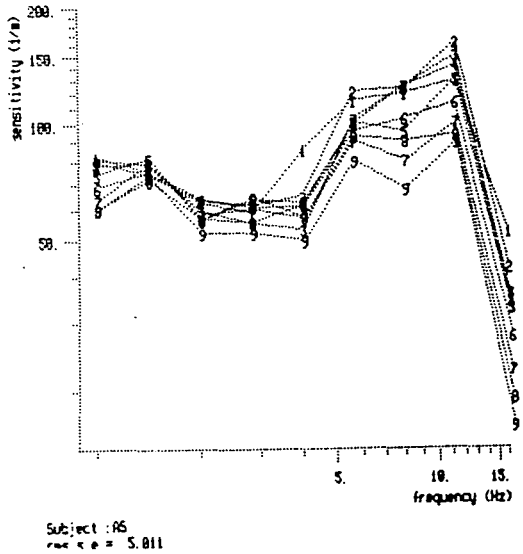

velocity	(cd m^{-2} s^{-1})
1·····1	279
2·····2	395
3·····3	559
4·····4	790
5·····5	1118
6·····6	1581
7·····7	2236
8·····8	3162
9·····9	4471

Figure 3.06 : Flicker sensitivity of each subject in all conditions of Experiment 3.2, plotted as a function of frequency with velocity as the parameter. Once again error bars have been omitted from the graph and the mean standard errors shown underneath.

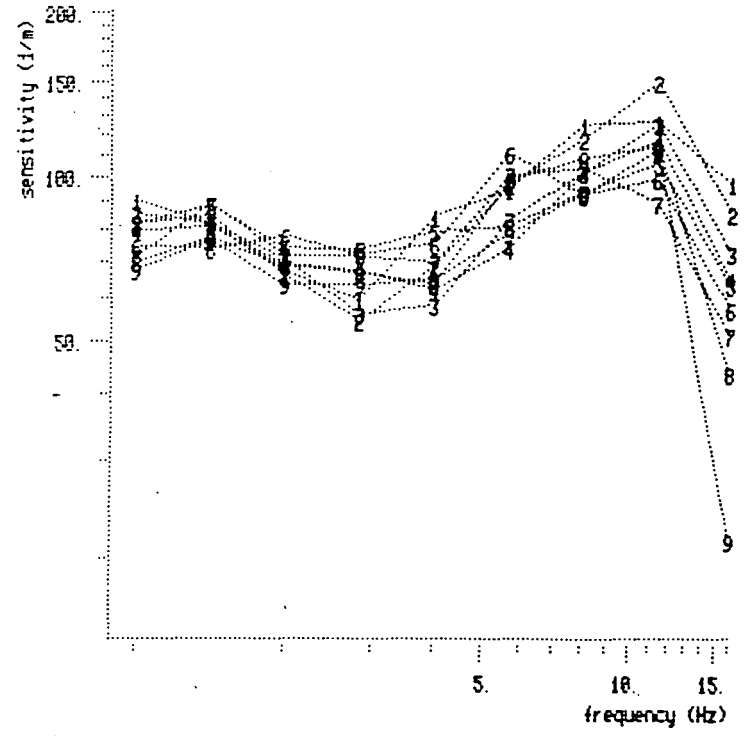

a

frequency (Hz)

1·····1	1.00
2·····2	1.41
3·····3	2.00
4·····4	2.83
5·····5	4.00
6·····6	5.66
7·····7	8.00
8·····8	11.31

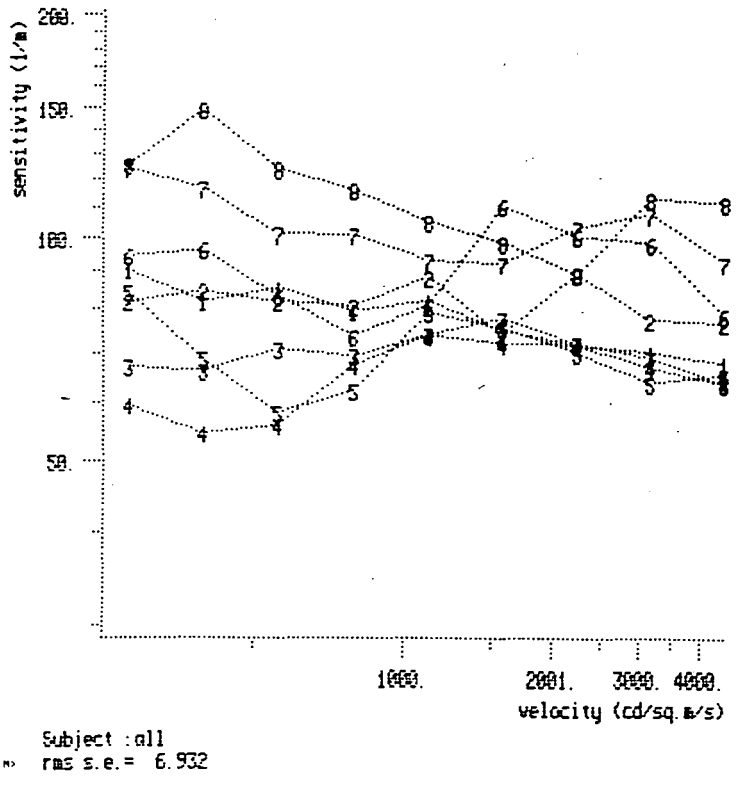

b

Figure 3.07 : (a) Mean flicker sensitivity across four subjects in Experiment 3.2.
(b) The same data replotted as a function of velocity, with frequency as the parameter. The 16 Hz condition (curve 9) was omitted at this stage since it was clearly different from the other conditions, showing a rising trend of sensitivity with velocity.

	Source	df	F	p
main effects	1.Velocity	8,24	4.5822	0.002
	2.Frequency	8,24	3.9939	0.00418
interactions	1 x 2	64,192	4.5185	<0.00001

Table 3.03 : Analysis of variance on the sensitivity data from Experiment 3.2 in Figure 3.06, all conditions.

	Source	df	F	p
main effects	1.Velocity	8,24	1.1565	0.36397
	2.Frequency	7,21	12.6905	0.00002
interactions	1 x 2	56,168	1.6084	0.01104

Table 3.04 : Analysis of variance on the sensitivity data from Experiment 3.2, 16 Hz condition removed.

primarily interested in low frequency processing it was decided to omit this condition from further analyses.

Repeating the analysis of variance with the 16 Hz condition removed (Table 3.04) reveals that although the main effect of velocity has disappeared, a significant interaction remains. The nature of this interaction is shown by replotting the data as a function of velocity, with frequency as the parameter - Figures 3.07b (mean data) and 3.08 (individual subjects). The resulting pattern of results is fairly complex, although essentially similar for all subjects. The insignificant main effect of velocity is due to opposite effects at different frequencies, leaving little or no net effect when averaged. As velocity increases, the extent to which the curves are spread out changes, although there is relatively little crossing over. That is, the relative order of frequencies remains unchanged but the absolute difference between them varies with velocity. The nonmonotonic function obtained when sensitivity is plotted against frequency (Figure 3.07a) shows how the relative ordering of frequencies in Figure 3.07b is derived. By varying the spread of curves, velocity is acting as a scaling, or gain, factor on the basic deLange function. This principle is illustrated in Figure 3.09. It should be emphasised that this is merely a hypothetical representation, illustrating the case where the scaling factor decreases monotonically with velocity. In fact, as will be seen, the scaling factor is a quadratic function of velocity. The hypothesis of velocity - dependent scaling may be tested by computing a gain factor according to the following algorithm:

$$G(v) = \frac{S_v - S_{v9}}{S_{v1} - S_{v9}} \qquad \text{Equation 3.02}$$

where S = sensitivity, v = velocity, v1 is the lowest velocity tested, and v9

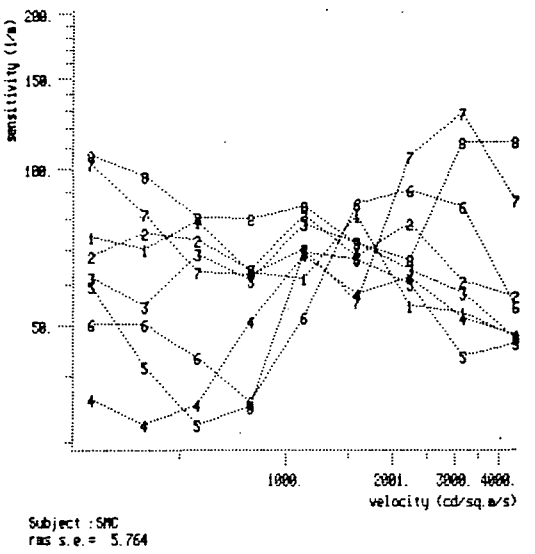

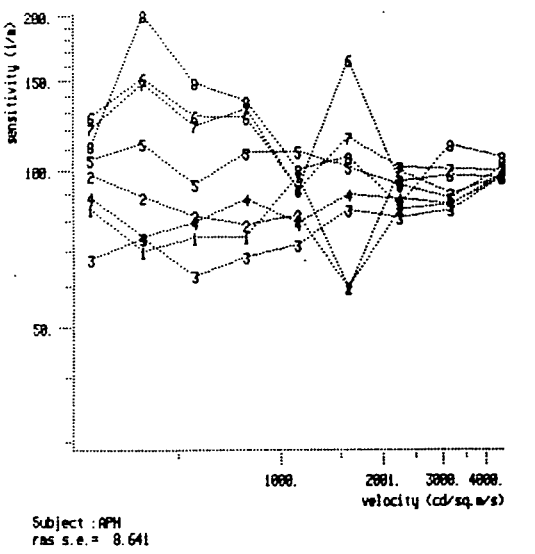

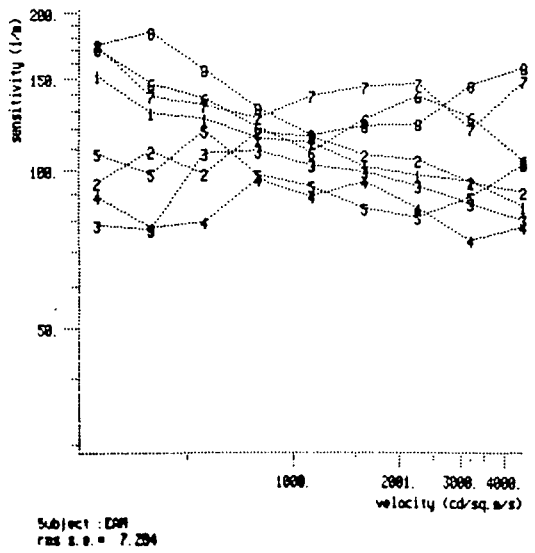

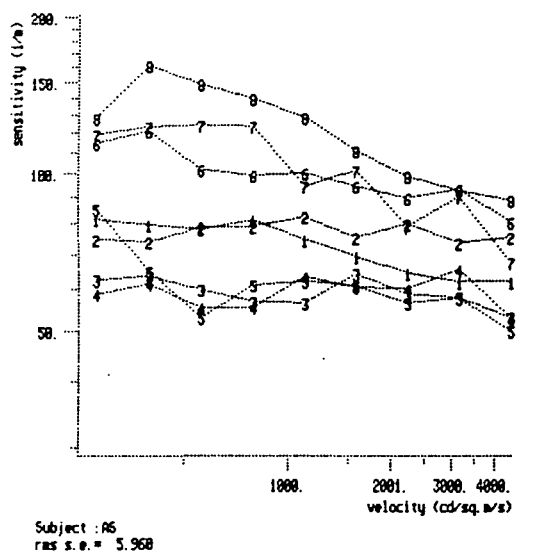

frequency	(Hz)
1·····1	1.00
2·····2	1.41
3·····3	2.00
4·····4	2.83
5·····5	4.00
6·····6	5.66
7·····7	8.00
8·····8	11.31

Figure 3.08 : The individual sensitivity curves of Figure 3.06 replotted as a function of velocity, with separate curves for each frequency.

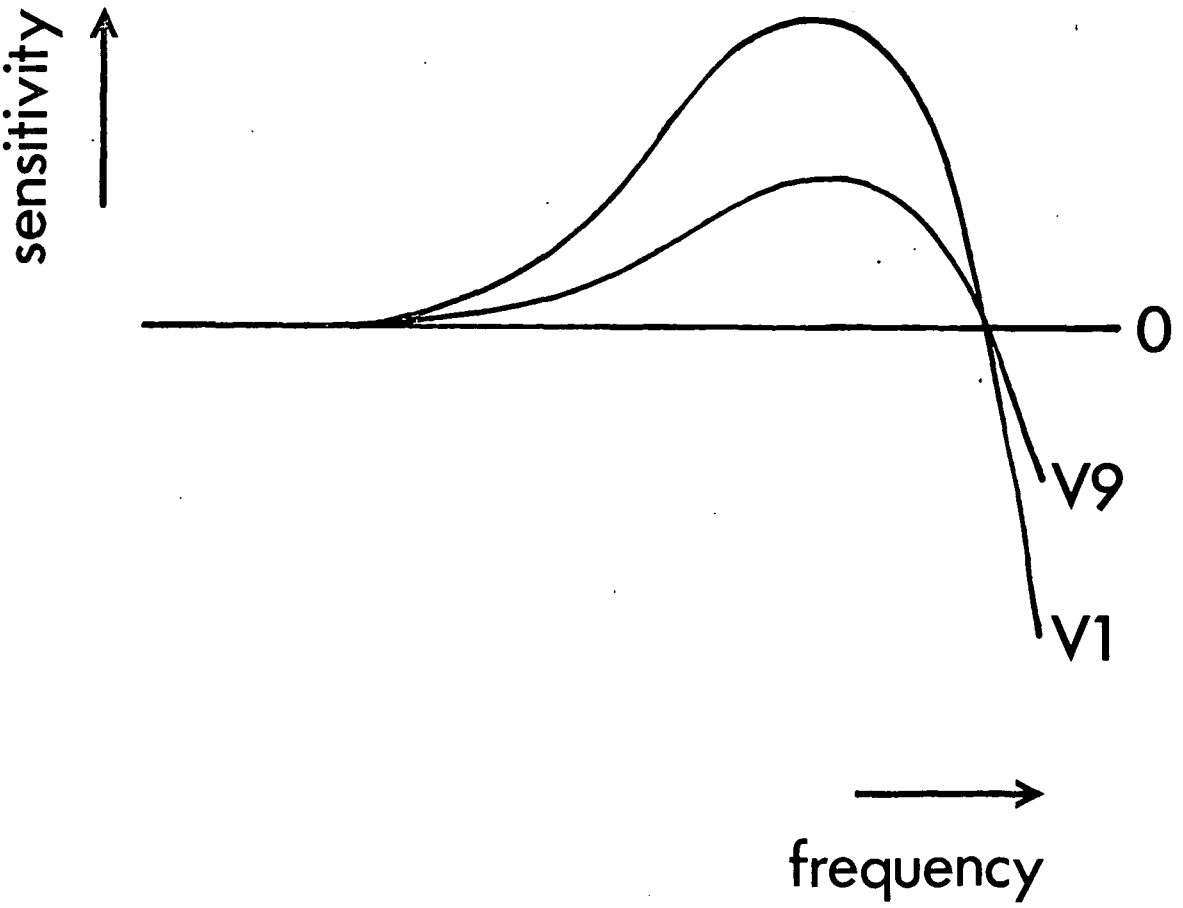

Figure 3.09 : Hypothetical analysis of the interaction between frequency and velocity. Velocity acts as a scaling factor on the basic deLange flicker sensitivity function. This illustrates the case where the scaling factor decreases as velocity increases from V1 to V9. As the scaling factor decreases the sensitivity function becomes flatter: when the scaling factor is at absolute zero threshold is independent of frequency. Thus the extent to which threshold is dependent on frequency varies as a function of velocity.

the highest velocity tested. The coefficient obtained is a measure of the gain relative to that at the two arbitrary fixed points, the lowest velocity (gain = 1) and the highest velocity (gain = 0). This gain function is plotted in Figure 3.10, together with the best fitting quadratic curve. As gain is reduced and the deLange curve becomes flatter, threshold becomes less dependent on frequency. The velocity - dependent scaling factor means that the extent to which sensitivity varies with frequency is determined by velocity. The U-shaped function in Figure 3.10 shows that the scaling factor is not linearly related to velocity. At about 1500 $cd \cdot m^{-2} \cdot s^{-1}$ threshold is maximally independent of frequency; above and below this point frequency is increasingly important.

3.4 Discussion

Experiments 3.1 and 3.2 both measured simple flicker thresholds to investigate whether the visual system is sensitive to the rate of luminance change within the flicker waveform. The first experiment measured thresholds for trapezoidal flicker at a number of adaptation levels. It was found that low frequency thresholds are dependent on mean luminance: threshold decreases with L_{mean}, but slightly less than predicted by a model of complete dependence. Two major studies of sinewave flicker have reached contradictory conclusions about the effect of adaptation level at low frequencies. It seems likely that Kelly's (1961a) finding that threshold is dependent on L_{mean} at photopic levels and independent of it at scotopic levels is the most complete explanation. The data of the first experiment appear to show a similar division, but closer analysis reveals a constant

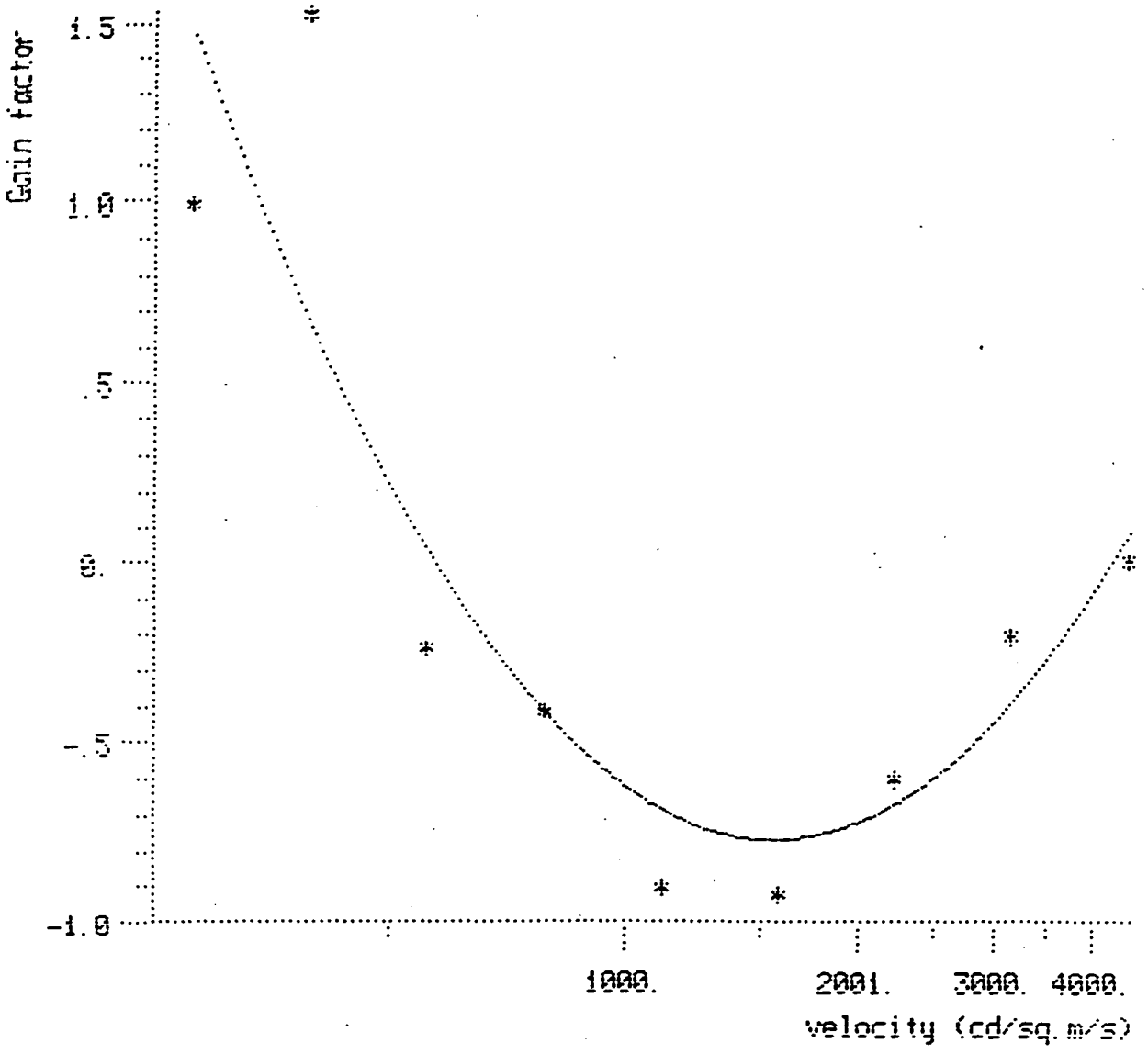

Figure 3.10 : The empirical scaling factor as a function of velocity. Scaling factors were computed • from Equation 3.02, taking each frequency separately then averaging to give a single figure for each velocity curve. The scaling, or 'gain', factor is not an absolute measure but is defined relative to the gains at the lowest (gain = 1) and highest (gain = 0) velocities. The main effect of velocity is significant ($F(8,24) = 2.94$, $p < 0.02$). The best fitting quadratic curve through the points has the form $Y = 4.03X^2 - 25.72X + 40.27$, where X = log velocity. Higher order components are not significant, $p > 0.65$. Only the means of the four subjects have been plotted, for the sake of clarity.

Figure 3.09 illustrated the effect on sensitivity of a scaling factor which decreased monotonically with velocity. This Figure shows that the obtained function is not as simple as this, with the deLange curve being flattest at midrange velocities.

trend across the 4 log units of luminance tested. The partial independence of threshold from adaptation level is thus not completely consistent with Kelly's model, but it is not possible to conclude that this is due to the nature of the waveform. More importantly, below 5 Hz threshold is largely independent of frequency, and hence also of velocity, because of the design of the waveform. This suggests that the ramp component of the trapezoid is not being detected by any system sensitive to non-abrupt transients. Rather, it seems likely that at threshold the ramps are short enough to be detected as steps, thus invalidating any possible conclusions about the luminance - dependent performance of a ramp detector.

In the second experiment the frequency and slope of the trapezoidal waveform were independently varied so as to look more closely at the possible effect of velocity on flicker thresholds. A significant interaction between the two variables was observed, indicating that the visual system is sensitive to velocity. In essence, velocity affects the degree to which threshold is dependent on frequency. As velocity changes, the deLange curve undergoes scaling so that threshold changes by a greater or lesser amount with frequency. The size of this effect seems to be independent of frequency, so that all parts of the deLange curve are scaled equally. Moreover, the scaling factor is a nonlinear function of velocity, reaching a minimum at about 1500 $cd \cdot m^{-2} \cdot s^{-1}$. All the conditions in this experiment were carried out at the same adaptation level: it may be interesting to look at how (or if) the form of the scaling function changes with L_{mean}.

It is possible to account for the findings of Experiment 3.2 within the electrical analogue models described in Chapter 1 by the inclusion of a separate velocity - sensitive stage acting on the overall characteristics of the rest of the filter network. However, such a detailed descriptive analysis is

not justified at this stage. The purpose of the first two experiments has been to establish that the visual system is sensitive to the luminance gradients in flicker. The next two chapters go on to present the results of four experiments designed to investigate more qualitative aspects of the analysis and detection of the luminance gradients in flicker waveforms.

CHAPTER 4

IS FLICKER ADAPTATION FREQUENCY OR VELOCITY SPECIFIC?

4.1 Introduction

This chapter continues the theme of whether flicker is detected on the basis of its temporal profile or its frequency. The experiment described uses the technique of adaptation to investigate this problem. The fundamental reasoning behind the technique is that prolonged exposure to a stimulus reduces the sensitivity of the mechanisms involved in the processing of that stimulus. Subsequent measurement of thresholds for an appropriate choice of test stimuli thus reveals the range of inputs to which these mechanisms are sensitive: thresholds will be raised for test stimuli mediated by the same channels as the adapting stimulus. Moreover, a quantitative estimate of relative sensitivity may be made by assuming that the thresholds of mechanisms detecting the test stimuli are raised in proportion to their sensitivity to the adapting stimulus. An equivalent assumption is that relative threshold elevation (RTE) is proportional to the sensitivity to the test stimulus of the mechanisms detecting the adapting stimulus. This assumption is invoked when a threshold elevation curve is used as an indication of the sensitivity profile of the mechanisms detecting the adapting stimulus.

A number of studies have investigated the effect of adaptation to a flickering stimulus on subsequent sensitivity to temporal modulation. Interest

in this problem has been stimulated by the work of Blakemore and Campbell (1969), suggesting that spatial contrast may be processed by channels that are sensitive to specific bands of spatial frequencies. This has led to a search for analogous channels tuned to specific temporal frequencies (Smith, 1970, 1971; Pantle, 1971), as the basis of a parallel filter model of temporal processing. Such an approach diverges from the conventional single - channel models discussed in Section 1.1.4, which were derived from simple threshold measures.

The studies of Pantle (1971), Smith (1970, 1971), and Nilsson et al (1975) used elevation of threshold as a measure of the temporal frequency specificity of flicker adaptation. Pantle found evidence of tuning at high frequencies (32 Hz), but a broadband elevation of threshold at lower frequencies (below 10 Hz). He suggested that this latter effect could have been due to masking by the high - frequency components of his squarewave stimulus. Smith (1971) eliminated this possibility by the use of sinewave modulation and showed, in contrast to Pantle's findings, that relatively narrowband threshold elevation occurs at 7 and 15 Hz, but not at 30 Hz. However, the tuning is broad, even in comparison with Blakemore and Campbell's spatial frequency channels. Further evidence for rather broad temporal tuning is provided by Nilsson et al (1975), who found that sensitivity to a given test frequency changed only gradually with changes in adapting frequency. In other words, peak threshold elevation shifts with the adapting frequency, but to a lesser extent. On the basis of these results they were unable to choose between a single and a multiple channel model.

Before rejecting a multiple channel model of temporal analysis, it is necessary to eliminate the possibility that the channels are selective for

parameters other than frequency. As discussed in Chapter 3, measuring amplitude thresholds in the conventional way (using sinewaves) does not allow control over the rate of luminance change. Several lines of evidence suggest that this may be an important variable. Thus, the experiment described in this chapter is designed to investigate whether adaptation effects may be specific to the rate of change rather than to temporal frequency.

In his report of a luminance aftereffect similar to the movement aftereffect, to be discussed in more detail in Chapter 5, Anstis (1967) claimed that the visual system adapts to the rate of change of luminance in sawtooth flicker. Although the published observations show evidence of specificity merely for the polarity rather than the rate of change, Anstis (personal communication) has demonstrated that the rate of the aftereffect is related to the frequency of the adapting sawtooth. There is strong neurophysiological evidence (reviewed by Jung, 1973) for two populations of neurones responsive selectively to increasing or decreasing luminance. It therefore becomes of interest to ask if channels which are sensitive to the sign of a luminance ramp also contain sub-units that are tuned to its slope.

A possible explanation of Smith's failure to find narrowband frequency tuning may lie in his use of sinusoidal modulation. A sinewave contains a single frequency component, but an infinite series of velocity components, since velocity varies cosinusoidally with luminance. Clearly, the best stimulus to test for velocity - specific adaptation is either a sawtooth or triangular waveform, containing only one velocity component. In Experiment 4.1 the basic paradigm is adopted of adaptation to flicker of one frequency, followed by measurement of flicker threshold across a range of frequencies. A comparison is made between two conditions:

1) Frequency condition, in which both test and adaptation stimuli contain only one frequency component, and

2) Velocity condition, in which stimuli contain only one velocity component.

During adaptation this is achieved by the use of sinewave flicker in the Frequency condition and triangle-wave flicker in the Velocity condition. During the test phase, modulation depth is adjusted in the normal way in the Frequency condition, but in the Velocity condition amplitude is varied by clipping the peaks of a triangle-wave, so that the slope of the function remains constant (see Figure 3.01). Thus, if flicker adaptation is frequency specific we would expect to find evidence of tuning in both the Frequency and Velocity conditions; if adaptation is velocity specific there should be tuning in the Velocity condition only.

4.2 Experiment 4.1

4.2.1 Apparatus

The CRT display was as described in Chapter 2. The digitisation and frame rate was 50 Hz in the Frequency condition and 5 kHz in the Velocity condition. Artificial pupils were not used, since mean luminance was constant throughout the experiment.

4.2.2 Design and Procedure

The adapting stimulus consisted of either sinewave (Frequency condition) or triangle-wave (Velocity condition) modulation of the entire screen at the adapting frequency and the maximum obtainable modulation: $(L_{max} - L_{min})/(L_{max} + L_{min}) = 0.71$. The amplitude of the basic triangle-wave in the Velocity condition was kept constant at 173 $cd \cdot m^{-2}$, so that velocity covaried with frequency:

$$V = 346f \qquad \text{Equation 4.01}$$

where V is velocity (in $cd \cdot m^{-2} \cdot s^{-1}$) and f is frequency (in Hz).

Four adapting frequencies were used, including a no flicker control condition (0, 2, 4, and 8 Hz). Each experimental session lasted about 40 minutes and consisted of adaptation to one frequency, followed by testing over a range of 13 frequencies covering the four octaves from 1 to 16 Hz at 1/3 octave intervals. Threshold estimates were made by the method of adjustment, with the subject varying the amplitude of flicker until it was at threshold. This method almost inevitably introduces a large element of variability into the results, since it does not control for spontaneous changes in either threshold or criterion.

Each session started with 50 seconds adaptation, after which the trial sequence started. A pilot study indicated that adaptation was effectively maximal after 1 minute, and adaptation effect was not observed to increase during the course of the experiment. Each trial consisted of 10 seconds topping-up adaptation, followed by a test phase during which the subject adjusted the amplitude by turning a knob until flicker was either just

detectable (setting from zero amplitude) or just undetectable (setting from maximum amplitude). The trial was terminated either by the subject pressing a button to indicate a threshold estimate had been made, or after 10 seconds, in which case the trial was repeated. Almost all estimates were made within the first 10 seconds, typically in 2 to 5 seconds. Five estimates were made at each test frequency, after which the next test condition was presented. Test stimuli were presented first in order of increasing frequency, with adjustment made from maximum amplitude. After a five minute rest period in dim illumination the conditions were presented in reverse order and thresholds set from zero amplitude to balance for short-term order effects. Ten threshold estimates were therefore obtained from each test/adapt combination. The four adapting conditions were run in order of increasing frequency on consecutive days, with a repeat of the first (0 Hz) condition on the fifth day. The Frequency condition preceded the Velocity condition, and the order of conditions was the same for all four subjects.

4.2.3 Results

The flicker sensitivity functions of all subjects in each adaptation condition are shown in Figures 4.01 (Frequency condition) and 4.02 (Velocity condition). Figure 4.01 shows the effect of adaptation to sinewave flicker on sensitivity to sinewaves; Figure 4.02 shows the effect of adaptation to triangular flicker on sensitivity to trapezoidal modulation. The unadapted sinewave sensitivity curves have the typical form of the deLange function for a uniform field of this size and mean luminance (Kelly, 1971a), that is an increase of sensitivity with frequency, reaching a peak at about 10 Hz. The sensitivity peak of subject APH appears to lie outside the

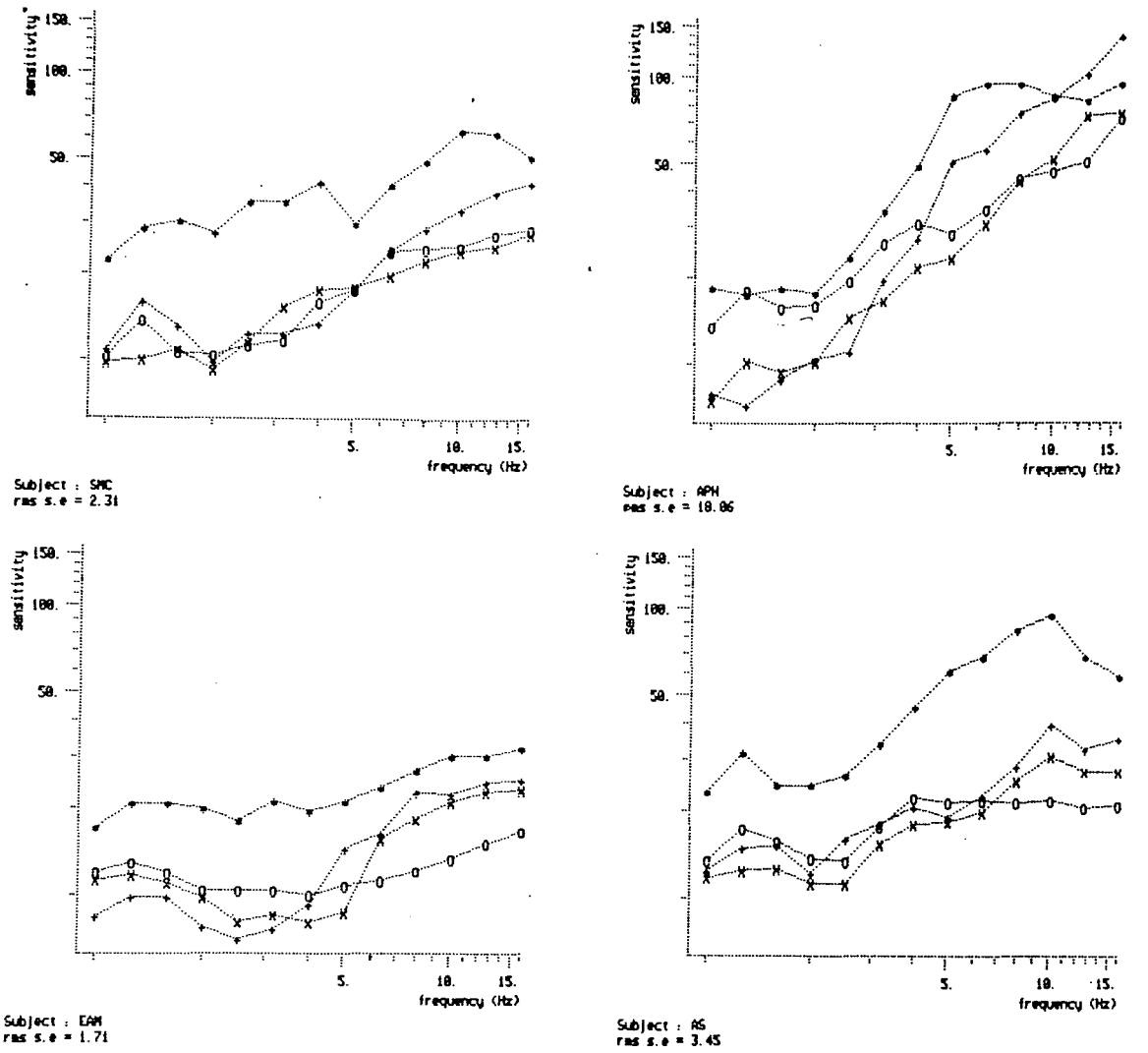

Figure 4.01 : Sinewave flicker sensitivity (the reciprocal of threshold modulation) of each subject in the Frequency condition of Experiment 4.1. The curve plotted with asterisks represents pre-adaptation baseline sensitivity, ie 0 Hz adaptation condition. The other three curves show sensitivity after adaptation to sinewaves at 2, 4, and 8 Hz. Mean standard errors across all conditions are shown below.

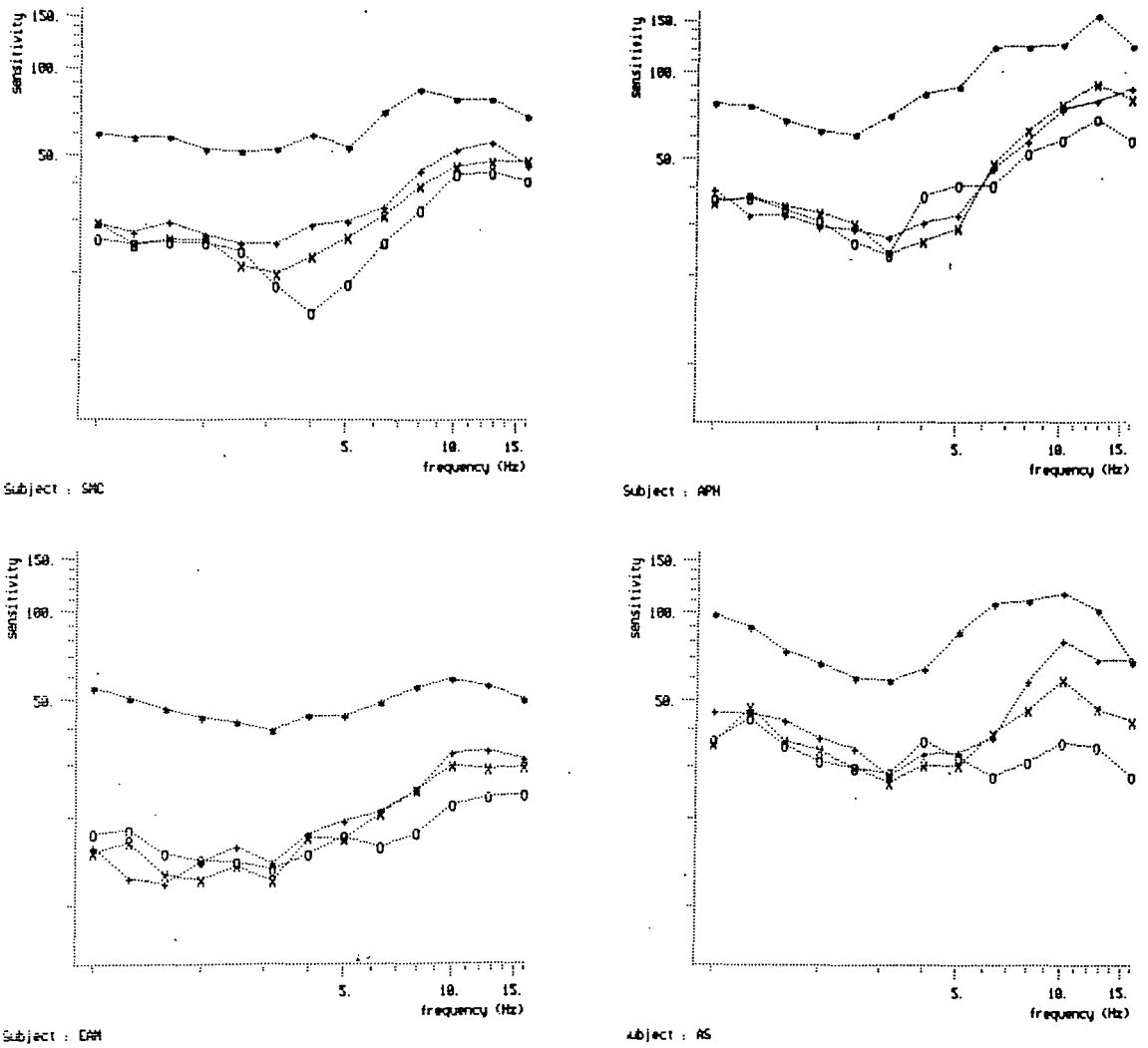

Figure 4.02 : Individual flicker sensitivity functions in the Velocity conditon of Experiment 4.1. The curves show sensitivity to trapezoidal flicker after adaptation to an unmodulated screen (asterisks) and to three frequencies of triangle-wave flicker.

frequency range tested. Subject EAM shows a marked lack of sensitivity to midrange and high frequencies, although her low frequency response is only slightly lower than that of other subjects. The inclusion of her results in the mean data has the effect of reducing the differential between the two ends of the frequency range. The unadapted sensitivity curves in the Velocity condition show the flattening at low frequencies already seen with the trapezoidal flicker in Experiments 3.1 and 3.2.

The adjustment method of threshold determination is inherently noisy, and is responsible for much of the intra-subject variability. For this reason the data shown in Figures 4.01 and 4.02 were averaged across subjects. The means thus obtained are plotted in Figures 4.03a and 4.04a respectively. It can be seen that adaptation to flicker produces a generalised drop in sensitivity to subsequent modulation, although detailed effects are less easy to observe. Any frequency - specific adaptation effects are more clearly revealed by replotting the data in terms of relative threshold elevation (RTE), defined as:

$$RTE = \log (S_{pre} / S_{post}) \qquad \text{Equation 4.02}$$

where S_{pre} is pre-adaptation baseline sensitivity, and S_{post} is post-adaptation sensitivity. A positive figure indicates a threshold increase, and a negative figure a threshold decrease. RTE provides a relative measure of the sensitivity of the mechanisms detecting the adapting stimulus to the test stimuli.

Mean RTE for the three adapting frequencies is shown for comparison below the mean sensitivity curves in Figures 4.03b (Frequency condition) and 4.04b (Velocity condition). In the Frequency condition each curve

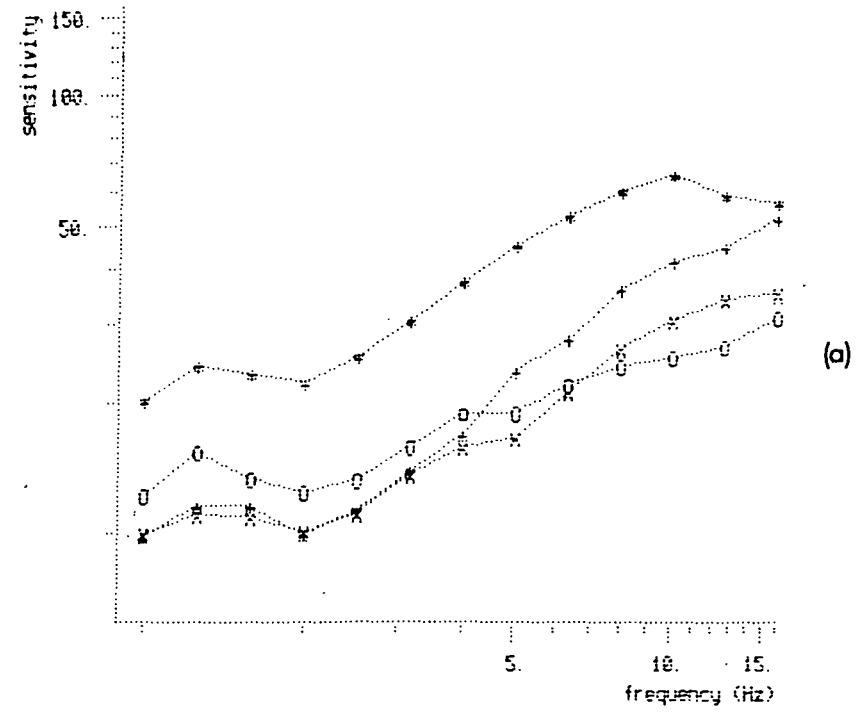

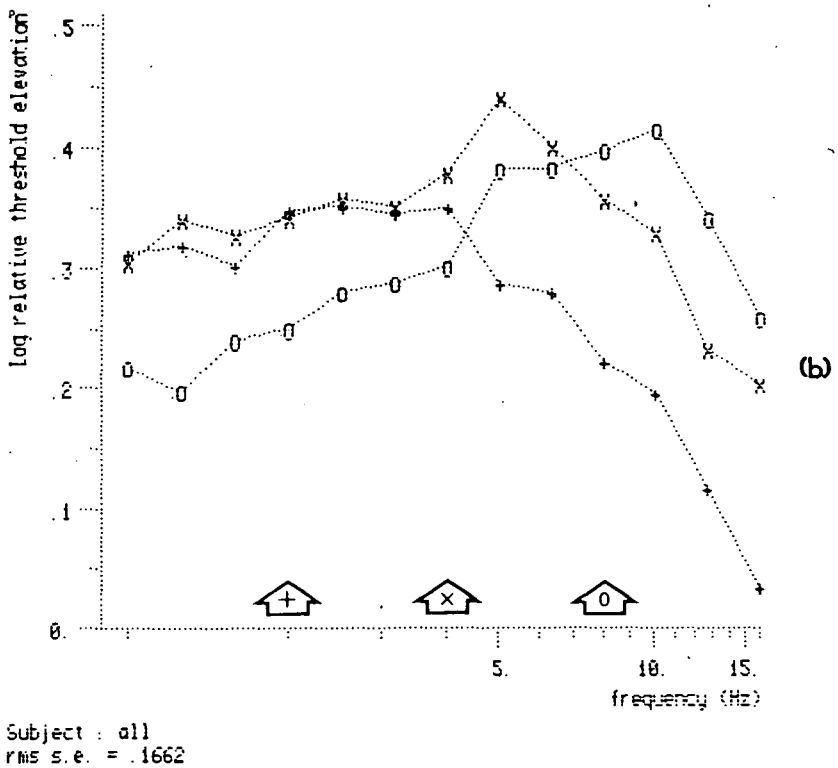

adapting frequency

+·····+ 2 Hz

×·····× 4 Hz

o·····o 8 Hz

Figure 4.03 : (a) Mean sensitivity across subjects in the Frequency condition.
(b) Relative threshold elevation, calculated by dividing pre-adaptation sensitivity by post-adaptation sensitivity for each subject individually, then averaging across subjects. A 0.3 log unit rise in threshold represents a drop in sensitivity by a factor of 2.

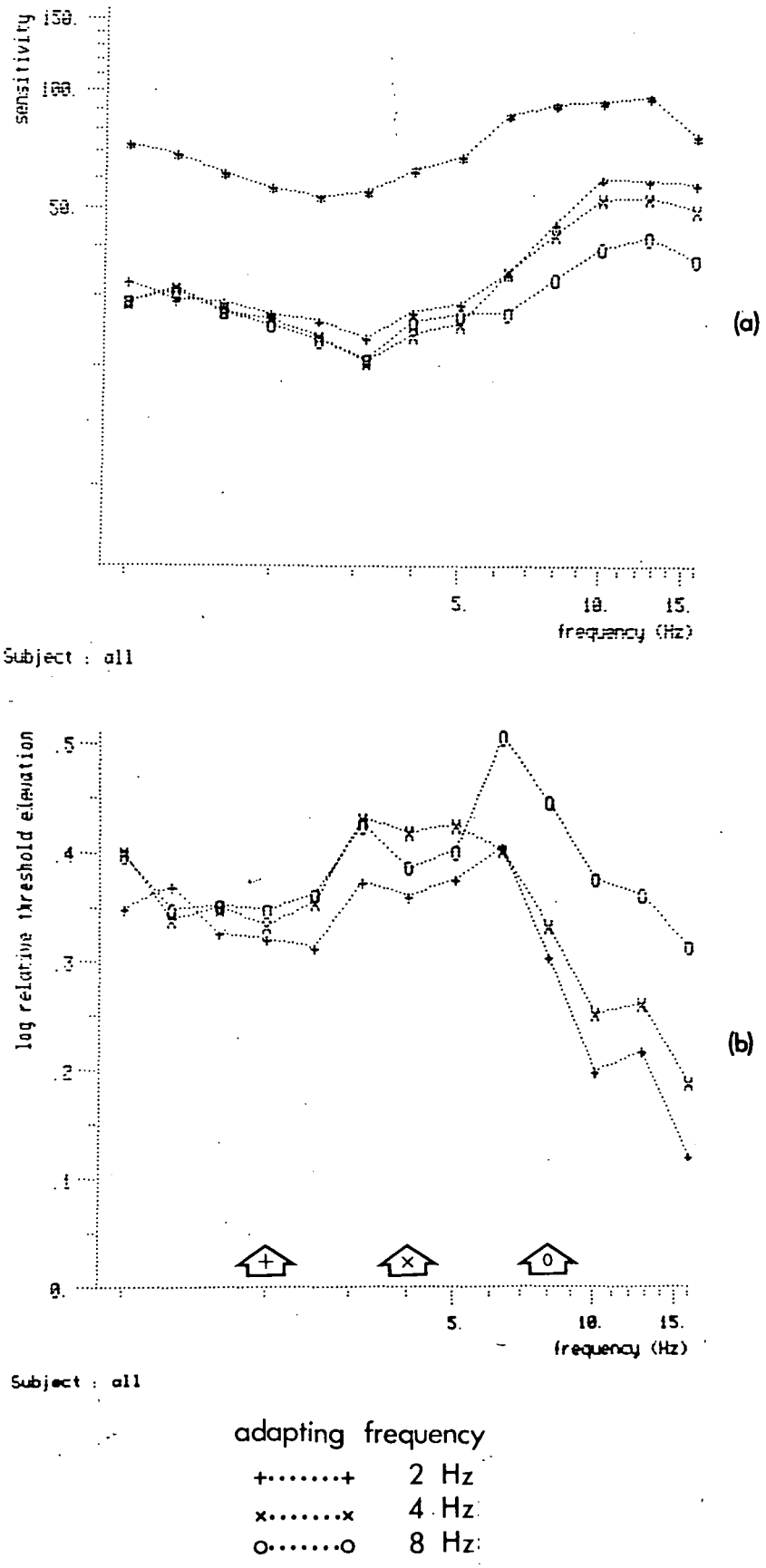

Figure 4.04 : (a) Mean sensitivity across subjects in the Velocity condition.
(b) Mean relative threshold elevation, calculated as for Figure 4.03b.

shows peak elevation of threshold near the adapting frequency. Thus the adaptation effect is frequency - specific, or tuned to temporal frequency. A further feature of the curves is their asymmetry about the peak, the fall-off in adaptation effect being more gradual below the adapting frequency than above. This effect increases at lower adapting frequencies, so that with 2 Hz adaptation sensitivity is hardly recovered at all below the point of adaptation. In the Velocity condition the convergence of the curves at low frequencies is even more marked. Below about 5 Hz adaptation effect is essentially independent of both test and adapting frequency; above 5 Hz the curves are displaced in the expected direction, once again showing some evidence of frequency - specificity. The results of an analysis of variance on the RTE data are shown in Table 4.01. The interaction between test and adapting frequency is highly significant ($p < 0.00001$), confirming that the adaptation effect is frequency - specific. However, neither the main effect of condition nor any of the interactions between condition and the two frequency variables are significant, indicating that the tuning effect is the same in both the Frequency and Velocity conditions.

4.3 Discussion

In the Introduction to this chapter the principle of regarding a threshold elevation curve as the sensitivity profile of the mechanisms detecting the adapting stimulus was discussed. In essence, it is assumed that the adapting stimulus raises the threshold of all those mechanisms sensitive to it, in proportion to their sensitivity. It is further assumed that the threshold for a stimulus is determined by the single mechanism most

	Source	df	F	p
main effects	1.test frequency	12,36	2.5131	0.01619
	2.adapt frequency	2,6	7.4800	0.02378
	3.F/V condition	1,3	1.0795	0.37665
interactions	1 x 2	24,72	5.7107	<0.00001
	1 x 3	12,36	0.7961	0.65236
	2 x 3	2,6	4.2555	0.07056
	1 x 2 x 3	24,72	1.0549	0.41466

Table 4.01 : Analysis of variance on the relative threshold elevation data from Experiment 4.1

sensitive to it. The threshold elevation curve then becomes a relative measure of the sensitivity of the adapted mechanisms to the test stimuli. The significant interaction between test and adapting frequency indicates that these mechanisms are specific, or 'tuned', to the temporal frequency of the adapting flicker. Considering firstly the sinewave data in the Frequency condition, this is analogous to the spatial frequency selective channels discovered with a similar technique by Blakemore and Campbell (1969). However, there are two important differences between the two sets of results. Firstly, the tuning of the temporal channels is extremely broad, with attenuation down by 0.3 log units at about 2.5 octaves above the peak frequency, compared to 0.5 octave for Blakemore and Campbell's spatial frequency channels. Secondly, and more importantly, the curves are clearly asymmetrical, unlike the spatial tuning curves. The mechanisms sensitive to 8 Hz flicker, for example, are more sensitive to lower than to higher frequencies. Furthermore, this asymmetry becomes more marked as adapting frequency is reduced, until at 2 Hz frequency - specificity has essentially disappeared.

A simple frequency - tuned system would show an equal fall-off in sensitivity per octave above and below its peak frequency. It appears therefore that sinewave flicker is not detected by such a simple tuned system. A point has been made throughout of referring to several systems underlying flicker detection. It is proposed that periodic luminance change is detected, at least in part, by a system sensitive to relatively slow luminance changes, irrespective of their periodicity. This system may be termed a 'nonperiodic' system, in contrast to a 'periodic' system, sensitive only to repetitive changes. The rate of change, or luminance velocity, varies cosinusoidally with luminance in sinewave flicker, so that even 8 Hz flicker contains slow changes around its peaks. These will have an adaptation

effect on a system detecting slow, nonperiodic changes, which would be seen as a raised threshold to lower frequency stimuli, which also contain slow changes. When summed with a 'pure' frequency tuning curve the asymmetries observed in Figure 4.03b are produced. As adaptation frequency decreases relative low-velocity content increases, producing greater nonperiodic adaptation and increased asymmetry. Below about 4 Hz the RTE curve is almost independent of frequency, suggesting that in this region sinewaves are detected almost entirely by the nonperiodic system.

Sinewaves present a broadband, lowpass filtered input to a velocity - sensitive system. The broadband threshold elevation observed after adaptation to low frequency sinewaves may thus be due either to the adaptation of a range of velocity - tuned channels, or to the operation of a single channel. These two possibilities are discriminable in the Velocity condition by the use of single - velocity test and adapting stimuli. Velocity covaries with frequency in the waveforms used, so that velocity - selectivity would appear as frequency - selectivity. Thus if the RTE curves were more narrowly tuned in the Velocity condition than the Frequency condition, particularly with 2 Hz adaptation, this would be evidence of velocity tuning. The obtained curves in fact show a slight trend in the opposite direction, although analysis of variance shows that the two conditions are not significantly different. We may conclude that, if a system exists which is sensitive to slow, nonperiodic luminance changes, it does not contain sub-units selectively tuned to the rate of change, at least over the range 346 to 5544 $cd \cdot m^{-2} \cdot s^{-1}$ (corresponding to 1 to 16 Hz with the waveforms used).

Experiment 3.2 provided evidence that the visual system is sensitive to luminance velocity, by showing that flicker thresholds are affected by

changes in velocity. However, the adaptation techniques of the present experiment failed to find evidence of velocity - selective channels, leaving open the question of how luminance velocity is analysed and coded. A more positive conclusion may be reached from the results of the Frequency condition. The asymmetrical tuning curves are consistent with the hypothesis that low frequency sinewaves are analysed on the basis of temporal luminance gradient, by a system sensitive to non-abrupt nonperiodic changes, rather than by their frequency content or periodicity. At test frequencies above about 5 Hz the threshold elevation curves are consistent with a system of multiple frequency - tuned channels. This distinction between high and low frequencies again parallels the many other empirical differences reviewed in Section 1.1.3. Furthermore, a change in the phenomenal appearance of flicker takes place at about the same point. Below 5 Hz the brightening and darkening phases are clearly discriminable, differences in frequency are easily seen, and the screen does not appear to 'flicker' in the normal sense. Above 5 Hz it is difficult or impossible to follow the variation in brightness, and the subjective impression of rapid flickering varies relatively little with changes in frequency. These observations suggest that an experimental investigation of frequency discrimination thresholds may provide further evidence of differences between the periodic and nonperiodic systems.

CHAPTER 5

IS FLICKER ADAPTATION WAVEFORM SPECIFIC?

5.1 Introduction

In the Conclusion to Chapter 4 it was suggested that low frequency sinewave flicker is detected by its temporal luminance gradients, and that the system performing this analysis is not tuned to the slope of the gradient. Parallels were drawn with similar findings on the analysis of low frequency spatial modulation. In this chapter two experiments are reported which again use an adaptation technique to investigate further the systems underlying the analysis of low frequency flicker.

Sinewave flicker not only contains luminance gradients, which may be detected by a 'nonperiodic' system, but is also a periodic stimulus. Squarewave flicker shares the periodic component, but contains luminance steps instead of gradients. By comparing sinewaves and squarewaves, Experiment 5.1 is designed to investigate the relative contribution of the periodic and nonperiodic systems to the detection of sinewave flicker. It is assumed that both sinewave and squarewave adapting flicker have identical effects on the sensitivity of the periodic system, but that only sinewave adaptation affects the nonperiodic system. A sinewave adapt / sinewave test condition thus provides a control measure of maximum adaptation effect. Comparing this with a squarewave adapt / sinewave test condition reveals the relative importance of the gradient in the detection of the sinewave test

stimulus. In the conventional frequency - tuning adaptation experiment, the spread of adaptation effect across frequency is measured by using test and adapting stimuli which differ only in frequency. Experiment 5.1 may be regarded as measuring the spread of adaptation effect across waveform, so that the test and adapting stimuli have the same frequency and differ only in waveform. The sinewave vs squarewave comparison is made across the 1 - 16 Hz range in order to study the contribution of the nonperiodic system as a function of frequency.

In Experiment 5.2 the principle of the spread of adaptation across waveform is applied to the question of the existence of separate channels for increasing and decreasing luminance. Jung (1973) has reviewed the neurophysiological evidence for separate populations of neurones selectively sensitive to the sign of luminance change. As mentioned briefly in Chapter 4, Anstis (1967) has reported a flicker aftereffect analogous to the movement aftereffect: after adaptation to full field sawtooth flicker, a steady field appears to change its brightness in the direction opposite to that of the slow phase of the sawtooth. Hanly and Mackay (1979) also adapted subjects to sawtooth flicker and showed that post-adaptation threshold was raised more for flicker of the same waveform than for that of the opposite polarity. However, neither study used flicker with a fundamental frequency higher than 5 Hz, leaving open the possibility that polarity - sensitivity is a property only of the system mediating LF flicker, or slow luminance gradients. Experiment 5.2 extends the Hanly and Mackay technique to the high frequency region, as well as testing the low frequency region more intensively.

A secondary aim of both Experiments 5.1 and 5.2 is the investigation of the relationship between the systems responsible for the analysis of low

frequency (LF) and high frequency (HF) flicker. All the theoretical models discussed in Section 1.1.4, for example that of Kelly (1971), consist fundamentally of two serial stages: a linear lowpass filter and a nonlinear network controlling LF sensitivity. An alternative model proposed by Roufs (1974a) suggests that LF sinewave flicker is processed by a system operating in parallel to the HF system (see Figure 1.09). It is suggested that this LF system is identifiable with the nonperiodic gradient detector. If flicker is detected by a system of serial filters, as suggested by Kelly (1971), then adaptation effect would be independent of flicker waveform. This would result even if the stages were differentially sensitive to the different waveforms. Any evidence of waveform selectivity is thus evidence against a serial model, and frequency - dependent selectivity would support the parallel model of Roufs (1974a).

5.2 Experiment 5.1

5.2.1 Apparatus

The standard visual display described in Chapter 2 was used, with a 1 kHz frame rate. The computer - generated flicker waveforms were output to the display monitor through a 12 bit multiplying D-A converter. Modulation depth was controlled by the subject with an adjustable voltage source, applied to the multiplying DAC. Artificial pupils were not used.

5.2.2 Design and Procedure

Each session consisted of the sequence:

1) 5 minutes adaptation to a steady field at mean luminance
2) measurement of flicker thresholds
3) 5 minutes adaptation to flicker
4) measurement of flicker thresholds

The measurement phase consisted of ten threshold estimates made by the method of adjustment from a starting point of either zero or maximum modulation, followed by a further ten made from the opposite starting point. The subject was instructed to adjust modulation depth until flicker was either just detectable (setting from zero) or just undetectable (setting from maximum). The final threshold was taken as the mean of all 20 estimates. Up to 10 seconds were allowed per trial for a setting to be made, indicated by the subject pressing a button which initiated the next trial. If no setting had been made after 10 seconds the trial was terminated automatically and repeated later in the sequence. Each trial was preceded by 10 seconds readaptation to the adapting stimulus, ie steady screen in the 1st measurement phase and flicker in the 2nd.

The purpose of Experiment 5.1 is to measure sensitivity to sinewave flicker after adaptation to both sinewaves (Sinewave condition) and squarewaves (Squarewave condition). Subjects were therefore adapted either to sinewaves at maximum obtainable amplitude (71%) or to squarewaves with a fundamental of the same amplitude, then tested with sinewave flicker of the same frequency. Each adaptation condition was repeated at 9 frequencies covering the range from 1 to 16 Hz at 1/2 octave intervals, giving a total of 18 conditions. These conditions were counterbalanced across the four subjects with respect to a) order of adjustment starting

point, b) order of adapting waveform, and c) order of frequency. Each session involved only one frequency, and sessions were separated by at least 6 hours to ensure no carry-over of adaptation effect.

5.2.3 Results

Experiment 5.1 is designed to isolate the contribution of the nonperiodic, gradient - detecting system to the detection of sinewave flicker. It is suggested that low frequency sinewaves are detected by both the periodic and nonperiodic systems, but that squarewaves are detected only the periodic system. [The possibility of a system sensitive to abrupt transients, or steps, is not directly relevant to the present argument.] To reiterate briefly the general considerations underlying the adaptation technique, outlined in Chapter 4, it is assumed:

a) that the adapting stimulus raises the threshold of all mechanisms sensitive to it, in proportion to their sensitivity.

b) that the test stimulus is detected at threshold by the single mechanism most sensitive to it.

c) that relative threshold elevation (RTE) is a measure of the sensitivity of the mechanisms detecting the adapting stimulus to the test stimulus.

In this experiment we need to compare RTE in the two adaptation conditions. The Sinewave adapt condition provides a control measure of maximum adaptation, since adaptation desensitises all the mechanisms detecting the test stimulus. The Squarewave adapt condition has an equal effect on the periodic system, but no effect on the nonperiodic system. RTE in the Squarewave condition is a measure of the sensitivity of the

mechanisms detecting squarewaves, ie the periodic system, to sinewaves. RTE in the Sinewave condition shows the sensitivity of both the periodic and nonperiodic systems to sinewaves. Any difference between the two conditions must therefore be due to the nonperiodic, gradient - detecting system.

Relative threshold elevation, calculated by Equation (4.1), in both the adaptation conditions is shown in Figures 5.01 (individual subjects) and 5.03a (mean across subjects). RTE in the Sinewave condition increases with frequency, as does absolute sensitivity (see Figure 4.03), validating assumption (a) above. The general pattern of results, shown by 3 out of the 4 subjects, is that sinewave threshold is raised more by adaptation to sinewaves than squarewaves at low frequencies, but that adaptation effect is independent of waveform at high frequencies, Once again the transition between the two types of behaviour occurs at about 5 Hz. Subject APH shows an unusually large effect of squarewave adaptation at low frequencies, resulting in little if any difference between the two conditions.

It is possible to derive from these data a measure of the sensitivity of the nonperiodic system alone. If the nonperiodic system were completely insensitive, as appears to be the case above about 5 Hz, then threshold elevation in the two adaptation conditions would be equal. This assumes that the periodic system is equally sensitive to sinewaves and squarewaves with the same amplitude fundamental. Any contribution to detection by the nonperiodic system is manifested as greater threshold elevation in the sinewave adapt than the squarewave adapt condition. For example, if RTE were twice as great in the sinewave than the squarewave condition, this would suggest that half the adaptation effect were due to the periodic system and half to the nonperiodic system. From assumption (c) above we

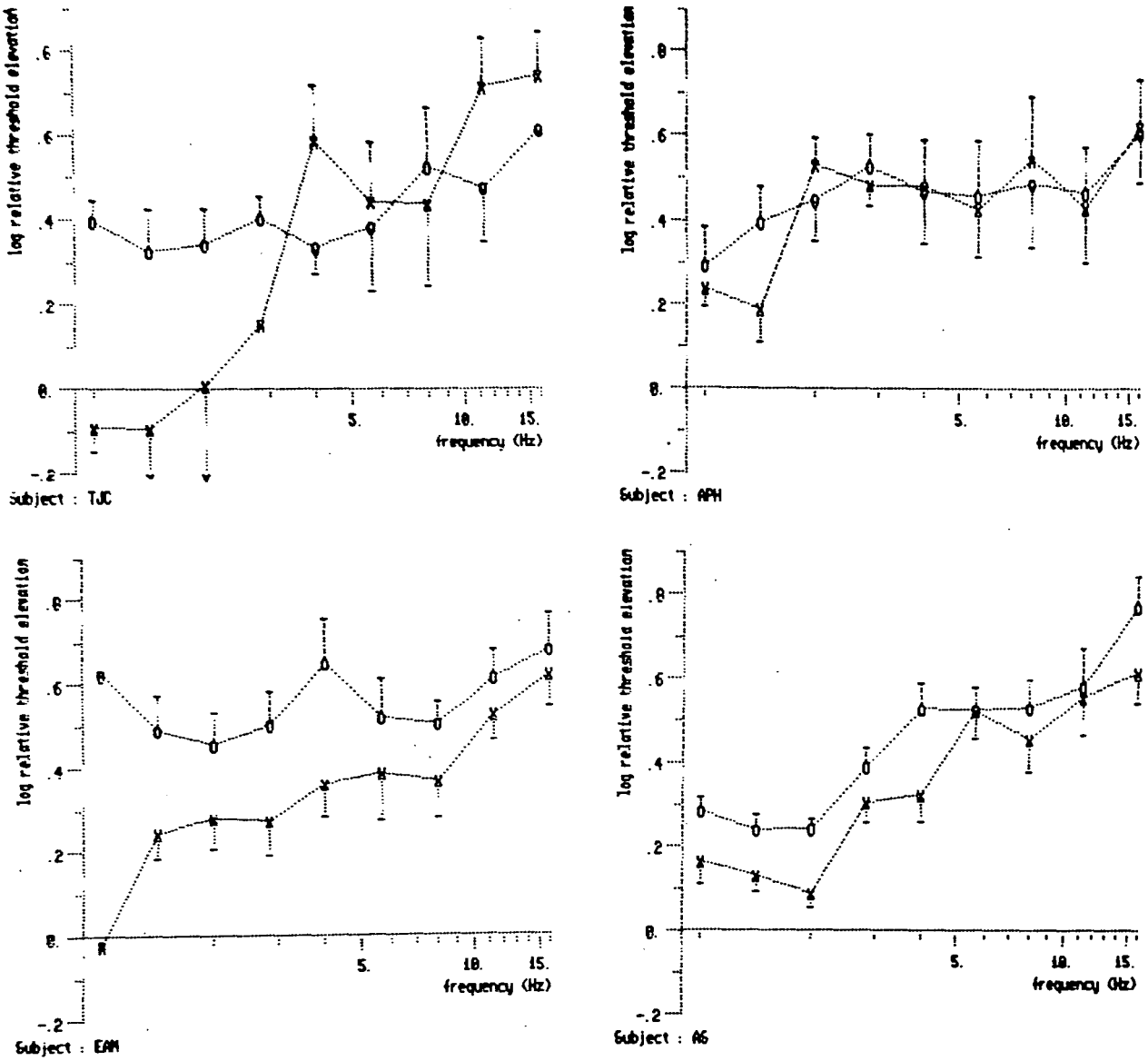

Figure 5.01 : Relative elevation of the threshold for sinewave flicker after adaptation to sinewaves (0) and squarewaves (X) of the same frequency and fundamental amplitude.

may conclude that in this case the two systems are equally sensitive to a sinewave stimulus. An index of the relative sensitivity of the nonperiodic system (RS_{np}), measured in terms of the sensitivity of the periodic system, may be derived by the following formulation:

$$RS_{np} = (Spost_{square} / Spost_{sine}) - 1 \qquad \text{Equation 5.01}$$

where Spost is post-adaptation sensitivity in the respective condition.. A figure of zero means that the nonperiodic system does not contribute at all towards detection thresholds, 1 that it is equally as sensitive as the periodic system, 2 that it is twice as sensitive, and so on. However, Equation 5.01 assumes that pre-adaptation sinewave thresholds are the same in the two conditions. An equivalent expression which takes possible baseline differences into account is:

$$RS_{np} = (RTE_{sine} / RTE_{square}) - 1 \qquad \text{Equation 5.02}$$

where RTE is derived according to Equation 4.01.

This relative sensitivity measure is plotted as a function of frequency in Figure 5.03b, averaged across subjects. The curves for individual subjects are shown in Figure 5.02. The predicted decline with increasing frequency may be observed, reaching zero at about 5 Hz. An analysis of variance on this data (Table 5.01) shows that the main effect of frequency is significant ($p < 0.04$). Trend analysis reveals that this effect is mainly due to the linear component ($F(1,27) = 13.198$, $p = 0.0012$) - higher order components are not significant ($p > 0.09$). Despite the wide range of individual differences the linear component accounts for 29.9% of the total variance ($r = -0.5464$; $p < 0.0001$, 34 df).

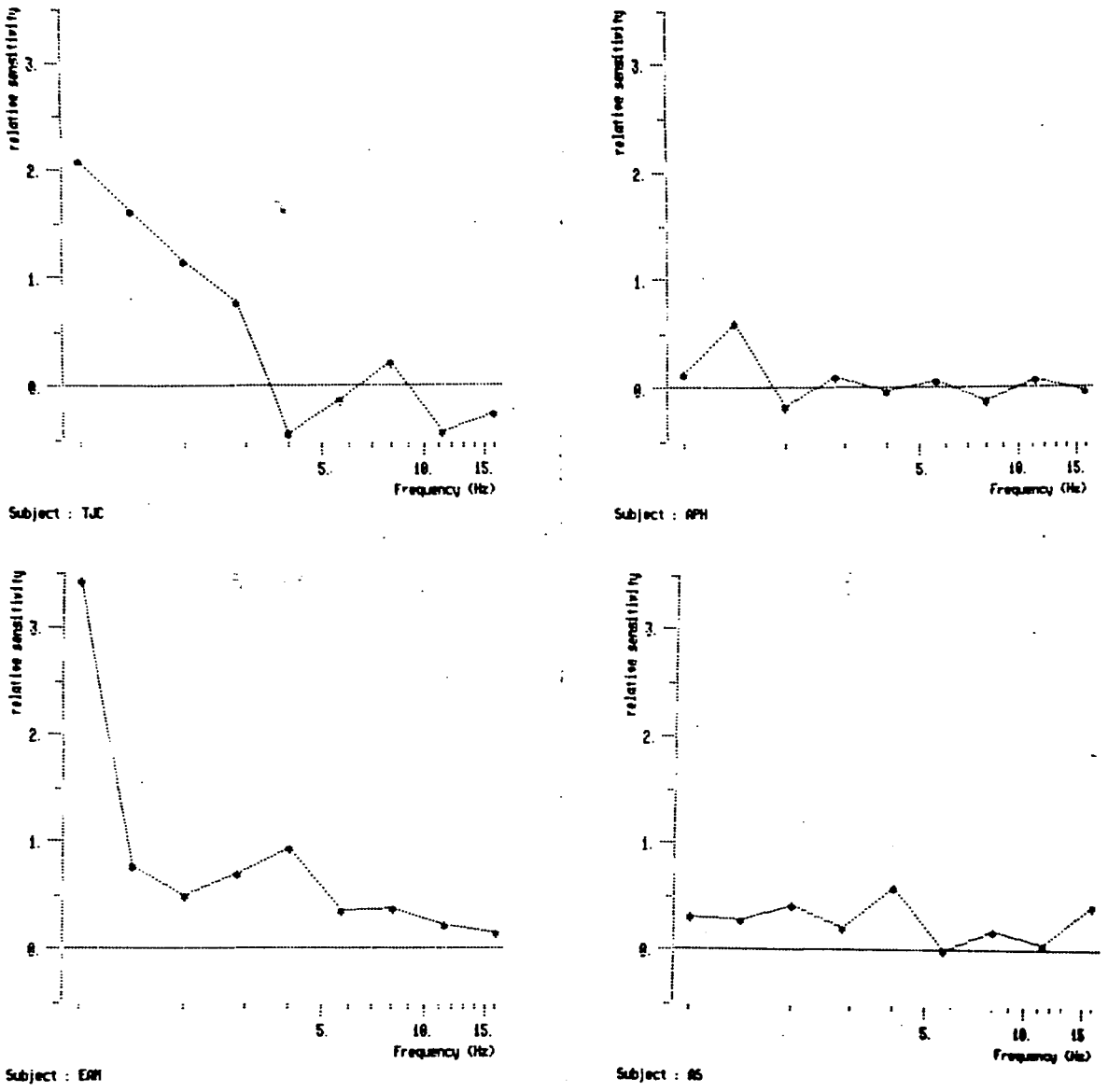

Figure 5.02 : Relative sensitivity of the mechanisms sensitive to sinewaves but not squarewaves, measured in terms of the mechanisms sensitive to both. The functions for each subject are plotted separately, calculated from the RTE data of Figure 5.01 by Equation 5.02.

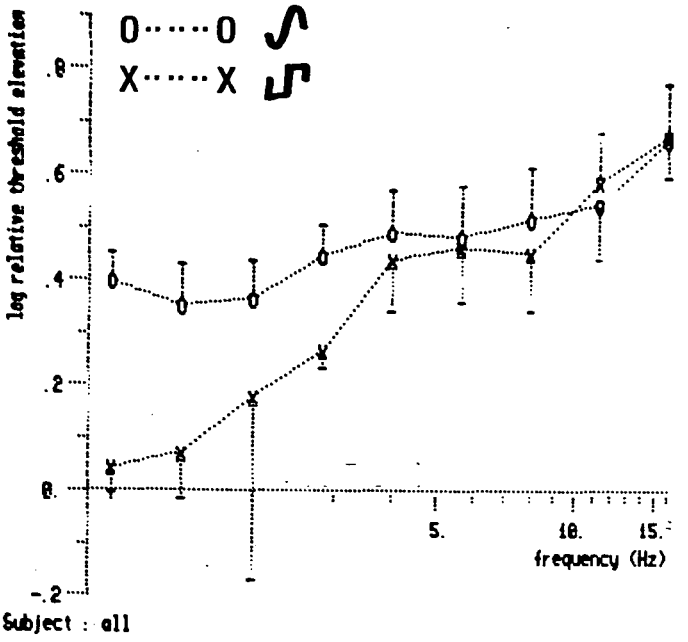

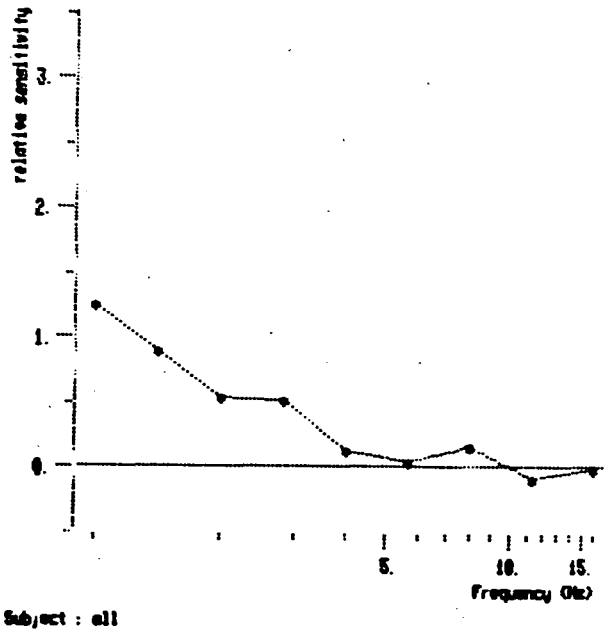

Figure 5.03 : (a) Mean log RTE for sinewave flicker; the data of Figure 5.01 averaged across subjects.
(b) Relative sensitivity of the sinewave - specific mechanisms, averaged across the three individual functions of Figure 5.02.

	Source	df	F	p
main effects	1.frequency	8,24	2.5339	0.03695

Table 5.01 : Analysis of variance on the relative sensitivity data plotted in Figure 5.03.

	Source	df	F	p
main effects	1.test waveform	1,2	10.7652	0.08055
	2.adapt waveform	1,2	7.1225	0.11652
	3.frequency	12,24	16.1281	<0.00001
interactions	1 x 2	1,2	4.2153	0.17736
	1 x 3	12,24	1.4190	0.22406
	2 x 3	12,24	3.0077	0.01053
	1 x 2 x 3	12,24	1.6586	0.14078

Table 5.02 : Analysis of variance on the relative threshold elevation data from Experiment 5.2, plotted in Figure 5.04. Note that adapting waveform is defined relative to the test waveform, ie the adapt variable is same / different polarity rather than positive / negative polarity.

We may conclude that sinewaves are detected at low frequencies by a system which is unaffected by squarewave adaptation. At 1 Hz this system is on average approximately 25% more sensitive to sinewaves than the periodic system. As frequency increases sensitivity declines, until by about 5 Hz it is effectively zero.

5.3 Experiment 5.2

5.3.1 Apparatus

The experimental setup was identical to that used in Experiment 5.1.

5.3.2 Design and Procedure

This experiment was designed to examine the polarity - sensitivity of the mechanisms underlying the detection of luminance change, using sawtooth flicker with both positive - going slow phase ('positive' flicker) and negative - going slow phase ('negative' flicker). All combinations of positive and negative flicker as test and adapting stimuli were presented, in a 2 x 2 design. The structures of both an entire session and individual trials were identical to those of Experiment 5.1. Within a session a single adapting polarity was used, but sensitivity to both test stimuli was measured, with both test and adapting flicker the same frequency. Each session thus contained both Same and Inverted conditions, referring to the polarity of the test and adapting waveforms. During the measurement phase

the subject made ten threshold estimates from one end of the adjustment range, followed by a further ten from the opposite end. Each block of ten trials consisted of five negative stimuli and five positive stimuli, randomly interleaved. Thus each data point represents the mean of 10 settings. The procedure was repeated at 13 frequencies from 1 to 16 Hz at 1/3 octave intervals. The order of both frequencies and adjustment starting point was counterbalanced across subjects, although the order of adapting waveforms was the same for all subjects.

5.3.3 Results

Relative threshold elevation functions for both positive and negative sawtooth flicker are shown for each of the three subjects in Figure 5.04. The data are presented according to the convention adopted for Experiment 5.1, that is thresholds for a single test waveform are plotted together, to show the differential effect of adapting waveform. Thresholds for positive sawtooth flicker are shown in the graphs on the left, for negative flicker in the graphs on the right. The two curves on each graph represent the two adapting waveforms. Adapting waveform is defined relative to the test waveform, so that the same plotting symbol is used on both graphs when the test and adapting stimuli have the same polarity. The mean RTE across subjects is shown in Figure 5.05.

The Same condition provides a baseline of maximum adaptation effect (RTE), so that any decrease from this maximum in the Inverted condition is an indication of polarity - specificity. The results of Hanly and Mackay (1979), together with the evidence of low frequency gradient detection provided by Experiment 5.1, predict that adaptation effect would be

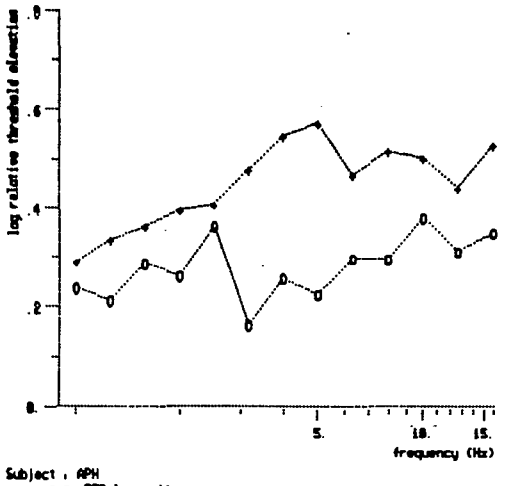

Subject : APH
rms s.e.= .078 log units
Test sawtooth positive

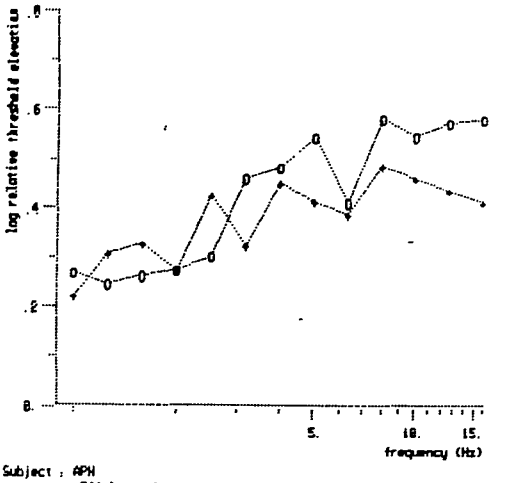

Subject : APH
rms s.e.= .044 log units
Test sawtooth negative

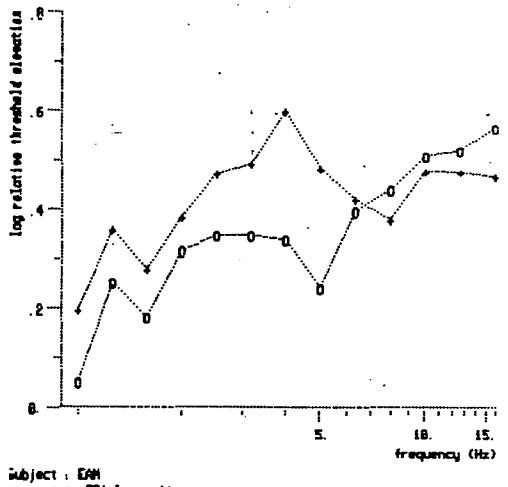

Subject : EAH
rms s.e.= .091 log units
Test sawtooth positive

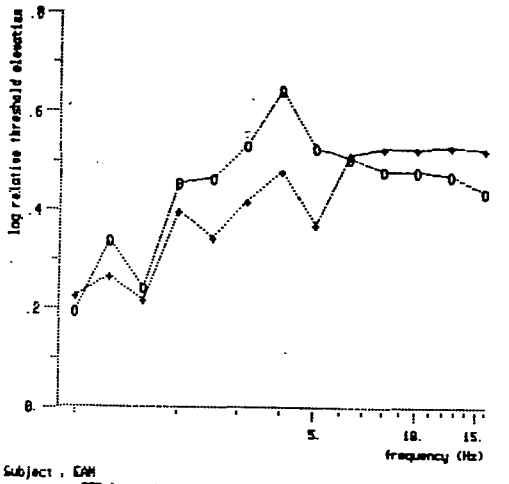

Subject : EAH
rms s.e.= .078 log units
Test sawtooth negative

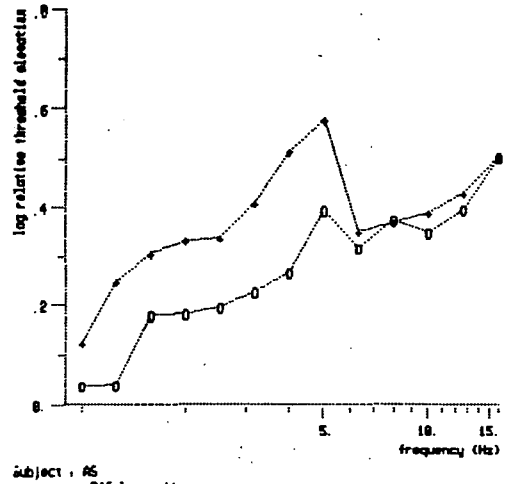

Subject : AS
rms s.e.= .046 log units
Test sawtooth positive

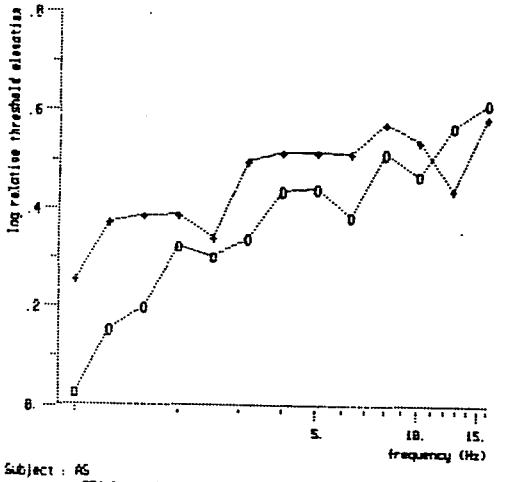

Subject : AS
rms s.e.= .034 log units
Test sawtooth negative

Figure 5.04 : Relative threshold elevation for sawtooth flicker in Experiment 5.2; data from each subject plotted separately. The left-hand column shows the results for sawtooths with a positive - going slow phase, the right-hand column for negative sawtooth flicker. Plotting symbols indicate threshold elevation after adaptation to flicker of the same (+) and of opposite (0) polarity.

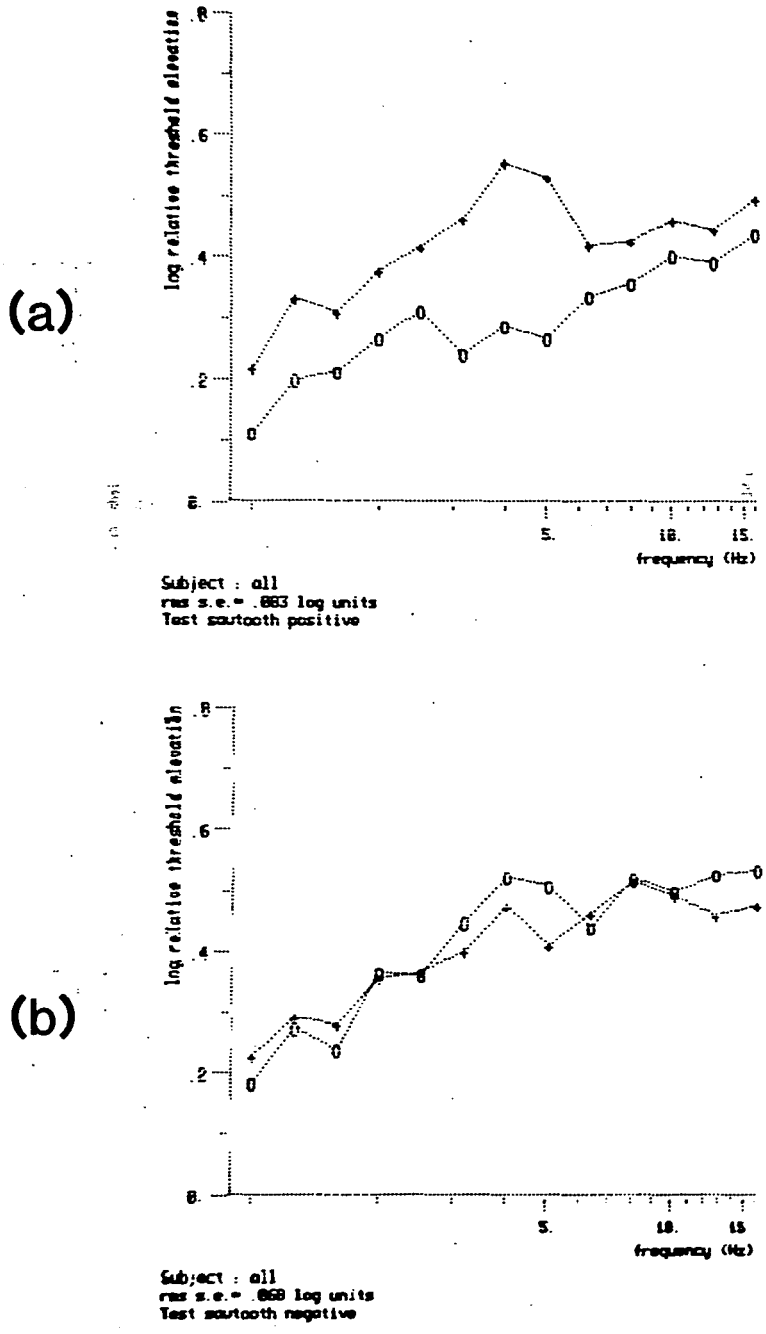

Figure 5.05 : Mean RTE across three subjects for positive (a) and negative (b) sawtooth flicker. Symbol conventions as for Figure 5.04.

polarity - specific at low frequencies but independent of polarity at high frequencies (above about 5 Hz). It is immediately clear from Figures 5.04 and 5.05 that such a clear-cut result is not obtained. Consider firstly the data for positive sawtooth flicker (left hand column). Although the expected pattern is shown by subject AS, the curves for the other two subjects appear to show a maximum difference at midrange frequencies, with a reconvergence at low frequencies. In subject APH this effect is so marked as to give exactly the opposite trend from that predicted. Averaged across subjects (Figure 5.05a) the nonmonotonic difference between the curves may be clearly seen, with a maximum at about 4 Hz and very little difference between high and low frequencies. Once again the two adaptation curves may be combined according to Equation 5.02 to yield a measure of the sensitivity of the polarity - specific system, measured relative to that of the non-specific system. The individual subjects' curves are plotted in Figure 5.06 and show a reasonable degree of correspondence, with a relative sensitivity peak at about 4 Hz in all subjects. When averaged across subjects (Figure 5.07a) the pattern becomes even clearer, with a peak of approximately 0.85 at 4-5 Hz and well-defined low and high frequency asymptotes of roughly equal value.

Turning to a consideration of the RTE curves for negative sawtooth flicker, the results are more disappointing. The individual subjects' curves in Figure 5.04 show little evidence of any systematic difference between the adaptation conditions. While subject AS shows a weak trend in the expected direction, the other two subjects both have a number of points where RTE is greater in the Inverted than in the Same condition. Overall these effects cancel out when averaged across subjects (Figure 5.05b) to give no overall effect of adapting waveform. Relative sensitivity curves for negative flicker are plotted for comparison against those for positive flicker in Figures 5.06

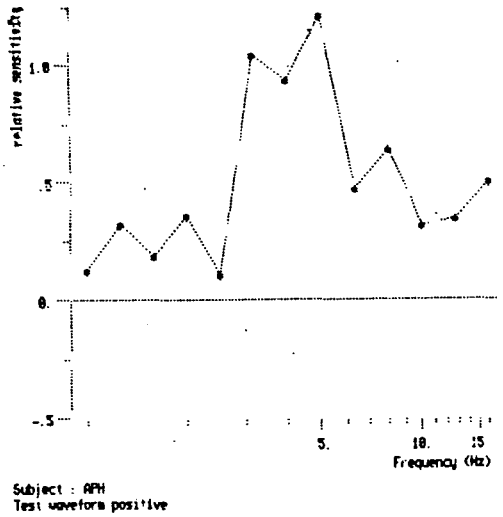

Subject : APH
Test waveform positive

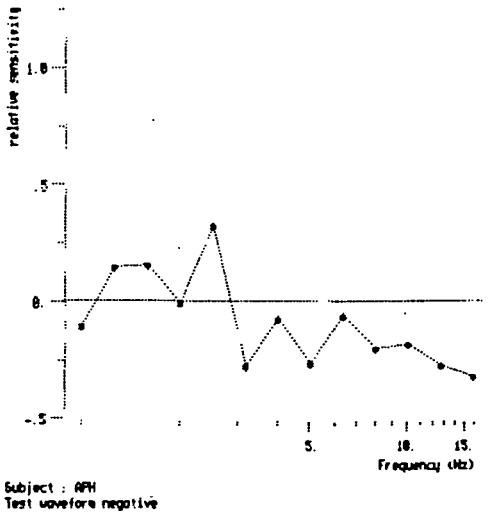

Subject : APH
Test waveform negative

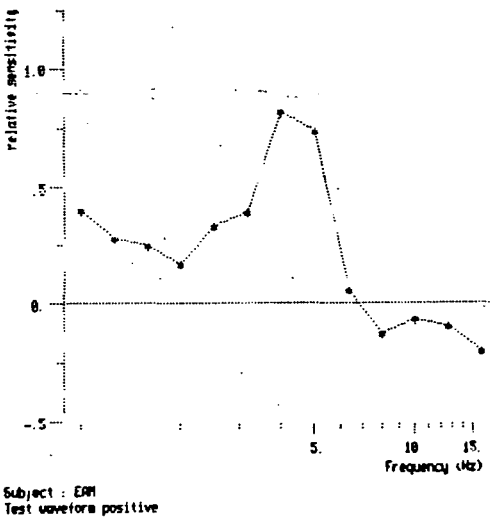

Subject : EAM
Test waveform positive

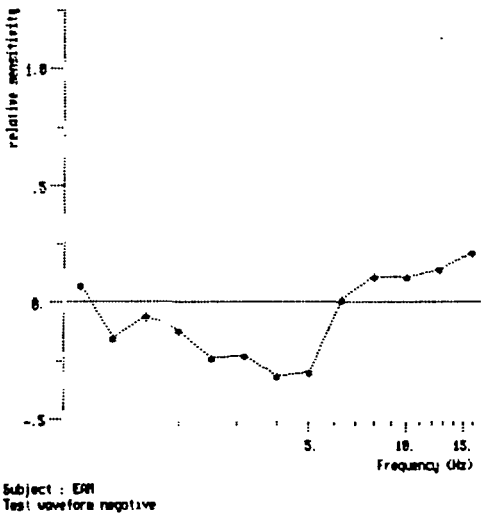

Subject : EAM
Test waveform negative

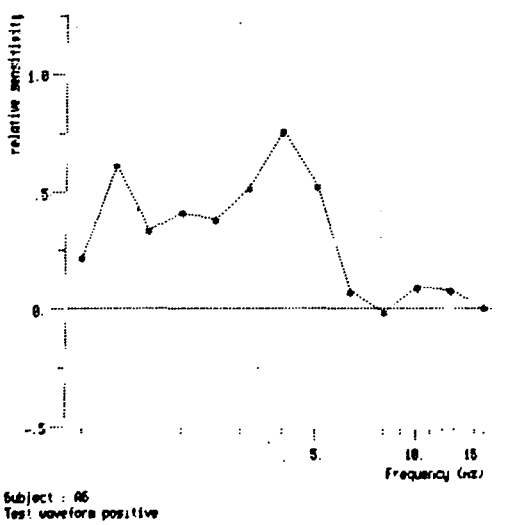

Subject : AS
Test waveform positive

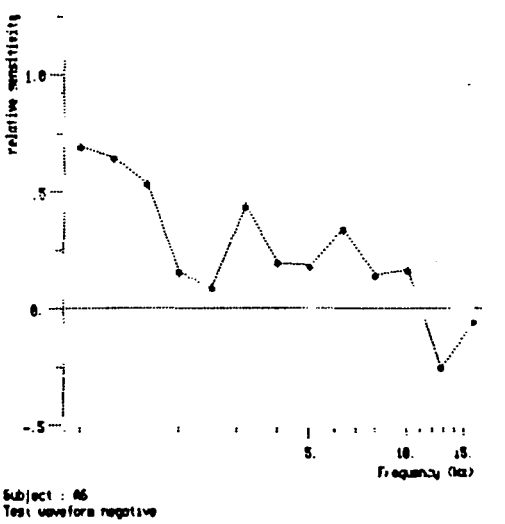

Subject : AS
Test waveform negative

Figure 5.06 : Sensitivity of the polarity - specific mechanisms, relative to that of the non-specific mechanisms. The functions are calculated from the RTE data of Figure 5.04 by Equation 5.02.

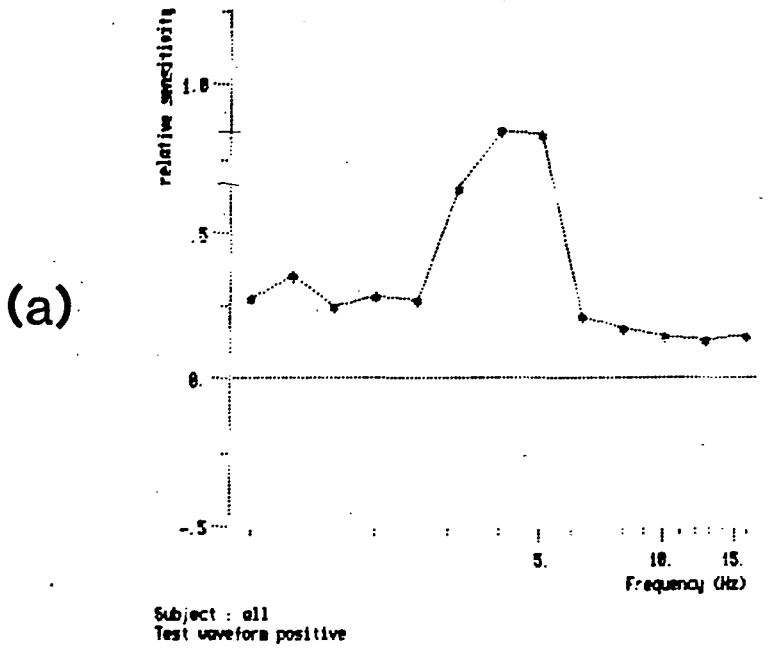

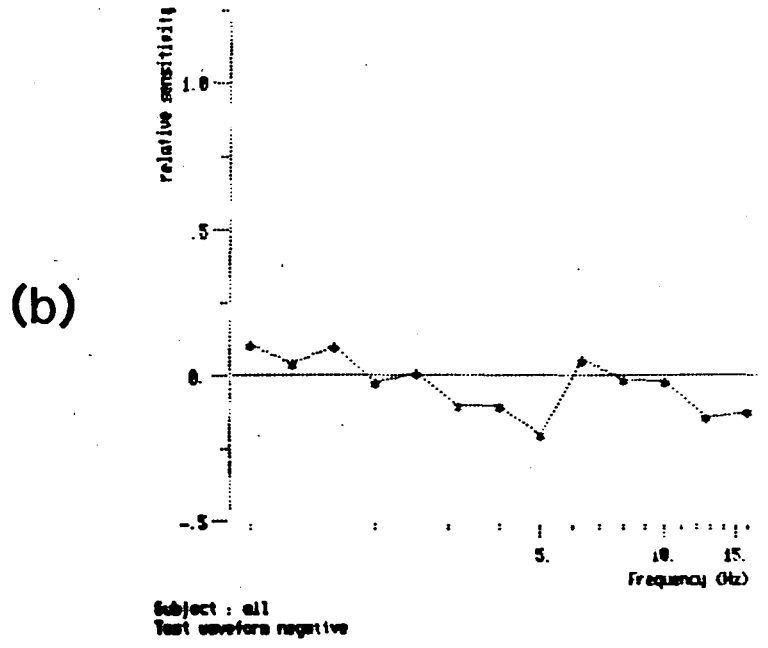

Figure 5.07 : Mean relative sensitivity of the mechanisms selectively sensitive to positive (a) and negative (b) sawtooth flicker, averaged across the functions for three subjects.

(individual subjects) and 5.07b (group mean). Figure 5.07 in particular highlights the surprising difference in polarity selectivity between the detection of positive and negative flicker.

In summary, it appears from this experiment that polarity - selective adaptation with sawtooth flicker is an uncommon phenomemon, occurring only between 3 and 5 Hz when testing with positive slow-phase flicker. However, the observation that polarity-specific adaptation takes place at all is of sufficient interest to justify further analysis, in particular to determine the factors behind the asymmetry between positive and negative sawtooth flicker. Possible reasons for this are discussed in the following section.

5.4 Discussion

The two experiments in this chapter both used the technique of adaptation in an unconventional way, looking at how far adaptation effect generalises to different waveforms, rather than to different frequencies as is typically the case. In both experiments a comparison was made between the condition where adapting and test stimuli were identical, and the condition where the two differ only in one important respect. In the latter condition the stimuli were designed to be as similar as possible in the frequency domain but have different time functions. The purpose of this manipulation was to demonstrate that flicker detection is determined by the temporal aspects of the waveform, independently of spectral composition. Experiment 5.1, comparing the effects of sinewave and squarewave adaptation on sinewave sensitivity, showed that as frequency decreases below about 5 Hz

sinewave detection is determined increasingly by the time function. It was suggested that detection in this region was mediated by a system responsive to slow, nonperiodic luminance change.

Following on from this, Experiment 5.2 used a similar technique to establish whether this 'nonperiodic' system contained independent subchannels selectively sensitive to the direction of luminance change. The results were equivocal but suggested that, at least under certain conditions, threshold is determined by directionally selective mechanisms. However, the expected monotonic increase of relative sensitivity of these mechanisms with decreasing frequency was not observed. One possible reason for this failure may be that the effects were masked by a system sensitive to the fast phase of the sawtooth. One assumption of the adaptation technique is that the test stimulus is detected at threshold by the single channel most sensitive to it. A fundamental problem with the technique of adaptation is that this channel is not necessarily the same under all conditions. We can never be sure whether the RTE function represents the response of a single system, or whether the identity of the most sensitive channel changes with frequency. For the selective adaptation technique of Experiments 5.1 and 5.2 to work, the unadapted channel must be more sensitive than the adapted channel. In Experiment 5.1 this was clearly the case, since low frequency sinewaves contain slow transitions that were increasingly unaffected by squarewave adaptation. The sawtooth stimuli of Experiment 5.2, on the other hand, contain both a slow and a fast phase. It is possible that, at threshold, these stimuli are detected at low frequencies by the fast, step phase rather than the slow phase. This interpretation is supported by the subjective impressions of all subjects that, after adaptation, low frequency sawtooths appear as steps, and that the slow ramp phase is not detectable. This analysis of the results of Experiment 5.2

contains three implications:

1) Sensitivity to the fast phase is much greater than to the slow phase. Even after adaptation step thresholds are lower than gradient thresholds.

2) The step detection system is not directionally selective. If we assume that the step - detectors are adapted by the fast phase of the sawtooth, then the experiment shows that sawtooths of either polarity have an equal effect. This suggests that, at least at threshold, step - detectors are equally sensitive to steps in either direction. This conclusion is supported by the step detection model of Rashbass (1976), including a rectifying element which squares the signal. However it is not consistent with the findings of Krauskopf (1980) who showed that adaptation to sawtooth flicker selectively reduced subsequent sensitivity to luminance steps in the same direction as the fast phase of the waveform.

3) The gradient detection system is not equally sensitive to ramps in either direction. Both the work of Hanly and Mackay (1979) and the evidence of polarity selectivity found in this experiment at midrange frequencies with positive flicker indicate the operation of polarity - selective gradient detectors. The fact that such evidence is only obtained with positive flicker suggests that the 'brightening' channel is more sensitive than the 'darkening' channel since, by the argument of (2) above, the latter is masked by the operation of the step-detecting system.

At a more global level, both experiments provide evidence in favour of the parallel filter of Roufs (1974a) and against a serial filter model of flicker processing (eg Kelly, 1971; Sperling and Sondhi, 1968). No model in which all flicker stimuli pass through a single channel can account for the finding (Figure 5.03a) that at 1 Hz squarewave flicker has no effect on sensitivity to sinewave flicker. The Roufs model, in which a linear bandpass filter operates in parallel with a nonlinear gradient - detection system, is more consistent with these observations.

The experiments in this chapter conclude the series of experiments concerning the detection of periodic stimulation. The experiments in Chapters 3, 4, and 5 have presented evidence that, at least at low frequencies, flicker detection may be modelled by a system sensitive to nonperiodic, nonabrupt luminance change. The logical next step is therefore to investigate these transient signals directly. As a first step, Chapter 6 presents the results of an experiment designed to find the threshold for ramp detection. Experiment 5.1 found that, above a certain frequency sinewaves are mediated by the same system as squarewaves, possibly implying that the sinewave gradients were too short to be detected. Experiment 6.1 investigates this implication by looking at the point at which a ramp becomes discriminable from a step.

CHAPTER 6

WHEN DOES A RAMP BECOME A STEP?

6.1 Introduction

The experiments reported so far have all been concerned with the detection of periodic temporal contrast. From the results, it has been argued that flicker detection is mediated by two separate systems, sensitive respectively to fast and slow luminance change, and that periodicity per se is an irrelevant feature of temporal contrast. Accordingly, the rest of the experiments to be reported now turn to a direct consideration of luminance ramps and steps, with the overall aim of describing the operation of the systems mediating each. As a first step, Experiment 6.1 is a simple investigation of the perceptual boundary between ramps and steps, assumed to reflect the operational division between the two hypothesised systems.

Nonperiodic luminance gradients have received relatively little attention in the literature. The relationship between thresholds for luminance gradients and for sinewaves was first demonstrated for spatial contrast (van der Wildt, Keemink, and van den Brink, 1976). Van der Wildt and Rijsdijk (1979) went on to show that a similar relationship holds for temporal contrast, in the only study to date of thresholds for temporal luminance gradients. They showed that thresholds for sinewave flicker are predictable from thresholds for luminance gradients, provided that the low-pass filtering effects of the visual system are taken into account. Their observation that

this relationship holds across the entire flicker threshold function would appear to suggest that sinewave flicker is detected at all frequencies on the basis of its component gradients, rather than just at low frequencies. However, the experiment was not designed in such a way as to provide information about the structure of the systems mediating contrast detection. Gradient thresholds were obtained using a 2AFC procedure, in which the subject chose between the gradient and a constant luminance stimulus. It is thus not possible to say whether the stimulus was detected as a gradient or as a step, and subjects' perceptions are not reported.

Van der Wildt and Rijsdijk showed that gradients predict flicker thresholds up to about 5 Hz almost perfectly, with a slight but consistent overestimate. Above 5 Hz flicker sensitivity is increasingly overestimated. The authors suggest that this is due to the action of a low - pass filter on the flicker stimuli, implying that the filter precedes the gradient - detecting stage. This filter has the effect of reducing the amplitude (and hence also the gradient) of a periodic stimulus. However, this analysis takes no account of the temporal characteristics of the gradient detectors themselves. The observed pattern is what would be expected if the gradient system were increasingly insensitive to flicker above 5 Hz because of increasing slope and / or decreasing duration.

The gradient threshold function of van der Wildt and Rijsdijk may be accounted for by a fairly simple model. In place of the smooth curve fitted by the authors (Figure 6.01a), the data are well fitted by two straight lines, intersecting at 536 ms (Figure 6.01b). Replotting the data in terms of threshold amplitude rather than gradient (Figure 6.01c) shows that ramp thresholds behave in a broadly similar way to pulse thresholds, both showing evidence of temporal energy integration up to a 'critical duration'.

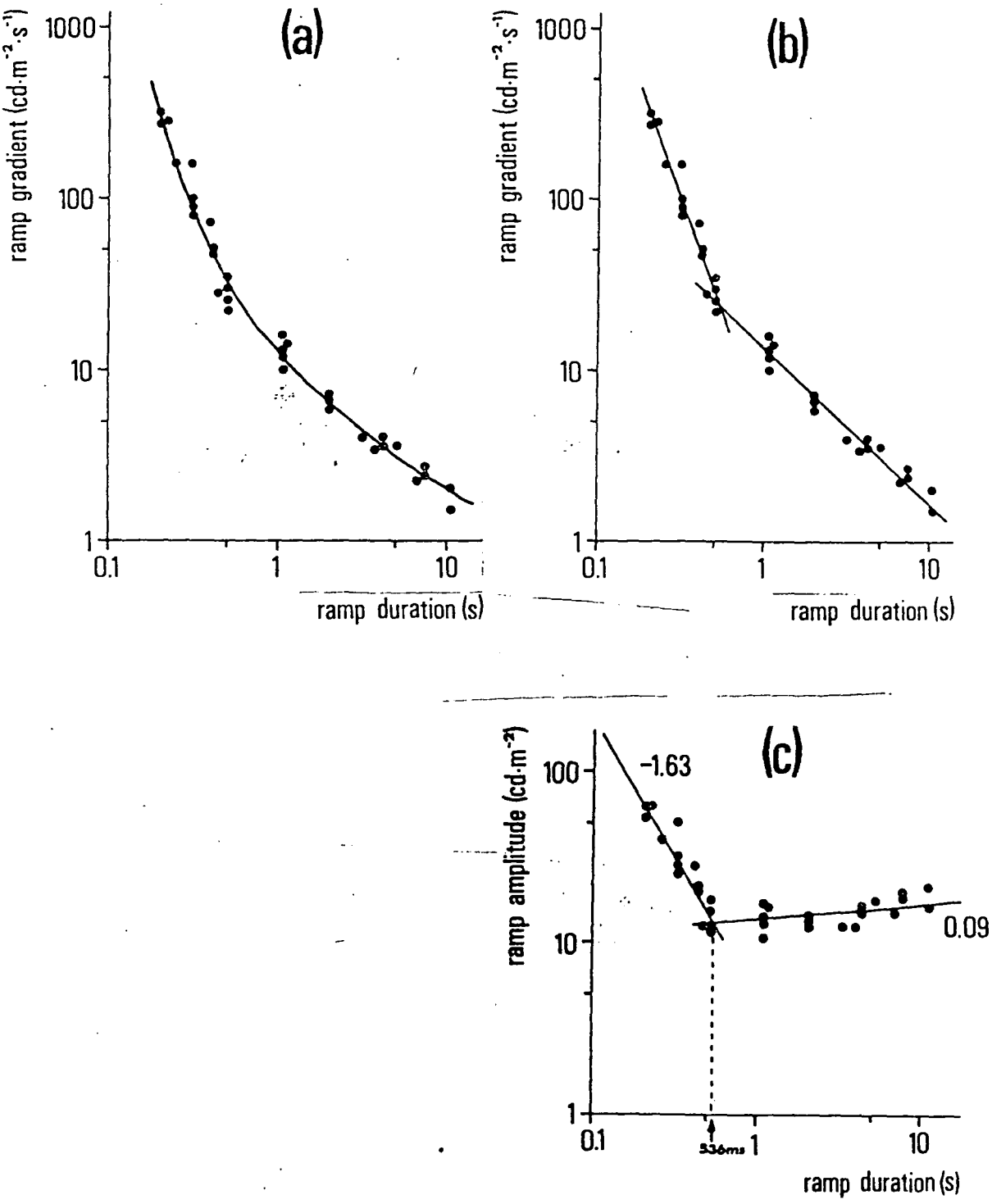

Figure 6.01 : A reinterpretation of the gradient threshold data presented by van der Wildt and Rijsdijk (1979).
(a) Threshold gradient as a function of ramp duration, with the unspecified smooth curve fitted by the authors.
(b) Two least - squares regression lines fitted to the same data.
(c) The data replotted as ramp amplitude, showing that ramp thresholds display Bloch's Law behaviour with an integration period of 536 ms.

Experiment 6.1 is designed to measure the discrimination threshold for ramps, as a function of their gradient. In purely physical terms, a step may be regarded as a ramp of zero duration and infinite slope. However, the finite bandwidth of any physical system means that a step input becomes extended in time, and thus more ramp - like. The two - channel visual system must establish a finite gradient criterion, below which stimuli are processed by the ramp system. Possible mechanisms for this process are considered in the final chapter; the present investigation is restricted to a descriptive level of analysis.

The van der Wildt and Rijsdijk (1979) study measured the simple detection thresholds for a ramp, by comparing it with a constant luminance in a 2AFC design. In contrast, the present experiment measures ramp discrimination threshold, using a 3AFC design in which the comparison stimuli are a step (infinite slope) and a constant level (zero slope). By establishing the boundary conditions for the ramp system, Experiment 6.1 complements the earlier study, providing an estimate of the detection threshold of the ramp system alone. Whereas van der Wildt and Rijsdijk measured threshold gradient as a function of ramp duration, the present experiment measures threshold duration with ramps of various slopes. The

ten gradients tested are chosen to correspond to the slopes of the triangular and trapezoidal flicker waveforms, from 0.5 to 11.31 Hz, in the Velocity condition of Experiment 4.1.

6.2 Experiment 6.1

6.2.1 Apparatus

The details of the visual display are given in Chapter 2. The frame rate and Z-update rate were 1 kHz, and the screen was viewed binocularly with natural pupils.

6.2.2 Design and Procedure

Thresholds for the ten ramp gradients were measured in a single experimental session. A quick and approximate estimate of the threshold for a given gradient was first obtained by the method of adjustment. This was then used as the starting point of a staircase procedure, to give a slower but more accurate final threshold.

The time course of trials in the initial phase of each condition is shown in Figure 6.02a. Ramps were presented repeatedly within a 1 second interval. In the following 500 ms interval the subject adjusted a knob whose setting determined the duration of the ramp in the following interval. All transitions to and from mean luminance in the setting interval were

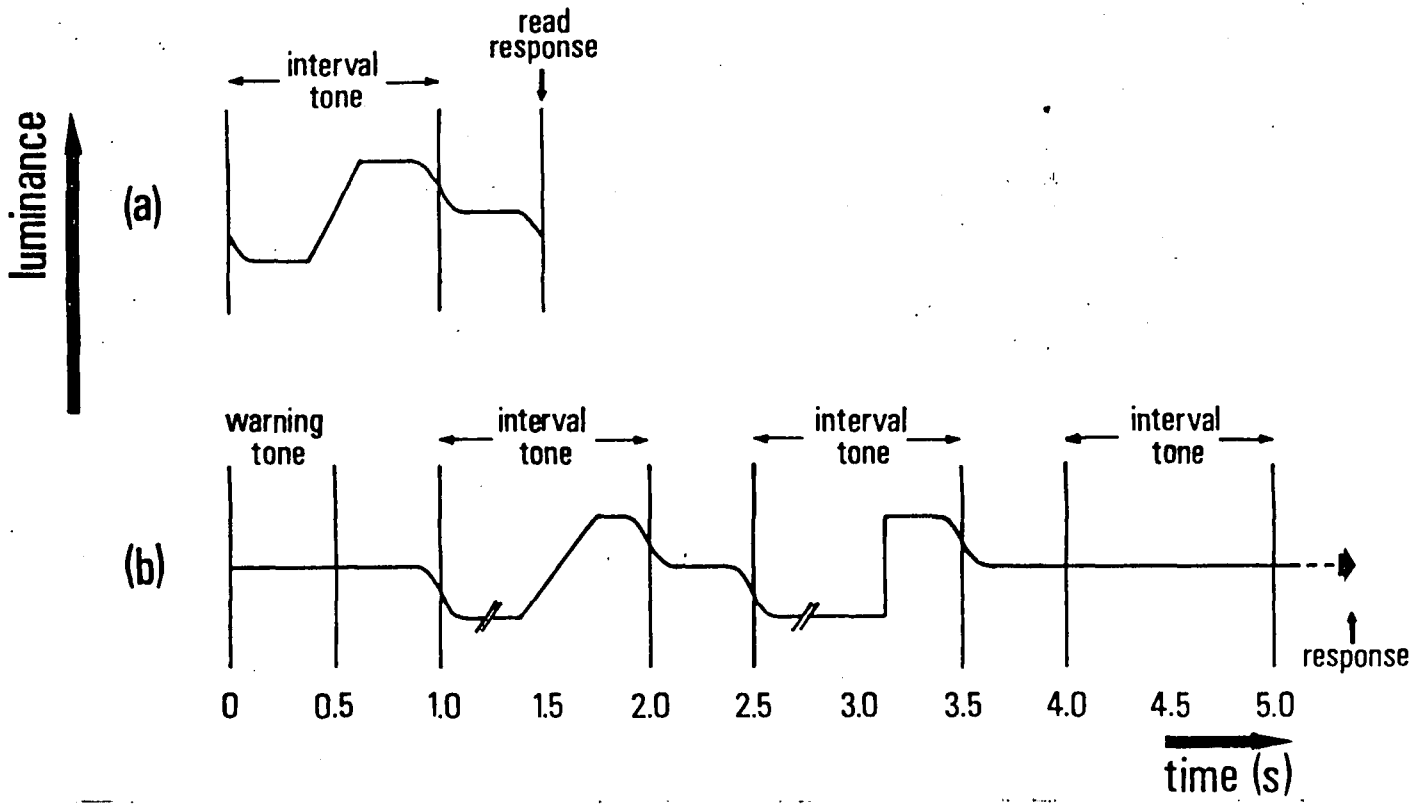

Figure 6.02 : Time course of the trials in Experiment 6.1:
(a) Initial phase. Ramps presented repetitively in 1 second intervals. In the following 0.5 second period the subject adjusted a knob whose setting determined ramp duration in the following interval.
(b) Main phase. Three 1 second intervals containing a ramp, a step, and mean luminance, in random order. The slashes indicate that the onset of both ramp and step was independently randomised within the interval. All periods of mean luminance were windowed with a 250 ms Gaussian function.

smoothed by an integrated Gaussian function of 250 ms duration. Subjects were instructed to adjust the ramp duration until it was just perceptible as a ramp.

When satisfied that an approximate threshold had been reached, subjects pressed a button to initiate the main phase of the condition. These trials consisted of three 1 second intervals, separated by 500 ms intervals during which the screen was at constant mean luminance. The time course of a single trial is shown in Figure 6.02b. On each trial the three intervals contained, in random order:

1) a luminance ramp. The gradient of the ramp was fixed, and the amplitude (and hence duration) determined by a staircase procedure. The temporal location of the ramp was randomised within the interval.
2) a luminance step. The amplitudes of the ramp and step were always equal, the step also being randomly positioned within its interval.
3) constant mean luminance.

Subjects were instructed to choose the interval in which they thought the ramp was presented, requiring a discrimination from stimuli of both infinite and zero gradient. Ramp amplitude on a particular trial was determined by the PEST staircase procedure (Taylor and Creelman, 1967), as modified by Findlay (1978). Since a 3AFC paradigm was being used, the PEST parameters were chosen so as to converge on the 66% correct response level. The staircase terminates when a pre-determined criterion response pattern is reached. The number of trials in a given run is thus variable, and largely determined by the consistency of response. PEST

typically returned a threshold estimate after 40 to 50 trials, with a range from 25 to over 400. On five conditions subject MJM failed to reach the response criterion after several hundred trials, and the condition was terminated without an estimate being made.

After the threshold for one ramp gradient had been measured, the procedure was repeated for the next gradient. Discrimination thresholds were obtained for ten gradients, from 173 to 3920 $cd \cdot m^{-2} \cdot s^{-1}$ at equal logarithmic intervals. Both positive - going and negative - going ramps were presented, to investigate possible polarity - dependent differences in threshold. The conditions were divided into two experimental sessions, with each session devoted to the ramps of a single polarity. The order of ramp gradient within a session and of ramp polarity between sessions was varied across subjects. Three subjects were used: see Section 2.1 for details.

6.2.3 Results

The amplitude at which a ramp is discriminable from both a step and a constant field, as a function of ramp gradient, is shown in the graphs on the left hand side of Figure 6.03. Also shown, in the right hand column of Figure 6.03, are the same data replotted as ramp duration. Two features of the data are immediately clear. Firstly, there is no systematic difference in discrimination threshold for positive - going and negative - going ramps. Secondly, threshold amplitude increases with gradient. Although the two measures are directly related, the duration threshold function appears more irregular because of the scaling of the y axis, chosen to make the data points fill the available space.

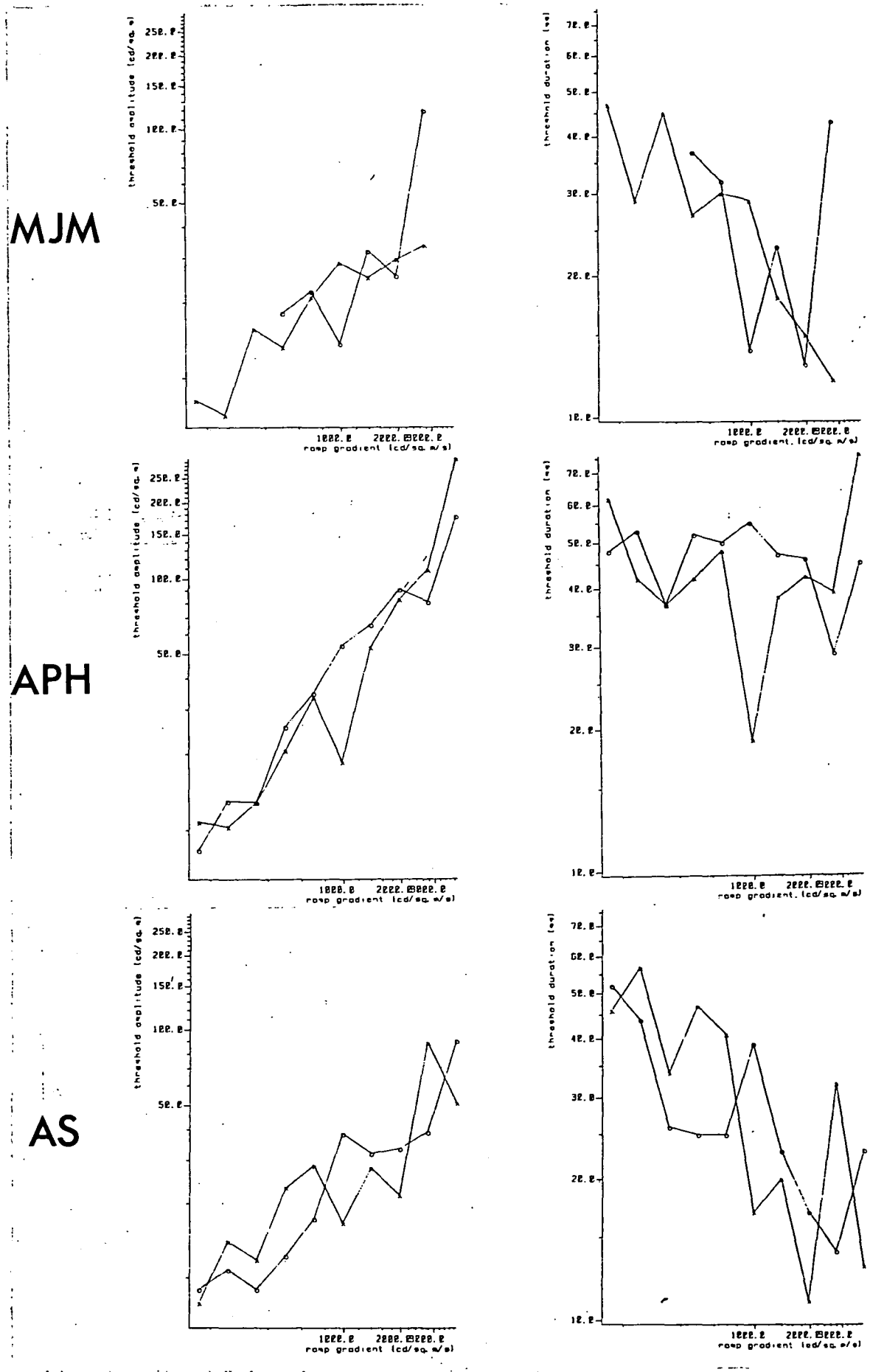

Figure 6.03 : Ramp discrimination threshold as a function of ramp gradient, for each of the three subjects in Experiment 6.1. The data are plotted on the left in terms of amplitude, and on the right in terms of duration. Thresholds for positive - going ramps are plotted with circles, for negative - going ramps with crosses.

The best - fitting linear regression functions across all data points are shown in Figure 6.04. The regression line for the amplitude threshold (Figure 6.04a) has a slope of 0.77, accounting for 75.04% of the total variance. A slope of 1 would mean that, at threshold, all ramps had the same duration, regardless of their gradient. The slopes of the amplitude and duration threshold functions are related, so that the regression line for the duration data (Figure 6.04b) has a slope of 0.77 - 1 = -0.23.

6.3 Discussion

The absence of any significant difference between the results obtained with positive - going and negative - going ramps greatly simplifies modelling of the mechanisms underlying ramp detection. On the basis of this experiment alone it is not possible to choose between a single system, insensitive to ramp polarity, and a pair of symmetrical systems. However, the polarity - specific adaptation effects of Experiment 5.2 would favour the latter interpretation.

The main purpose of Experiment 6.1 is the simple empirical one of establishing the boundary conditions for ramp perception, rather than the development of a theoretical model of the gradient detecting system. Possible mechanisms involved in the mediation of nonabrupt temporal contrast are discussed further in Chapters 8 and 9. The boundaries of ramp perception are measured by the discrimination threshold for ramps, when presented with stimuli of zero and infinite slope. Assuming that perception of a ramp results from stimulation of the gradient system, then the

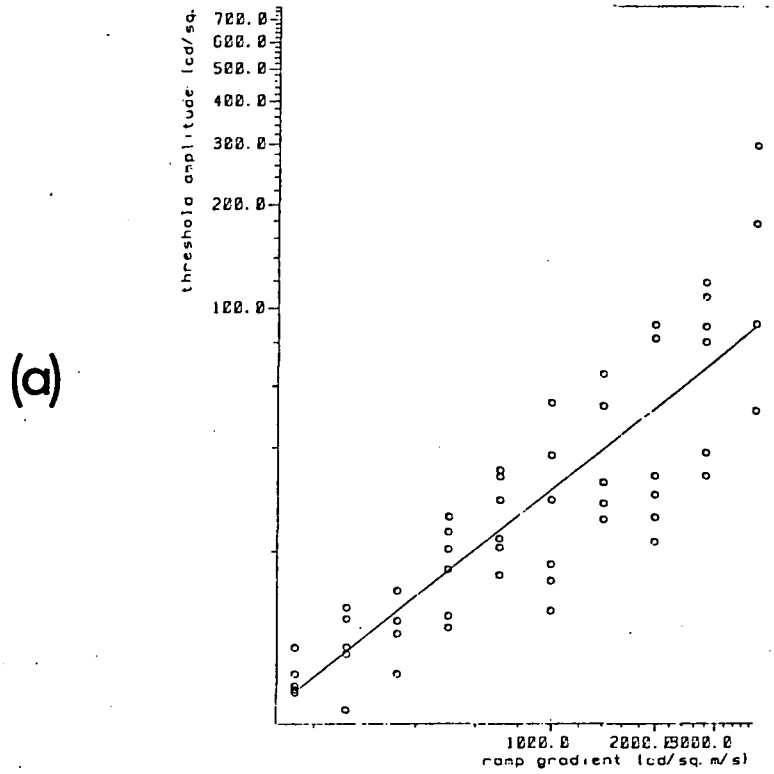

(a)

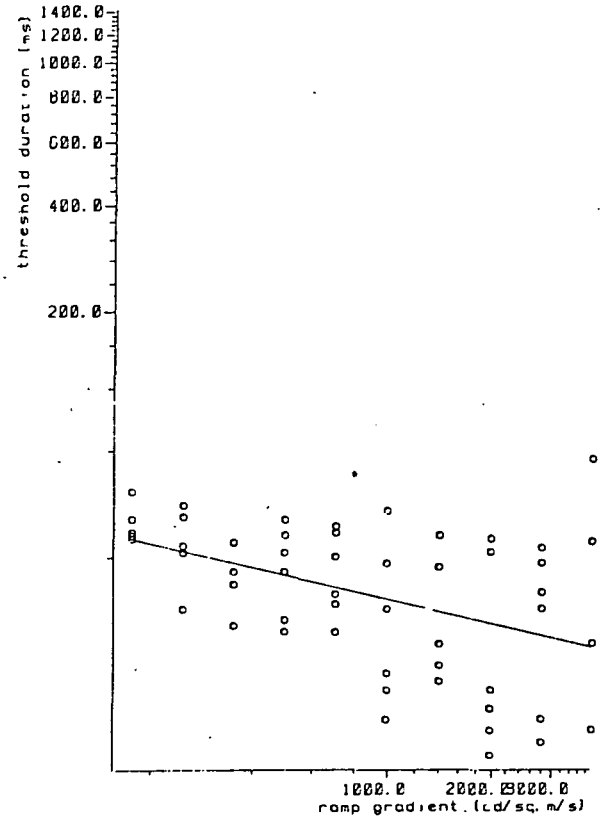

(b)

Figure 6.04 : The threshold data from all three subjects, plotted as amplitude (a) and duration (b), together with the least - squares linear regression lines. The axes are scaled to give equal - size log units. The equations of the regression lines are:

(a) $\log y = 0.77 \log x - 0.83$

(b) $\log y = -0.22 \log x + 2.15$

threshold functions thus obtained may be regarded as threshold functions of the gradient system alone. This is in contrast to the ramp detection thresholds of van der Wildt and Rijsdijk (1979), which confounded the ramp and step systems by disregarding subjects' perceptions of the stimulus.

The pooled data of Figure 6.04a show that the temporal contrast threshold of the ramp system increases with increasing gradient. The function is linear in log-log co-ordinates, with a slope of less than 1. A slope of 1 would mean that the system has a fixed temporal window, with any change in level taking place wholly within the window being seen as a step. As Figure 6.04b shows, log threshold duration decreases linearly with increasing log gradient, but with a fairly shallow slope. If the data were replotted as amplitude vs duration, as was done for the data of van der Wildt and Rijsdijk in Figure 6.01c, the regression line would have a slope of -3.36. This figure, while less than the vertical line of a fixed window system, is considerably greater than the slope of -1.63 derived from the earlier study, suggesting that the two experiments are looking at different processes.

Van der Wildt and Rijsdijk (1979) compared their ramp thresholds with thresholds for sinewave flicker, showing that a close relationship exists between the two across the flicker frequency spectrum. The arguments for two systems presented throughout this thesis would suggest that, when the ramp system is considered alone, flicker sensitivity would be increasingly underestimated above about 5 Hz, since in this region flicker perception is mediated largely by the step system. In Figure 6.05, the sinewave flicker thresholds predicted from ramp thresholds are plotted, together with an actual flicker sensitivity curve obtained under similar conditions. The

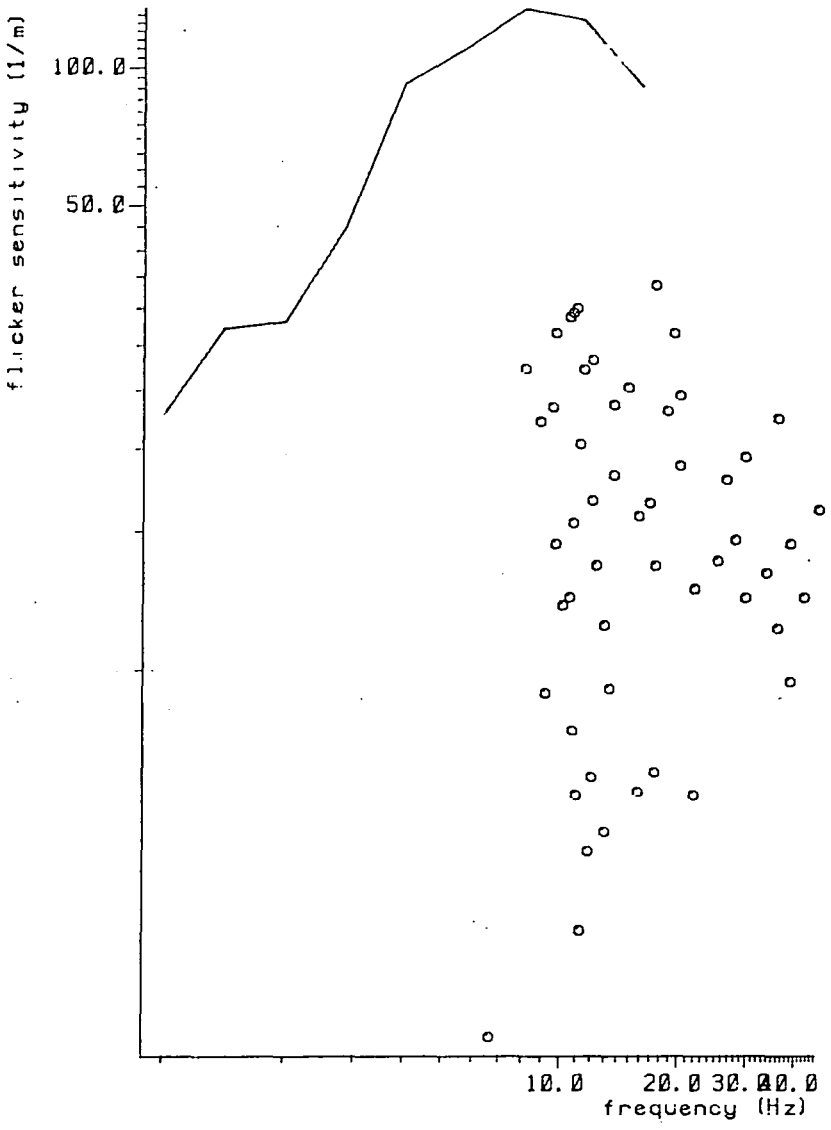

Figure 6.05 : A comparison between measured flicker sensitivity and that predicted from ramp thresholds. The data points are derived from those of Figure 6.06 as follows. Peak - peak flicker amplitude is assumed equal to ramp amplitude, and converted to modulation by dividing by 2.Lmean [2 x 122 cd/sq.m = 244]; sensitivity is the reciprocal of threshold modulation. Ramp duration is assumed equal to half a flicker cycle, so that f = 1/(2t) where f is frequency and t is ramp duration. Equal gradient contours become positive diagonals on these axes. The solid line shows actual sinewave flicker sensitivity, from 1 to 16 Hz, measured under similar conditions in Experiment 5.1.

expected flicker thresholds are derived by the same method used by van der Wildt and Rijsdijk, in which the sinewave is approximated to a triangular waveform and effects of probability summation are disregarded. This analysis shows that high frequency flicker thresholds are indeed higher than would be expected from the ramp system alone, as predicted, providing further evidence for the operation of two systems in the detection of sinewave flicker. While not directly conflicting with the conclusions of van der Wildt and Rijsdijk, this confirms the suggestion that the methods of the earlier study had confounded measurement of the step and ramp systems.

Simple thresholds such as these may be seen as a one-dimensional measurement of the peak excursion of the internal response to a stimulus. In the remaining two experimental chapters we extend the investigation of nonperiodic stimuli into two dimensions by looking at the time course of the internal response. In addition we attempt to increase the power of the findings by looking for the first time at suprathreshold stimuli.

CHAPTER 7

WHAT IS THE INTERNAL RESPONSE TO A STEP?

7.1 Introduction

7.1.1 Internal responses

Linear systems theory allows us to predict the internal response to an arbitrary external stimulus from the modulation and phase transfer functions. However, the necessary assumptions about linearity and phase are not unquestionably valid under all conditions. For this reason it is desirable to try to measure the internal (ie post-filter) representations of visual stimuli directly, rather than infer them from general systems properties. The three experiments reported in this and the following chapter form a sequence of studies with the end goal of measuring the time course of the response to a series of suprathreshold luminance ramps. These experiments have been inspired by a technique devised by Jacques Roufs at IPO in the Netherlands for the probing of internal responses to subthreshold stimuli (Roufs and Blommaert, 1975; 1981). The present experiments aim to extend the Roufs technique from subthreshold steps and pulses to suprathreshold ramp stimuli. Chapter 7 examines the implications of some essential modifications to the Roufs technique; Experiment 8.1 then goes on to apply the method to ramps.

7.1.2 Subthreshold summation

One common technique for the psychophysical investigation of internal responses is that of subthreshold summation. This method consists of taking the stimulus to be studied (the test stimulus) and presenting a short pulse (the probe stimulus) at various intervals before, during and after the test. The test stimulus is below threshold, and the threshold for the probe stimulus is measured as a function of the time between onsets (stimulus onset asynchrony: SOA). The underlying reasoning is that the responses to the two stimuli will summate to determine the combined threshold, which is assumed to be invariant with SOA. Thus as the probe is moved relative to the test, variations in its threshold will reflect the response to the test stimulus.

This type of temporal summation technique was first described by Granit and Davis (1931), using a 0.6 ms test pulse of fixed amplitude followed by a probe pulse of the same duration. They found that threshold amplitude of the probe increased monotonically with SOA, following an exponential function for the first 30 ms and then a linear function up to 80 ms. This function may be regarded as the inverse of the excitation pattern following the offset of the test pulse. Thresholds were not measured for probe pulses occurring before or during the test, nor was the response followed after 80 ms. Possibly for these reasons the biphasic and triphasic responses reported in later studies were not observed.

More recent studies of subthreshold temporal summation have tended to use pairs of stimuli with a fixed amplitude ratio, rather than the fixed amplitude test of Granit and Davis. Bouman and van den Brink (1952) used two identical pulses of fixed amplitude and duration and, using

probability of detection as an index of summation, found once again a monotonic transition from complete to zero summation. Ikeda (1965) measured temporal summation as a function of SOA for pairs of positive pulses, pairs of negative pulses, and pairs of opposite - sign pulses, using a range of amplitude ratios. Her 'summation index' is a measure of the integration of the two responses, based on the thresholds of the stimuli in combination relative to their thresholds when presented alone. With pairs of same - sign pulses summation is complete at short intervals, and based on probability alone at long intervals. At intermediate intervals summation decreases to reach a minimum of zero at about 50 ms SOA, suggesting that inhibition is occurring, and hence that the internal response is biphasic. Ikeda suggested that the monophasic responses found in earlier summation studies were due to the use of lower luminances and smaller stimuli, both known to reduce the bandpass characteristics of the temporal MTF (Kelly, 1971). A hypothetical impulse response was derived from the results of varying the amplitude ratio and of using pairs of opposite - polarity pulses. This impulse response is biphasic, asymmetrical with respect to time, but approximately mirror - symmetrical for positive and negative pulses.

7.1.3 Perturbation

The interpretation of two-stimulus thresholds as internal responses depends on a constant relationship between the onset of the probe stimulus and the peak of the combined response, ie the point that determines its threshold. If the individual responses do not have a single dominant phase, then the peak of the combined response may be caused by different combinations of peaks as the responses are shifted relative to each other. This difficulty was identified by Roufs and Blommaert (1975, 1981) in the

development of their 'perturbation' technique. This variant of subthreshold summation has two main features:

a) the probe stimulus is chosen so as to have one dominant phase.

b) the amplitude ratio is fixed so that the amplitude of the test stimulus is always small compared to that of the probe. Typically a test : probe ratio of 0.2 is used.

Once again it is assumed that the two responses sum linearly, and that detection occurs when the amplitude of the combined response reaches a fixed criterion level. The perturbation technique is designed to reduce the probability of unwanted combinations of peaks reaching threshold, so that the extreme value of the combined response will always coincide with that of the probe response.

The principles of the technique, as described by Roufs and Blommaert (1981), are syntactically complex but semantically fairly straightforward. It is based fundamentally on the theorem that, at threshold:

$$(A_p \cdot R_p) + (A_t \cdot R_t) = d \qquad \text{Equation 7.01}$$

where A is the amplitude of the stimulus,

R is the gain of the internal response at a given point in time,

p and t relate to the probe and test stimuli respectively,

d is the internal detection criterion.

As internal responses, both R_p and R_t vary as a function of time: the final aim is to describe the R_t function. R_p may be considered to be a fixed value, rather than a complete function, since we are concerned only with the peak of the probe response. If the two stimuli have a constant amplitude ratio, r, such that $A_t = r \cdot A_p$, then Equation 7.01 simplifies to

$$\frac{R_p}{d} + \frac{r \cdot R_t}{d} = \frac{1}{A_{p\ comb}} \qquad \text{Equation 7.02}$$

where $A_{p\ comb}$ is the threshold amplitude of the probe pulse in combination with the test stimulus. In other words, when the probe and test are presented together the sum of their responses, measured in terms of the detection threshold, is a linear function of sensitivity to the probe stimulus, which can be measured directly.

Measuring probe threshold as a function of probe - test SOA, Equation 7.02 can be used to obtain the shape of the test response, superimposed on a pedestal of peak probe response. However, because the effects are so small, and the investigations thus required so prolonged, potentially severe problems can arise from drifts in sensitivity (d) both within and between sessions. To counteract these, the absolute value of Equation 7.02 may be converted to a dimensionless normalised response by dividing by R_p / d:

$$\frac{R_t}{R_p} = \frac{1}{r}\left(\frac{1}{A_{p\ comb}} \cdot \frac{d}{R_p} - 1\right) \qquad \text{Equation 7.03}$$

The left-hand term represents the test response measured in terms of the peak probe response. When the probe stimulus is presented alone, ie when $A_t = 0$, Equation 7.01 shows that its threshold amplitude ($A_{p\ alone}$) equals d / R_p. Thus Equation 7.03 can be rewritten as

$$\frac{R_t}{R_p} = \frac{1}{r}\left(\frac{A_{p\ alone}}{A_{p\ comb}} - 1\right) \qquad \text{Equation 7.04}$$

This drift - correcting technique is based on the assumption that changes in sensitivity will affect both probe thresholds equally. The method of Equation 7.04, using a probe in combination and a probe alone, is a special case of the situation where the probes are in combination with two test stimuli of different ratios. The normalised response for the general case is obtained by solving Equation 7.02 for two values of r, r_1 and r_2. Equation 7.04 then becomes:

$$\frac{R_t}{R_p} = \frac{A_{p2} - A_{p1}}{r_1 A_{p1} - r_2 A_{p2}} \qquad \text{Equation 7.05}$$

where the subscripts 1 and 2 refer to the different test stimuli. In Equation 7.04 $r_2 = 0$, and hence $A_{p2} = A_p$ alone. Further simplification is possible if $r_1 = -r$ and $r_2 = +r$, that is if probe threshold is measured with two test stimuli of equal amplitude ratio but opposite sign. In this case Equation 7.05 reduces to

$$\frac{R_t}{R_p} = \frac{1}{r} \cdot \frac{A_{p-} - A_{p+}}{A_{p-} + A_{p+}} \qquad \text{Equation 7.06}$$

where A_{p+} and A_{p-} are the thresholds of the probe pulse in combination with the positive and negative test stimuli respectively.

Using this analysis, Roufs and Blommaert (1975, 1981) obtained a triphasic impulse response, in contrast to the biphasic response of Ikeda (1965) and the monophasic response of Bouman and van den Brink (1952). It is possible that this disagreement is due to differences in pulse duration (Roufs and Blommaert: 2 ms; Ikeda: 12.5 ms) and luminance level (1200 td vs 328 and 61.2 td); indeed an impulse response obtained by Roufs and

Blommaert at 2 td seems to be essentially biphasic. Another possibility, noted by Watson (1982), is the failure by Roufs and Blommaert to take account of probability summation effects. Using estimates of probability summation obtained by Quick (1974), Watson showed that this effect could make a biphasic impulse response appear to be triphasic in combination with a second impulse response.

7.1.4 Experiment 7.1

In addition to their impulse response, Roufs and Blommaert used the perturbation method to measure the response to a luminance step. Just as the step is the integral of an impulse function, they showed that the step response is the integral of the pulse response, confirming the linearity of the system being measured. Experiment 7.1 is essentially a replication of this investigation of the step response, carried out under the conditions used in the other experiments in the sequence. Both the visual display, its type and characteristics, and the psychophysical procedure used differ greatly from those of Roufs and Blommaert. As the starting point to the study of suprathreshold ramps in Experiment 8.1, it is designed to establish that the summation technique is valid in these particular conditions, using a paradigm with an expected outcome.

One methodological change is made to the basic Roufs technique described in the previous section. Instead of probing two test stimuli of different sign with a single probe pulse, the situation is reversed so that a single test stimulus is measured with two probes of opposite sign. It has already been shown (Roufs, 1974a; Roufs and Blommaert, 1975) that the responses to steps and pulses of opposite sign are mirror - symmetrical, so

that inverting a step stimulus may be assumed to invert the response. However, this symmetry has not yet been shown to be true of the response to a ramp. The results of these experiments are intended to be comparable with those of Experiment 8.1, in which the test stimulus is a ramp. Thus the design of a single polarity test with opposite polarity probe pulses was adopted to capitalise on existing data. Experiment 8.1 could then concentrate on the effects of varying ramp gradient, rather than the less interesting problem of ramp polarity. The reasoning in Section 7.1.3 is unaffected, since Equation 7.01 is true for all combinations of probe and test polarity. However, it does require the additional assumption that changes in sensitivity will affect decremental and incremental thresholds (d_+ and d_-) symmetrically. The derivation of test response given in Equation 7.06 remains valid, provided that the absolute values of probe thresholds are taken:

$$\frac{R_t}{R_p} = \frac{1}{r} \cdot \frac{|A_{p-}| - |A_{p+}|}{|A_{p-}| + |A_{p+}|} \qquad \text{Equation 7.07}$$

where A_{p+} and A_{p-} are the thresholds of positive and negative probes respectively.

7.1.5 Experiment 7.2

In the second experiment in this chapter, the test stimulus is once again a step. However, two further modifications are introduced to the basic Roufs technique:

1) The step has a fixed absolute amplitude, rather than being a fixed

ratio of the probe pulse. The amplitude is set so that the stimulus is below threshold when presented alone. The ramp stimuli to be investigated in Experiment 8.1 are specified in terms of duration and gradient, and hence have a fixed amplitude. Experiment 7.2 will establish whether the response revealed by probe techniques to a fixed amplitude stimulus is comparable with that to a fixed ratio stimulus, obtained in Experiment 7.1.

2) The procedure is designed to measure the discrimination threshold for the pulse and test combination against the test stimulus alone. The original Roufs method measured simple detection threshold for the combination against a null stimulus. This approach is restricted to subthreshold test stimuli; since subsequent experiments use both sub- and supra-threshold stimuli, it is desirable to establish at this stage the implications of the discrimination procedure.

The method used in this experiment may be seen as a signal detection paradigm, with the test stimulus providing the noise against which the probe must be detected. This technique is known as masking, and is a common method in auditory psychophysics. With the test stimulus in both intervals, it will compete with the probe stimulus rather than co-operate with it as in subthreshold summation. The presence of a test stimulus will thus cause probe threshold to increase in the masking situation and decrease in the summation situation. The amount of threshold elevation provides a measure of the power of the test response in the same channel as the probe response. The reversal of the effects of the test stimulus on probe thresholds has the effect of changing the polarity of the derived internal response.

Measuring the threshold elevation due to masking requires a different analysis than the summation analysis of Equation 7.07. It is assumed that, at threshold, it is the signal / noise ratio that is constant, rather than the signal amplitude. That is

$$\frac{S_p}{N_r + N_t} = k \qquad \text{Equation 7.08}$$

where S_p is the probe signal (equal to $A_p \cdot R_p$), N_r is random background noise, and N_t is the 'noise' due to the test stimulus. If k is constant for all combinations of probe and test, then

$$\frac{S_{p\ comb}}{N_r + N_t} = \frac{S_{p\ alone}}{N_r + 0} \qquad \text{Equation 7.09}$$

which may be rearranged to give

$$\frac{N_t}{N_r} = \frac{S_{p\ comb}}{S_{p\ alone}} - 1 = \frac{A_{p\ comb}}{A_{p\ alone}} - 1 \qquad \text{Equation 7.10}$$

The left - hand term gives the internal response due to the test stimulus, measured in terms of the background noise. This figure will be referred to as the normalised response, since it is directly analogous to the scaling by the probe threshold of Roufs (Equation 7.03). Note, however, that the polarity of this function is opposite to that derived from the Roufs formulation, due to the opposite effects of masking and summation. Measuring the response in log units, we arrive at the following formula for the normalised response (NR):

$$NR = \log(A_{p\ comb} / A_{p\ alone}) \qquad \text{Equation 7.11}$$

Note the close similarity between this and the relative threshold elevation (RTE) measure used in the adaptation experiments in Chapters 4 and 5.

7.2 Experiment 7.1

7.2.1 Apparatus

As mentioned in Chapter 2, the visual display used in Experiments 7.1, 7.2, and 8.1 differed in several respects from that of earlier experiments. The display monitor was viewed through binocular 3 mm artificial pupils, giving a mean retinal illumination of 47.6 td. The maximum available pulse amplitude, measured as a deviation from this mean level, was $\pm$33.5 td. The screen was masked with black card to give a sharp - edged circular field of 5° diameter. The display was refreshed at a frame rate of 1 kHz.

7.2.2 Design and Procedure

Experiment 7.1 measures the threshold for detection of both a positive (incremental) and a negative (decremental) luminance pulse, in combination with a luminance step. The independent variable is the interval between the onsets of the two stimuli (SOA). Threshold estimates were made using the Adaptive Probit Estimation (APE) procedure of Watt and Andrews (1981).

This procedure samples responses from within a moveable range of stimulus values, and fits a probit curve (Finney, 1948) to the observed response probabilities. To determine whether the fitted psychometric curve is a valid description of the data points, they are then checked for normality of distribution with a chi-squared test. The curve parameters allow the stimulus level corresponding to any given response probability to be estimated. The threshold was chosen as 1 standard deviation away from the 'point of subjective equality' (PSE), that is the inflection point of the curve. This corresponds to a response probability of approximately 84%. The APE procedure has three important advantages in the context of these experiments:

a) optimum information use. The final probit curve parameters are based on information gained throughout the run. The power : length ratio obtainable is thus in principle higher than that from conventional staircase procedures with a limited 'memory'.

b) automatic correction for interval - bias. In a two - alternative forced choice design (2AFC), the psychometric function may be considered as the probability of responding with a given interval choice (eg P(2)), as stimulus level varies from high in one interval through zero to high in the other interval. Any interval bias will shift the curve along the stimulus dimension, but will not affect its slope. The 1 s.d. threshold point returned by APE is measured relative to the curve's inflection point, and is thus independent of interval bias. The stimulus interval on a particular trial is selected by APE so as to equalise <u>response</u> probabilities between the intervals. This contrasts with conventional 2AFC procedures in which <u>stimulus</u> probability is equal in the two intervals.

c) thresholds may be obtained outside the stimulus range tested. This unique feature of APE is due to its ability to extrapolate the probit curve outside the confines of the data points. For this to be successful the points on which the curve is based must be extremely well distributed. Even so the thresholds thus obtained must be treated more cautiously than those within the tested range. Although the threshold pulses in Experiments 7.1 and 7.2 were generally well within the 33.5 td range available, the unexpected magnitude of the effects in Experiment 8.1 resulted in thresholds which were much greater than the luminance range of the oscilloscope display.

Each experimental session was started with at least 5 minutes adaptation to the display screen at mean luminance. The design of an individual trial is shown in Figure 7.01. Two 500 ms intervals were presented, one containing the probe pulse and test step, the other containing constant mean luminance. The subject was required to indicate in which interval they thought the stimuli occurred. As noted above, the stimulus level for each trial was selected by the APE procedure.

The response immediately initiated the next trial; incorrect responses were signalled by a tone. The amplitude of the probe was five times that of the step ($r = 0.2$) throughout the experiment. The interval between the stimulus onsets (SOA) was fixed within a run, but the location of the stimuli was randomised within the chosen interval. To minimise drifts in sensitivity, thresholds for positive and negative flashes were measured simultaneously, using two randomly interleaved APEs. If the responses obtained on either of these reached the $p < 0.05$ level on the chi-square

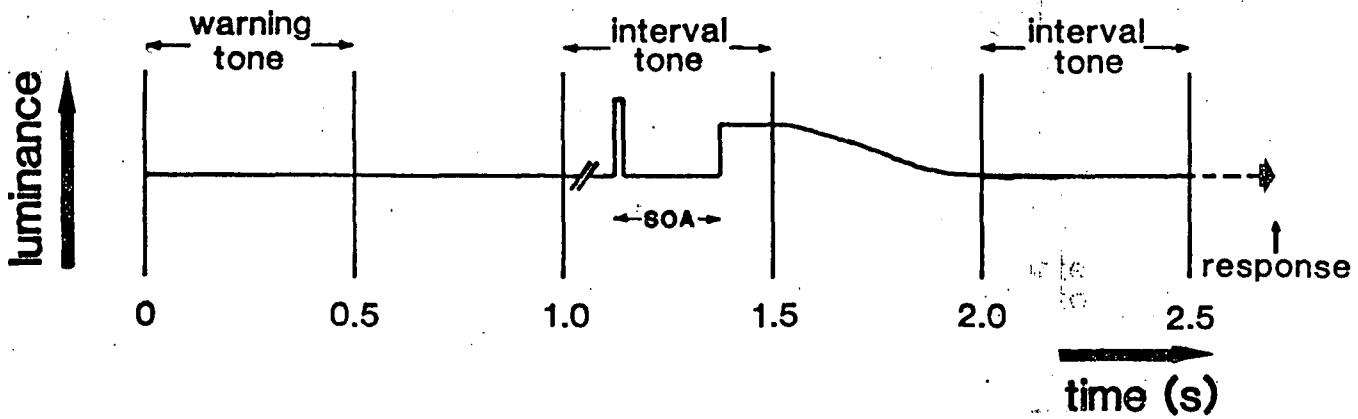

Figure 7.01 : Time course of the trials in Experiment 7.1. The stimulus onset asynchrony (SOA) between the 5 ms probe pulse and the test step is fixed within a session, and the stimulus pair presented in one of the two 500 ms intervals. The slashes indicate that the timing of the stimulus was randomised within the interval. Luminance returns to the mean level by a Gaussian function in the 500 ms following the stimulus interval. The subject's response initiates the next trial.

test, both thresholds were discarded and that SOA condition repeated. Each threshold estimate was made after 120 trials, the total of 240 trials per condition lasting approximately 30 minutes.

SOA is measured relative to the test stimulus onset, so that a negative figure indicates the probe preceding the step. With subject APH thresholds were measured at every 20 ms from -110 ms to +110 ms SOA, and additionally at every 10 ms between ±30 ms. Subject AS was tested over the range -50 ms to +100 ms at 10 ms intervals. SOAs were presented from negative to positive for one subject, with the order reversed for the other subject. Typically three SOA conditions were run within a single session.

The duration of the probe pulse must be chosen so that it lies within the integration period of the system being measured. A pilot experiment was carried out to measure the threshold amplitude of a positive pulse as a function of its duration, under identical conditions to those of the main experiment. Experimental procedure was as described above. The results, shown in Figure 7.02, follow the expected Bloch's Law function, with a 'critical duration' or integration time of about 100 ms. On the basis of these results it was decided to use a probe pulse of 5 ms, with a baseline threshold of approximately 5 td, for all subsequent experiments.

7.2.3 Results

The thresholds of positive and negative pulses are shown for subject AS in Figure 7.03 (a and b) and for subject APH in Figure 7.04 (a and b). Data from the two subjects are plotted on different scales because of the large differences in absolute sensitivity. The SOA axis is arranged to

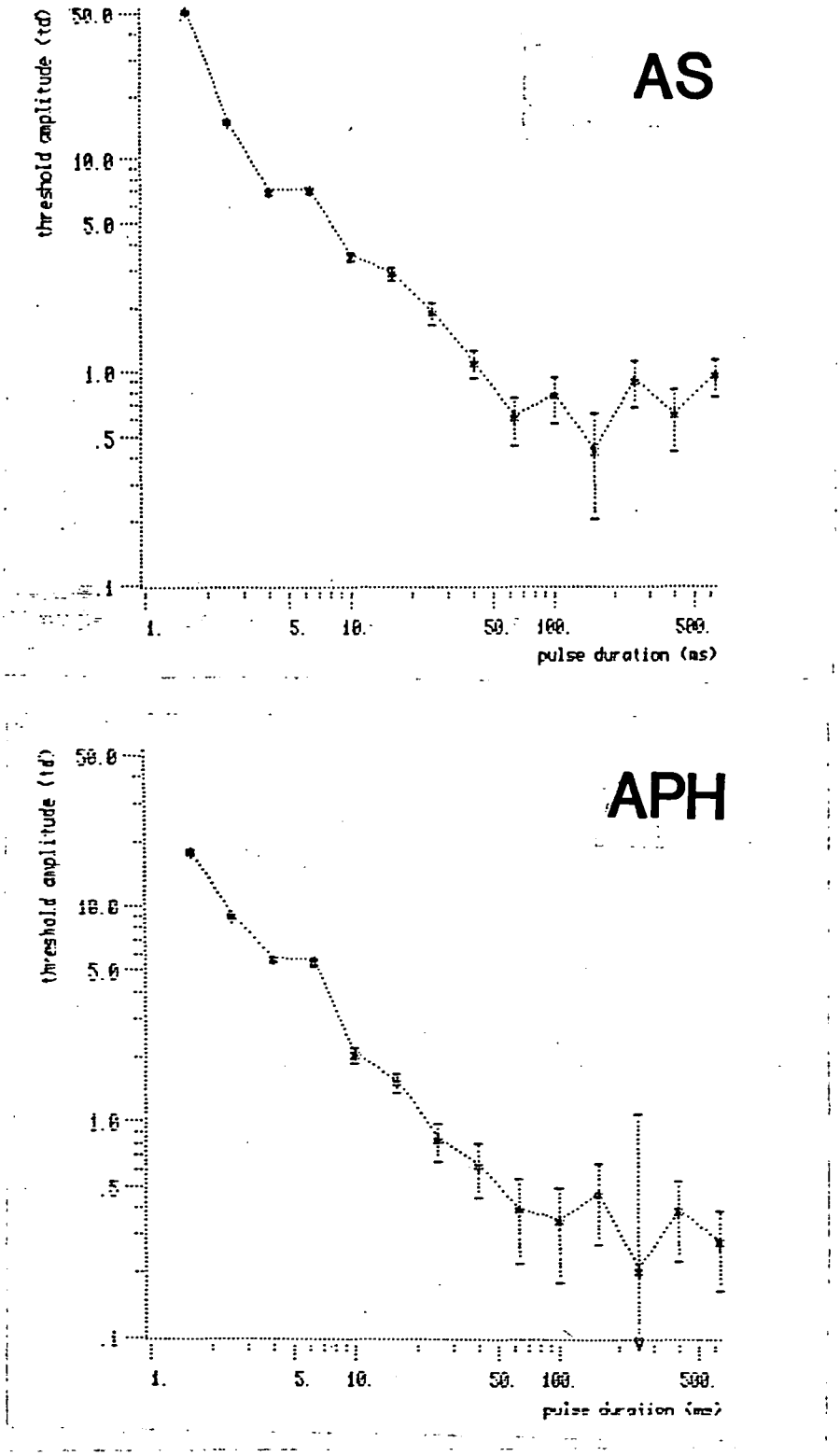

Figure 7.02 : Threshold luminance of a luminance pulse as a function of its duration, for two subjects. These are the results of a pilot experiment to determine the temporal integration period of the visual system under the conditions used in subsequent experiments. On the basis of these data, a probe pulse duration of 5 ms was selected.

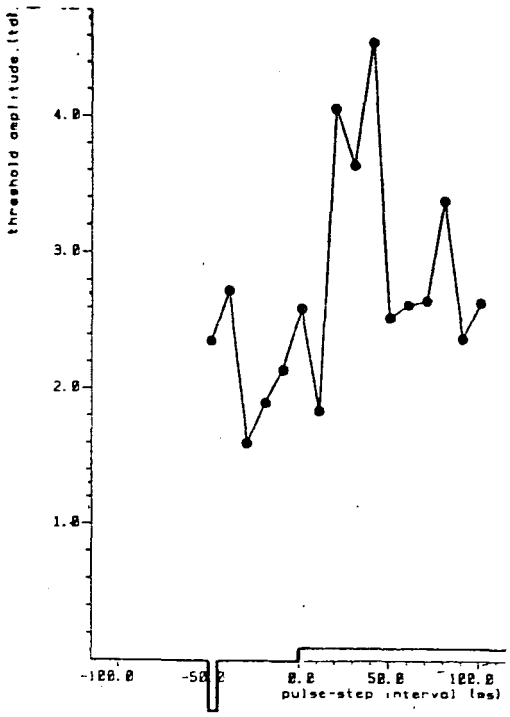

(a)

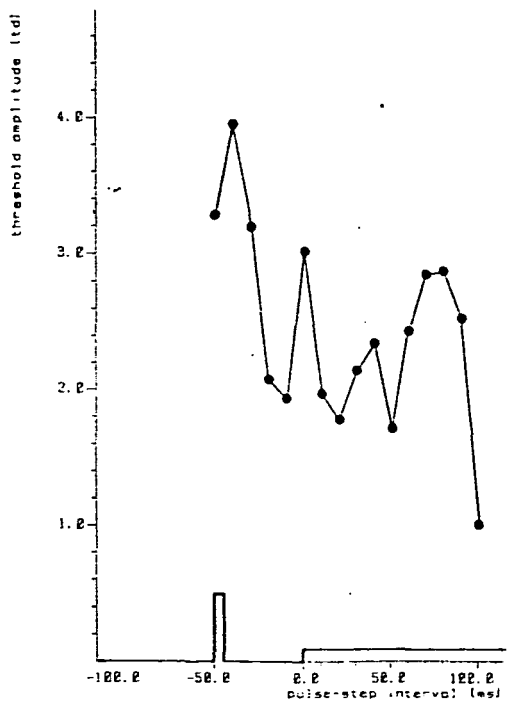

(b)

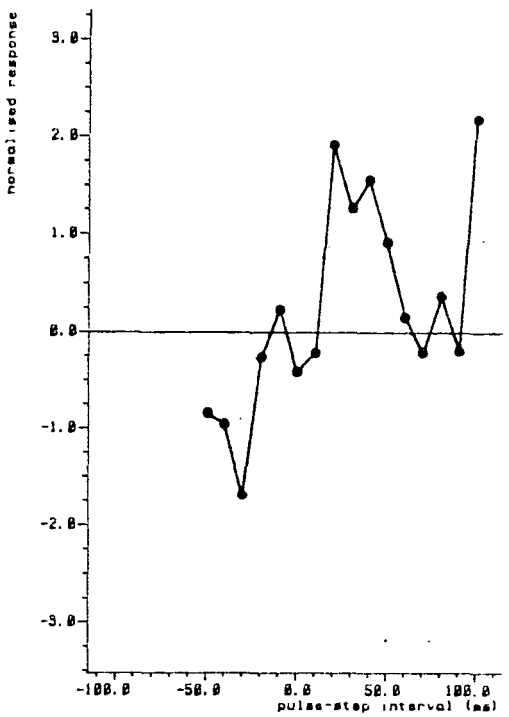

(c)

Figure 7.03 : Results of subject AS in Experiment 7.1.
(a) Threshold for a 5 ms negative pulse in combination with a positive step, as a function of their separation. The step / pulse amplitude ratio was fixed at 0.2. The stimulus is shown schematically at the bottom of the graph.
(b) Threshold for a step and positive pulse combination.
(c) The hypothetical internal step response, derived from the functions in (a) and (b) by Equation 7.07.

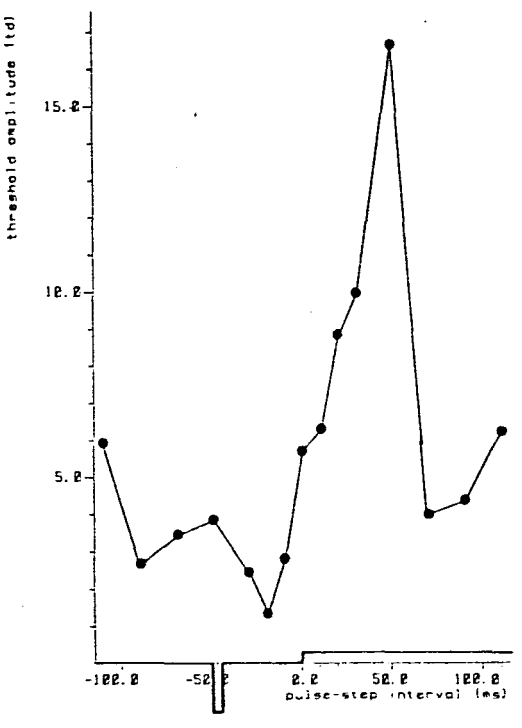

(a)

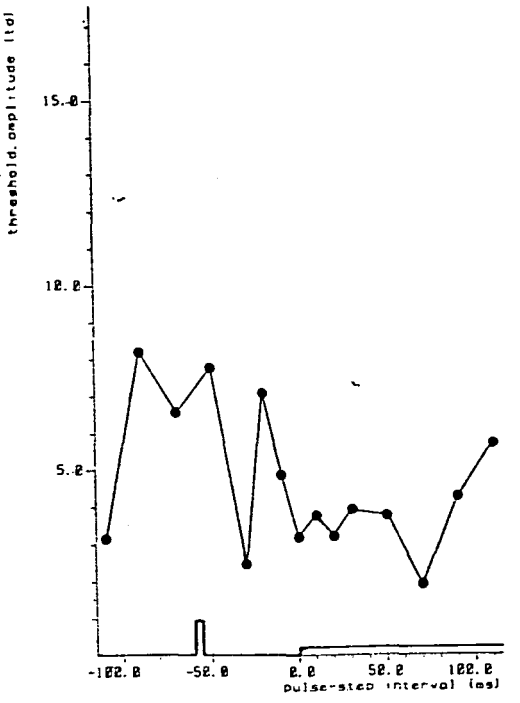

(b)

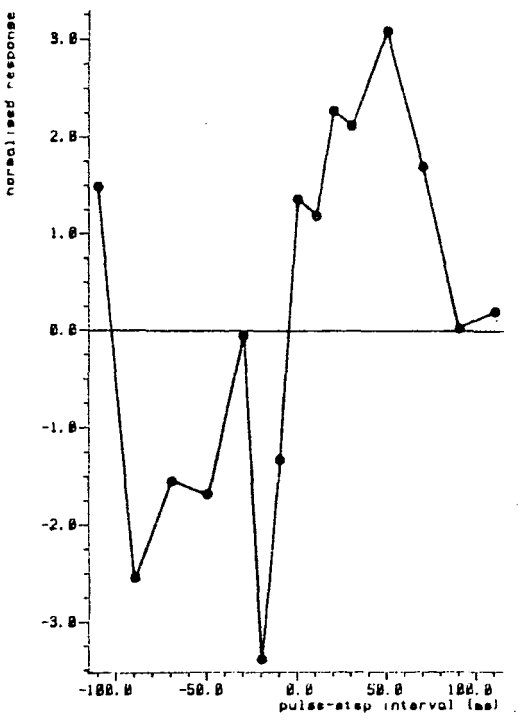

(c)

Figure 7.04 : As Figure 7.03, for subject APH.

represent time running from left to right, with the test step occurring at 0 ms. Although somewhat noisy, the overall result, shown by both subjects, is that thresholds for positive pulses reach a peak at about 50 ms before the step, while those for negative pulses reach a peak about 50 ms after the step. The data for subject AS are particularly noisy, due perhaps in part to the fact that the thresholds being measured are extremely low. The point at +100 ms in Figures 7.03b and c is almost certainly inaccurate.

Figures 7.03c and 7.04c show the normalised response to the step stimulus, calculated by Equation 7.07. The response so derived is biphasic, centred on 0 ms, and with peaks at approximately $\pm$30 ms for subject AS and $\pm$50 ms for APH. The existence of an effect at negative SOAs does not imply that the response precedes the stimulus: the absolute position of the response relative to the stimulus is not known, all points being measured relative to the peak of the probe response.

Since Equation 7.07 normalises the test response with respect to the probe response, we might expect it to have a maximum value of $\pm$1. The fact that the measured response is greater than this may be taken as evidence that the response to a step is much greater than that to a pulse. The positive phase of the response is related to an increase in negative pulse thresholds; similarly the negative phase is related to a rise in positive pulse thresholds. For the normalised response to have a maximum value of 1, these threshold changes would need to be accompanied by equal and opposite effects on the threshold of the complementary pulse. However, examination of the pulse thresholds reveals that decreases in threshold below the asymptotic level are not reliably obtained. For example, Figure 7.04 shows that while negative thresholds increased almost sixfold from a baseline level of about 3 td to a peak of 17 td at +50 ms, positive pulse thresholds

remained virtually unchanged.

7.3 Experiment 7.2

7.3.1 Apparatus

As for Experiment 7.1

7.3.2 Design and Procedure

The psychometric procedure and the overall structure of the experiment were the same as for Experiment 7.1. Unlike the simple detection threshold measured in that experiment, however, Experiment 7.2 measured the threshold for discrimination between the pulse and test combination and the test stimulus presented alone. The design of each trial is shown in Figure 7.05. Both intervals contained a step, whose position within the interval was randomised within the constraints imposed by the SOA. The interval containing the pulse was again selected by APE to compensate for bias. The amplitude of the step was fixed throughout the experiment at 1 td, chosen on the basis of informal observations as being approximately 1/3 of the threshold amplitude.

Both subjects AS and APH took part in the experiment. However, subject APH was withdrawn after her thresholds for negative pulses became so high that they could not be reliably determined. Thresholds for subject

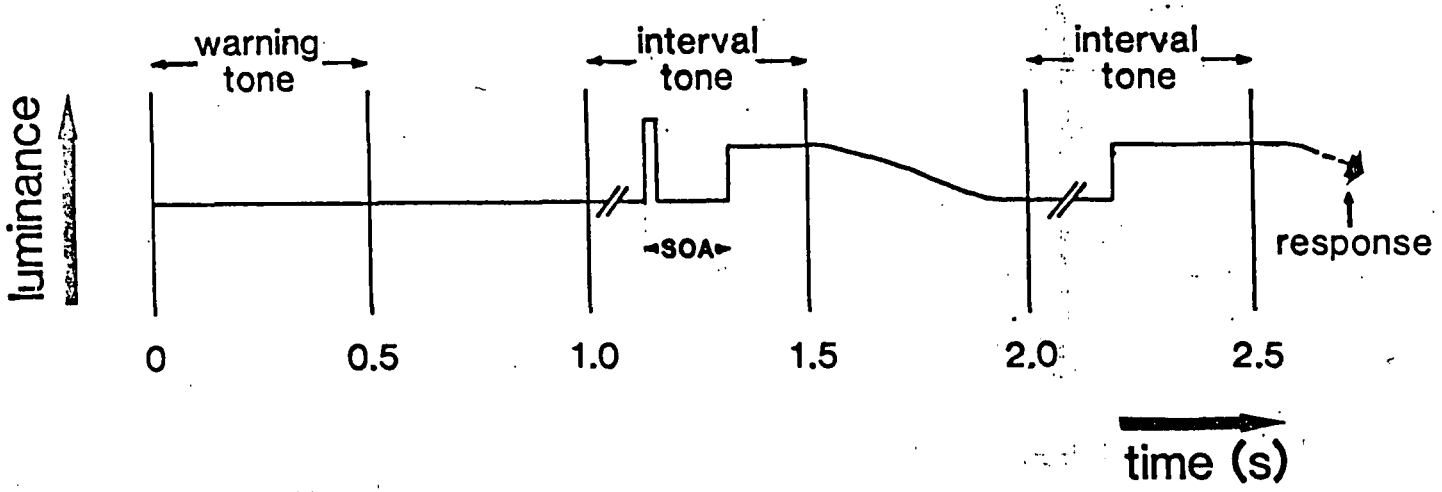

Figure 7.05 : Design of the trials in Experiment 7.2. A luminance step is presented in both 500 ms stimulus intervals, with the probe tone in only one interval. The stimulus onsets are independently randomised, and luminance returns to the mean level by a Gaussian function in the 500 ms following each interval. The next trial is initiated by the subject's response.

AS were obtained for positive and negative pulses, randomly interleaved, over the range -100 to +150 ms SOA at 10 ms intervals.

7.3.3 Results

The pulse threshold functions for subject AS are shown in Figure 7.06a and b, in the same format as previously. The curves show essentially the same features as those obtained with a fixed ratio step. Threshold for positive pulses reaches a peak at about 50 ms before the step and negative threshold peaks at 50 ms after the step. However, the effects of the step on the two pulses are markedly asymmetrical, with the rise in the negative threshold being much greater. To give an indication of the scale of this effect, the step stimulus is drawn to scale at the bottom of the graphs in Figure 7.06. Pulses greater than 33.5 td could not be generated with the display used, so that threshold estimates greater than this should be regarded as more qualitative than quantitative. Some of these conditions were repeated several times before the responses were sufficiently normally distributed to be fitted by the probit psychometric curve.

Two features of these results are clear:

1) The two thresholds behave independently as a function of SOA. As noted in the previous experiment, neither curve is affected as the other rises to a peak.
2) Thresholds are increased but not decreased by the presence of the test stimulus. It is assumed that raw probe threshold, $A_{p\ alone}$, is equal to the values at the extremes of the measured SOA range. The results provide evidence of masking but not summation.

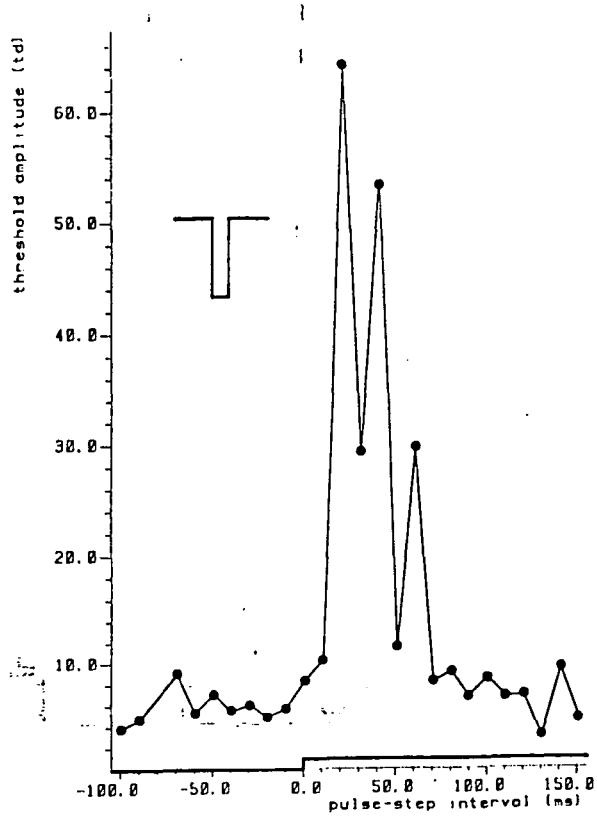

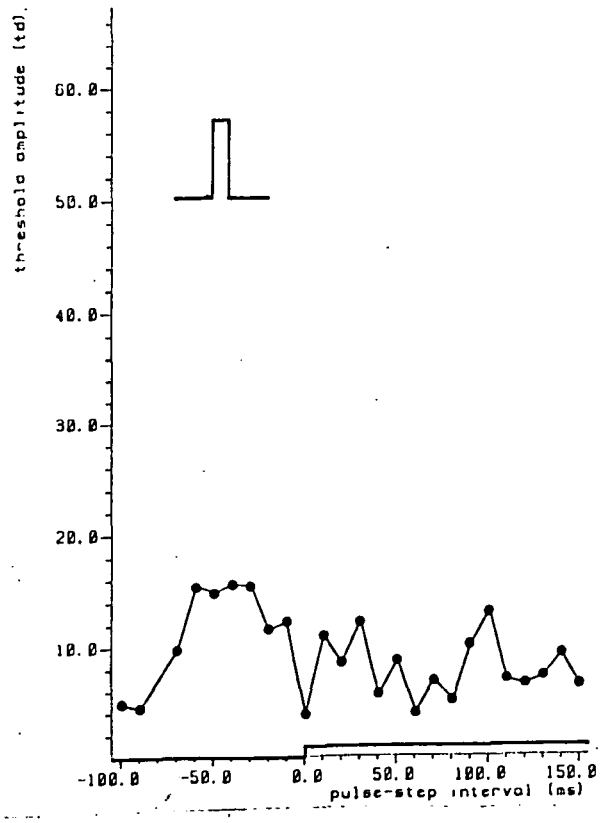

Figure 7.06 : Results of subject AS in Experiment 7.2. Threshold amplitude of a negative (a) and positive (b) 5 ms pulse in combination with a 1 td step. The step stimulus is drawn to scale at the bottom of each graph.

An approximate estimate of $A_{p\ alone}$ may thus be obtained by averaging across the lower of the two threshold functions in Figure 7.06 at each SOA. This gives a figure of 6.74 td (±0.44 td s.e.). Dividing each data point in Figure 7.06 by this value (Equation 7.11), the two normalised response curves plotted in Figure 7.07a are obtained. These two curves represent the magnitude of the test response in the two channels sensitive respectively to the positive and negative probe pulses. The test response is measured in terms of intrinsic system noise.

The two opposite responses appear to be mutually exclusive, suggesting that a single test response can be either positive or negative at any given moment; the opposite response is always zero. This zero response implies that the opposite pulse threshold is equal to $A_{p\ alone}$. The complete biphasic response may thus be obtained by:

$$NR = \log(A_{p+} / A_{p-}) \qquad \text{Equation 7.12}$$

This formulation has the advantage of eliminating changes in A_p due to shifts in sensitivity and criterion, since A_{p+} and A_{p-} are measured simultaneously. The data points are replotted according to Equation 7.12 in Figure 7.07b. The response is symmetrical with respect to time, peaking at ±40 ms. However, it is still asymmetrical with respect to amplitude, with the negative phase approximately twice as great as the positive phase. As noted above, this function is inverted relative to those plotted in Figures 7.03c and 7.04c, due to differences in experimental procedure.

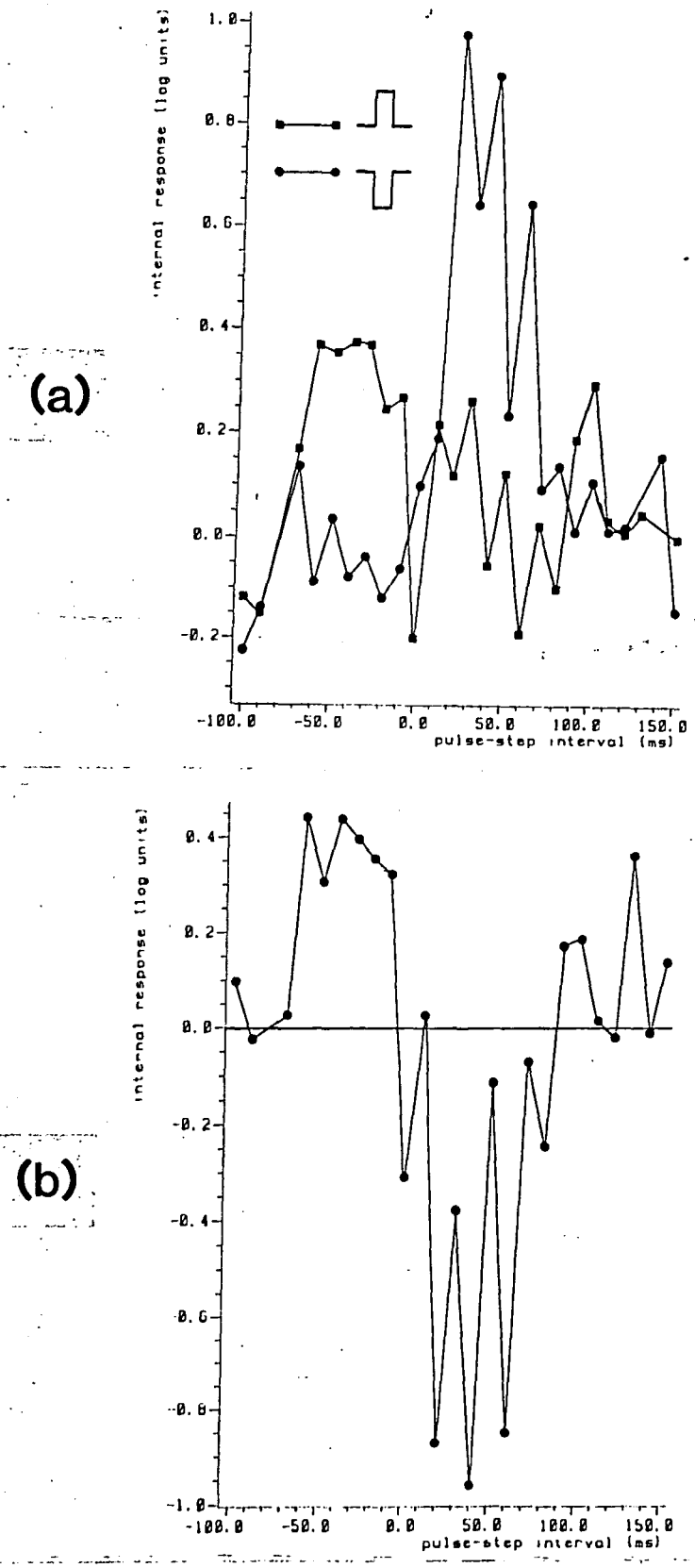

Figure 7.07 : (a) Elevation of threshold for positive and negative pulses, as a function of their separation from the step. The baseline threshold for the pulse presented alone is taken as the lower of the two thresholds, averaged across SOA. Threshold elevation is then calculated according to Equation 7.11.
(b) The hypothetical internal step response, calculated from the positive and negative pulse thresholds by Equation 7.12.

7.4 Discussion

The experiments reported in this chapter were designed to measure the internal response to a subthreshold step stimulus. In Experiment 7.1 the response was measured using a variation of subthreshold summation called the perturbation technique, devised by Roufs and Blommaert (1975, 1981). In Experiment 7.2 the amplitude of the test stimulus was held constant, and the internal response was measured by a masking technique. Rather than these responses being of intrinsic interest, the data were obtained for two purposes:

a) to establish the validity of the masking technique by comparing its results with those of the well - documented perturbation method.

b) to characterise the system mediating step detection for comparison with that mediating ramp detection, measured in Experiment 8.1.

The forms of the step responses obtained in the two experiments are broadly in agreement with those reported by Roufs and Blommaert (1981). That is, a biphasic response, centred on 0 ms SOA, whose first phase is somewhat smaller than the second. The Roufs response is faster, with the peaks occurring at $\pm$20 ms rather than at $\pm$40 ms, a difference attributable to the greater mean luminance in the original study (1200 td vs 47.5 td). The normalised Roufs response peaks at the expected maximum of 1, indicating that it is equal to the peak of the pulse response. However, the peak of the response in Experiment 7.1 (Figure 7.03c), measured in essentially the same way, is greater than 1. The immediate cause of this discrepancy lies in the asymmetrical effect of the test stimulus on probe thresholds. The perturbation technique depends on two critical assumptions:

a) linear summation of responses, and

b) a constant peak detection criterion.

One corollary of these assumptions is that the sum of the probe amplitudes will remain constant at threshold: as threshold of one pulse increases, that of the opposite pulse decreases. The amplitude ratio, r, acts as a scaling factor on this response, taking values from 0 (no response) to 1 (response reaches d).

The probe thresholds obtained in the two experiments do not obey this complementarity rule. Positive thresholds increase before the step and negative thresholds increase after the step, as Roufs reports. Particularly in the latter case the size of the effects is impressive. However, these changes are not accompanied by equal and opposite changes in the thresholds of the opposite - polarity probe. Using a fixed amplitude test, the data of Experiment 7.2 (Figure 7.06) show these effects particularly clearly. The independence of the two thresholds suggests that, at least under these conditions, the assumption of linear summation is not valid. Since this assumption is central to the perturbation analysis, the following discussion of the characteristics of the systems involved will rest on the results of Experiment 7.2.

An analysis of the system detecting luminance steps must start with the measured step response, plotted in Figure 7.07b. For a linear system, the transfer function is the Fourier transform of the derivative of the step response. However, the probe - specific curves of Figure 7.07a show that the system is nonlinear, hence this simple analysis is invalid. Linear techniques may still be applied to that part of the system preceding the nonlinearity. Any fast transient in a physical system will become extended in time due to the smoothing effects of the low-pass elements in the system. The response curve of Figure 7.07b has two distinct peaks, but

little evidence of an overall difference between initial and resting levels, suggesting that the system is maximally responsive to the onset and offset of a smoothed step.

This type of response has much in common with that of the spatial contrast system proposed by Marr and Hildreth (1980). This effectively operates by taking the 2nd derivative of the output of a Gaussian smoothing filter. Marr (1976, 1980; Marr et al 1979) points out that this is an efficient way of removing redundant intensity information in the spatial array, while at the same time preserving and enhancing information about the location and sign of contours. There are a number of possible filter shapes which will perform this function. Marr and Hildreth, from a computational perspective, proposed an array of medium bandpass filters. Taking physiological realisability into account, Watt and Morgan (1983) argue that the difference of Gaussians (DOG) filter of Wilson and Bergen (1979) offers a good compromise between structural simplicity and the functional demands of the Marr and Hildreth mathematical model. The sensitivity profile of the DOG filter is the difference between two unit - area Gaussian functions with unequal standard deviations:

$$DOG(t) = \frac{\exp(-t^2/2S_+^2)}{S_+(2\pi)^{0.5}} - \frac{\exp(-t^2/2S_-^2)}{S_-(2\pi)^{0.5}} \qquad \text{Equation 7.13}$$

where S_+ is the standard deviation of the excitatory surround, S_- that of the inhibitory centre, and the function is centred on $t = 0$. Watt and Morgan suggest that a ratio of $S_+ / S_- = 1.75$ gives a good approximation to the ideal Marr and Hildreth model. The DOG impulse response may thus be seen as deriving either from a single bandpass filter or from an opponent pair of low-pass filters with different cut-off frequencies. The implications

of this choice of filter for systems analysis are considered in more detail in Chapter 9.

The validity of the DOG filter as a model of the mechanisms underlying detection of temporal transients may be tested by convolving it with the step stimulus. The output is a biphasic function symmetrical with respect to both time and amplitude. In order to fit the measured step response (Figure 7.07b), some differential scaling must be applied to the positive and negative output of the DOG filter. With the ratio of the time constants fixed, a theoretical curve may thus be fitted to the data with only two parameters: one time constant and the scaling ratio.

The data of Experiment 7.2 were first fitted by the mathematical model of Marr and Hildreth (1980), by varying the standard deviation of the smoothing Gaussian. The peaks of the best-fitting curve, by a least - squares criterion, were found to lie at $\pm$32.89 ms. This point is therefore the point of intersection of the two Gaussians of the DOG filter (Equation 7.13). With $S_+ / S_- = 1.75$ (Watt and Morgan, 1983), this gives best fitting values of $S_+ = 22.32$ ms and $S_- = 12.76$ ms. These values were substituted in the DOG filter, and the theoretical step response obtained by convolution. The remaining free parameter, the scaling ratio, was then estimated by independently varying the amplitude of the positive and negative phases until the overall squared deviations were minimised. A scaling ratio of $k_+ / k_- = 1.425$ gives the best fit to the data, where k_+ and k_- are the reciprocals of the scaling factors applied to the positive and negative responses respectively.

The best fitting DOG filter curve is plotted as a solid line in Figure 7.08, together with the data points from Experiment 7.2. Also plotted, as

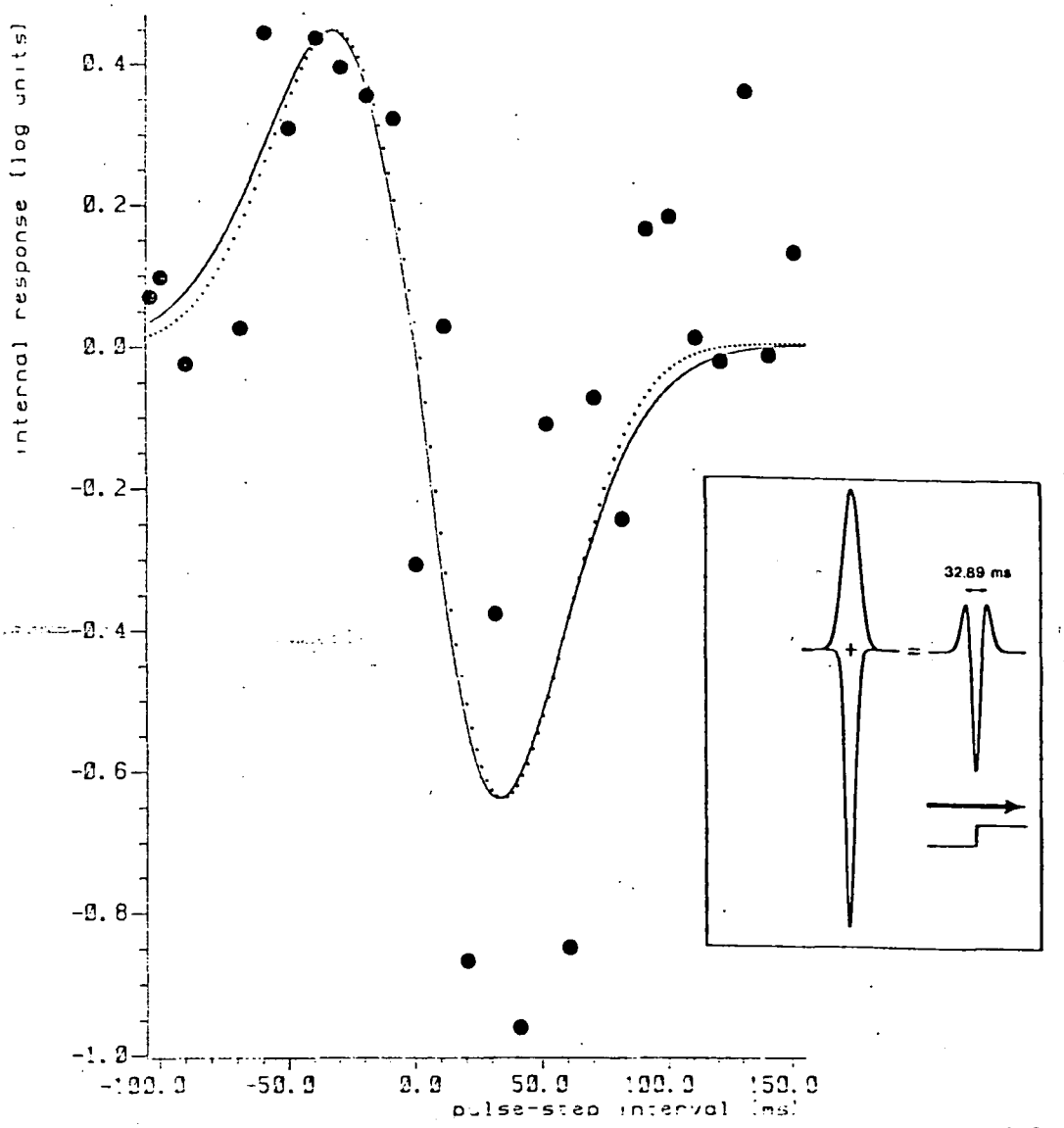

Figure 7.08 : The solid line shows the step response of a difference - of - Gaussians bandpass filter, with parameters chosen to give the best fit to the data of Experiment 7.2. The curve is obtained as illustrated in the panel. The DOG function is the difference of two Gaussian functions whose standard deviations (time constants) have a preset ratio of 1.75. The output of the convolution of this function with a step is differentially scaled, so that negative responses are 1.425 times greater than positive responses. The dotted line represents the 2nd differential of a step, after smoothing with a single Gaussian filter with a time constant of 32.89 ms.

a dotted line, is the 2nd derivative of a Gaussian smoothed step (the Marr and Hildreth model), also differentially scaled. The effect of the DOG approximation is a slight broadening of the peaks, resulting in a marginally worse fit to the data. Overall, however, the fit is reasonable, suggesting that this is a tenable model of the mechanisms involved. By this analysis polarity selectivity occurs only in the response to the 2nd derivative, arguing strongly that the rectification process follows the bandpass filtering stage, but precedes the differential scaling. This relationship is expressed in a block diagram of the proposed model shown in Figure 7.09.

Figure 7.09 incorporates the results of Experiment 7.2 into a hypothetical model of the mechanisms mediating the detection of fast transients. The DOG filter is represented by an opponent pair of low-pass Gaussian filters, rather than as a single bandpass element. The gain function of these filters does not have a linear high frequency asymptote, thus the curve is characterised not by the corner frequency but by the -3 dB or half - power frequency (f_{-3dB}). This frequency is calculated by:

$$f_{-3dB} = \frac{2^{-0.75}}{\pi S} \qquad \text{Equation 7.14}$$

where S is the standard deviation of the Gaussian impulse response. With S_- = 12.76 ms for the 'centre' or inhibitory filter, f_{-3dB} = 14.83 Hz; for the excitatory 'surround' filter, S_+ = 22.32 ms is equivalent to f_{-3dB} = 8.48 Hz. The difference of the output of these filters is then subjected to half - wave rectification, in order to separate the positive and negative parts of the response. Each part is then handled by a separate nonlinear detection stage. In order to fit the measured response of Experiment 7.2 most accurately, the negative phase must be 1.425 times greater than the

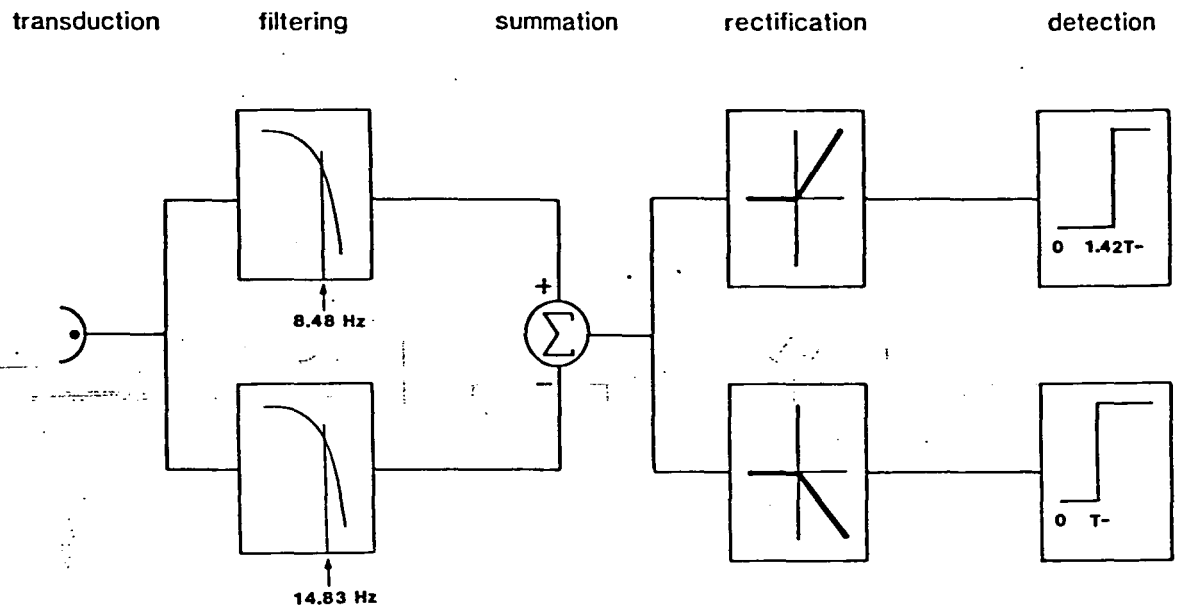

Figure 7.09 : Block diagram of the proposed system mediating the detection of fast transients, based on the results of Experiment 7.2. The incoming time - varying signal is passed through a bandpass filter, composed of an opponent pair of lowpass filters. The -3dB points on the transfer functions are indicated. The filter output passes through a pair of half - wave rectifiers to separate positive and negative phases of the response. The final, polarity specific detection stages have unequal threshold levels to account for the apparently greater negative response. See text for details of the model's operation and performance.

positive phase. Instead of applying differential attenuation or amplification, this is handled in the model by differential sensitivity in the detection stage.

The question of differential sensitivity deserves further comment. From this experiment alone it is not possible to determine whether sensitivity is dependent on the sign or on the temporal order of the response, since the two are confounded by the use of only one step polarity. The response to a negative step should reverse the response phases, thereby showing whether sensitivity is greater to the negative or to the second phase. For the sake of simplicity the effect is shown to be polarity - dependent in the model of Figure 7.09.

In the next chapter the techniques of Experiment 7.2 are repeated with a ramp stimulus in place of a step. With a quantitative model of the step - detecting system, it will then be possible to decide whether ramps are detected by the same system, or by a filter with different characteristics. The ramp stimulus is particularly interesting from the point of view of a 2nd derivative bandpass system, since we may expect:

a) that smoothing will have less effect in shifting the response relative to the stimulus, and

b) an extended zero response will be seen between the two peaks as ramp duration increases.

CHAPTER 8

WHAT IS THE INTERNAL RESPONSE TO A RAMP?

8.1 Introduction

In Experiment 7.2 the step response of the visual system was measured, using a masking technique, and a possible mechanism was proposed to account for the findings. In this chapter the same technique is used to measure the ramp response of the visual system, so that the characteristics of the system sensitive to luminance ramps may be described.

The step stimuli in Experiment 7.2 were always presented at subthreshold levels. However, the masking technique (unlike that of subthreshold summation) is not restricted to the measurement of subthreshold test stimuli. The three ramps chosen for investigation in Experiment 8.1, the only experiment in this chapter, extend from subthreshold to suprathreshold levels. Thus, not only is this the first investigation of the time course of the response to nonabrupt transients, it is also the first in which such a continuum of levels has been used. There is a traditional distinction in the literature between subthreshold and suprathreshold stimuli. Chapter 7 included a review of some of the work on subthreshold responses, thus Experiment 8.1 will be introduced with a short discussion of the main findings on suprathreshold responses, so as to complete the review of studies of internal temporal responses.

As luminance level (L_{mean}) increases, so also does the increment (ΔL) required for detection, so that the ratio ΔL / L_{mean} remains constant. We can measure the time course of this change by measuring the threshold (ΔL) of a pulse presented at different times before and after a change in adaptation level. This increment threshold technique was first described by Crawford (1947), who used a 10 ms probe pulse to follow the change in threshold associated with an increase in luminance of 10, 30, and 100 $c \cdot ft^{-2}$ lasting 52 ms. He found that threshold started rising before the stimulus onset, reached a peak around the point of luminance change, then dropped to a new asymptotic level. The offset of the test stimulus was not accompanied by a threshold peak except at the highest levels tested. The apparent anticipation of the onset of the test stimulus was attributed by Crawford to a difference in neural transmission times between the weak probe pulse and the strong test pulse.

Baker (1953) found a similar effect to Crawford with a single negative step, using a 20 ms probe flash. Threshold rose just before the stimulus to reach a peak at the luminance offset. Baker suggested for the first time that this apparent anticipation was due to a negative phase of the off-response. Probe threshold never decreased below the asymptotic level in either the Crawford or the Baker studies.

Boynton and Kandel (1957) followed the response to a 121 $cd \cdot m^{-2}$ step at different adaptation levels with a 40 ms probe flash. When adaptation level was zero, they found that probe threshold reached a maximum at about 50 ms after the step. As adaptation level increased, the threshold increase started later and peaked at a lower level. These changes were assumed to reflect the neural on-response to the test step. Once again, at no time interval did probe threshold decrease below its baseline

level.

Crawford's method has much in common with the masking technique of Experiment 7.2. The major difference, which may account for the failure to find a biphasic response, is that a negative probe is used to follow negative responses and a positive probe to follow positive responses. These earlier studies confirm that the method is equally applicable to test stimuli above and below threshold. The internal responses to ramps are interesting both in their own right and also because of their relationship to the detection of fast transients. Roufs (1974a) proposed a model of temporal contrast analysis consisting of two parallel channels, sensitive respectively to high and low frequencies. It has been argued throughout this thesis that the low frequency channel of the Roufs model is sensitive primarily to luminance ramps. Roufs has investigated the high frequency system directly by measuring the impulse and step responses (Roufs and Blommaert, 1975; 1981). It is a logical extension of this work to apply essentially the same techniques to the low frequency system, measuring the response to luminance ramps.

In Chapter 7 a quantitative model of the system sensitive to luminance steps was proposed, based on the measured step response. By measuring the ramp response in a similar way, it is possible to determine the characteristics of the system sensitive to ramps. The Roufs model proposes thst steps and ramps are mediated by separate systems, suggesting that the fit of the step system to the ramp response will not be good.

The responses to three ramps are measured, so as to observe the effects on the ramp response of ramp amplitude, duration, and gradient. The three conditions are illustrated and tabulated in Figure 8.01. Ramp 1

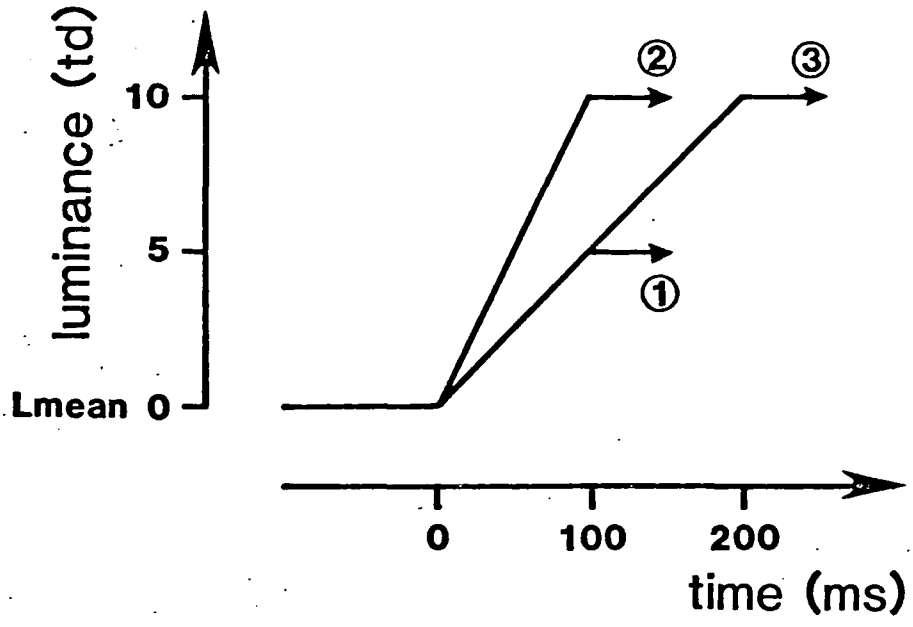

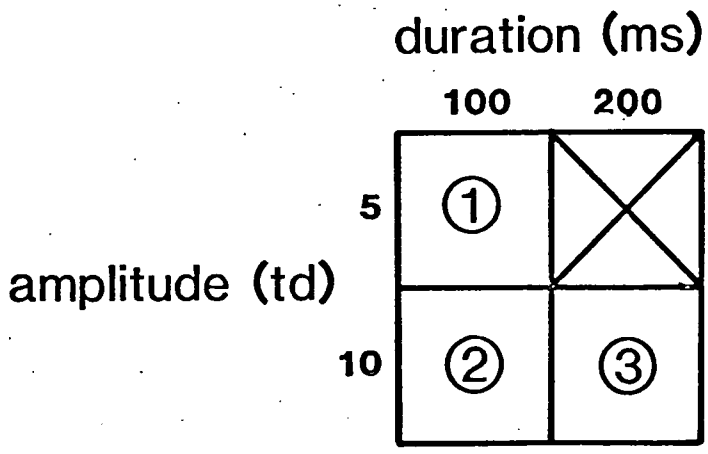

Figure 8.01 : The three ramp stimuli used in Experiment 8.1. The grid shows how the crossed design allows amplitude, duration and gradient to be varied independently. The three stimuli are illustrated in the graph above.

has an amplitude of 5 td and a duration of 100 ms; ramp 2 has twice the amplitude (10 td) but the same duration; ramp 3 has the same amplitude as ramp 2 but twice the duration (200 ms). The values are chosen so that two ramps have the same value of any given parameter, with the third ramp being either twice or half that value:

a) amplitude. Ramps 2 and 3 are 10 td; ramp 1 has an amplitude of 5 td.

b) duration. Ramps 1 and 2 are 100 ms; ramp 3 is 200 ms.

c) gradient. Ramps 1 and 3 have a slope of 50 $td \cdot s^{-1}$; ramp 2 is 100 $td \cdot s^{-1}$.

8.2 Experiment 8.1

8.2.1 Apparatus

The physical set-up was identical to that of Experiments 7.1 and 7.2, described in Section 7.2.1.

8.2.2 Design and Procedure

The overall design of the experiment and the APE psychometric procedure were similar to that described for Experiment 7.1.

The design of each trial is shown in Figure 8.02. In each 500 ms

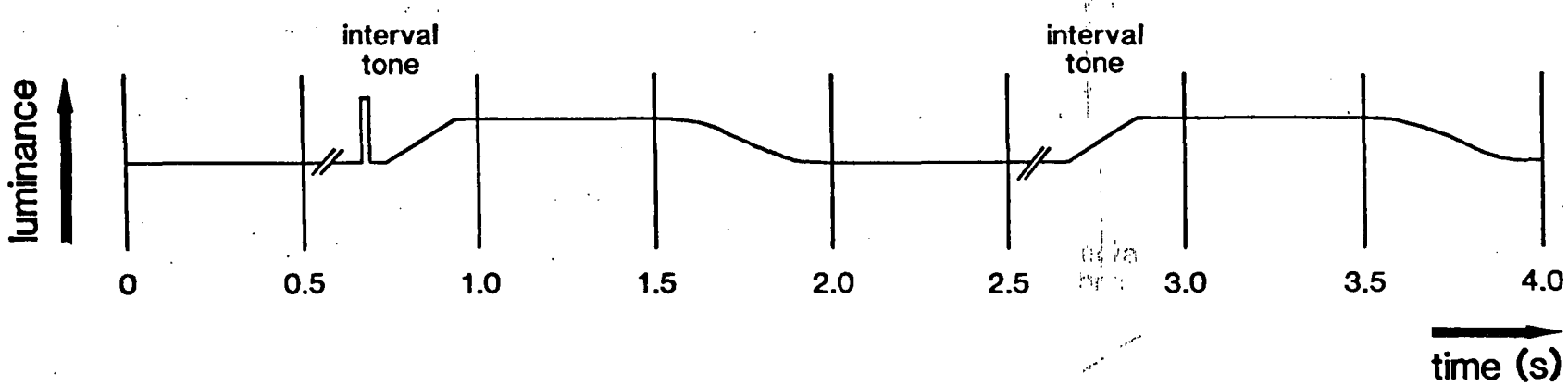

Figure 8.02 : Design of the trials in Experiment 8.1. Each of the 500 ms stimulus intervals contains a ramp, and one interval also contains the 5 ms probe pulse. The stimulus intervals are flanked on either side by 500 ms intervals of constant luminance, and luminance returns to the mean level by an integrated Gaussian function. Responses are collected at any time after the second interval. The next trial starts either at the end of the current trial or after the subject's response, whichever is the later.

stimulus interval the test ramp was presented, at a latency randomised within the constraints imposed by the SOA. One interval also contained the probe pulse, and the subject was required to indicate which interval he thought this was. Incorrect responses were followed by a tone. The APE procedure selected both the interval for the probe and its amplitude on a given trial.

The three test stimulus conditions are illustrated in Figure 8.01. In each ramp condition thresholds were measured from 150 ms before the ramp to 150 ms after the end of the ramp. For subject AS measurements were taken at every 10 ms, and for subject JMAH at every 20 ms. Thresholds for positive and negative probe pulses were measured simultaneously with randomly interleaved trials. Estimates were made after 80 trials, giving a total of 160 trials in each SOA condition, lasting approximately 20 minutes. Threshold estimates were only accepted when the chi-squared tests showed that responses to both pulses were normally distributed. If either chi-square was significant (at $p \leq 0.05$), the condition could be repeated at least five times before being abandoned. Only in this case is a threshold reported that is not paired with the opposite threshold measured simultaneously.

For subject AS the ramp conditions were presented in the order 2, 1, 3, and SOA conditions from negative to positive intervals. Both orders were reversed for JMAH.

The problems of measuring the very high thresholds encountered meant that approximately two runs were required on average for every successful data point obtained. Thus the entire experiment consisted of over 60,000 trials, occupying 130 hours of observation time.

8.2.3 Results

The raw pulse thresholds are presented in Figures 8.03 to 8.05. Each subject's data are presented separately, because of the large differences in pulse sensitivity. However, the scales for each subject are the same in each condition, to allow a direct comparison between conditions.

The most obvious effect of a ramp is to raise the threshold for positive pulses around its onset and raise the threshold for negative pulses around its offset. These effects were much greater than expected. For example, the 5 td ramps (Figure 8.03), which were close to or below the detection threshold, were found to cause a 10 to 20-fold increase in pulse threshold. Because of this, many thresholds lay outside the range obtainable from the display screen (33.5 td), and thus had to be estimated by extrapolation of the psychometric curve. Although this is a questionable practice, many of the estimates obtained in this way are within the expected ranges. However, the extrapolation requires an extremely good distribution of responses in the measurable region. The difficulty of achieving this inevitably led to the loss of some data points around the ramp onsets and offsets. However, in no condition was a threshold unobtainable from both subjects. In general the thresholds of JMAH were higher than those of AS, although her responses were more normally distributed. Thus, although more extrapolation was necessary, it is likely to be more reliable.

The thresholds for positive and negative pulses show some slight evidence of reciprocity, in contrast to the conclusions reached in Chapter 7. An example may be seen in Figure 8.03d, in the 5 td / 100 ms condition for JMAH. However, the effect is not consistently observed in other

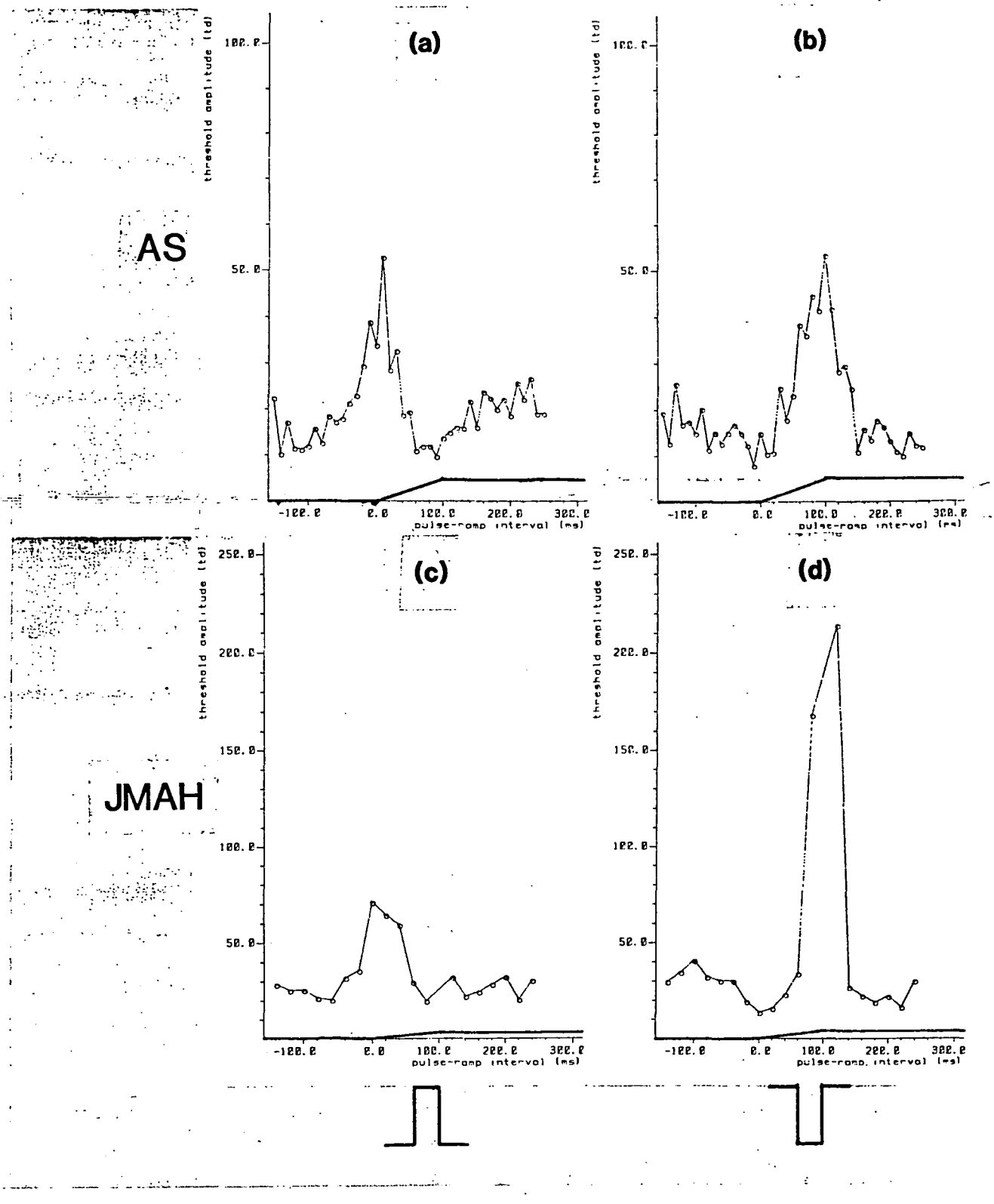

Figure 8.03 : Absolute pulse thresholds in the 5 td / 100 ms ramp condition. Thresholds for subject AS are shown in (a) and (b), those for JMAH in (c) and (d). Different scales have been used for the two subjects because of the large differences in sensitivity. Positive pulse thresholds are shown on the left in (a) and (c), negative pulse thresholds on the right in (b) and (d). The stimulus ramps are drawn to scale at the bottom of each graph.

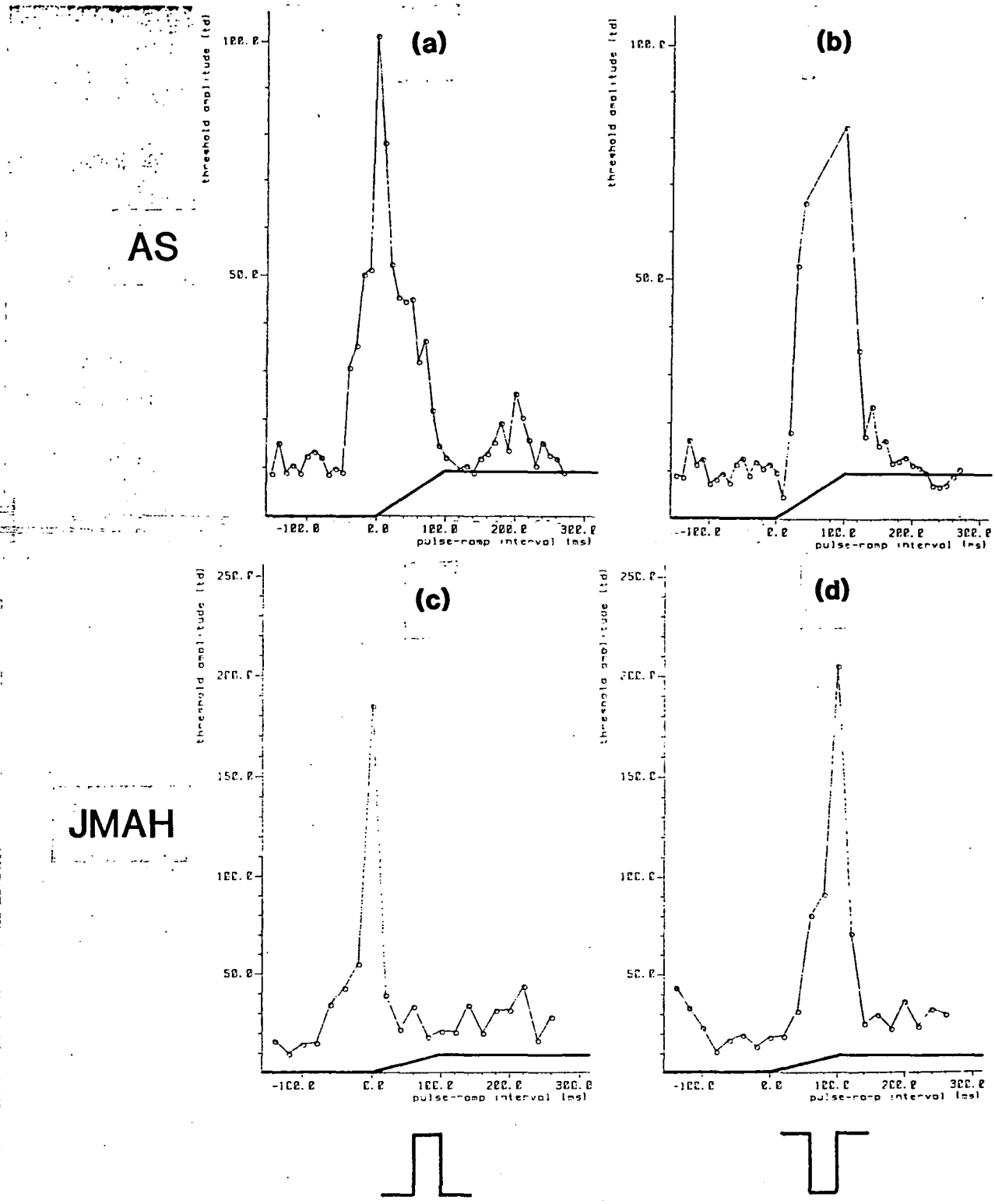

Figure 8.04 : As Figure 8.03, for the 10 td / 100 ms ramp condition. This ramp is shown on each graph. The same scales are used as in the previous Figure.

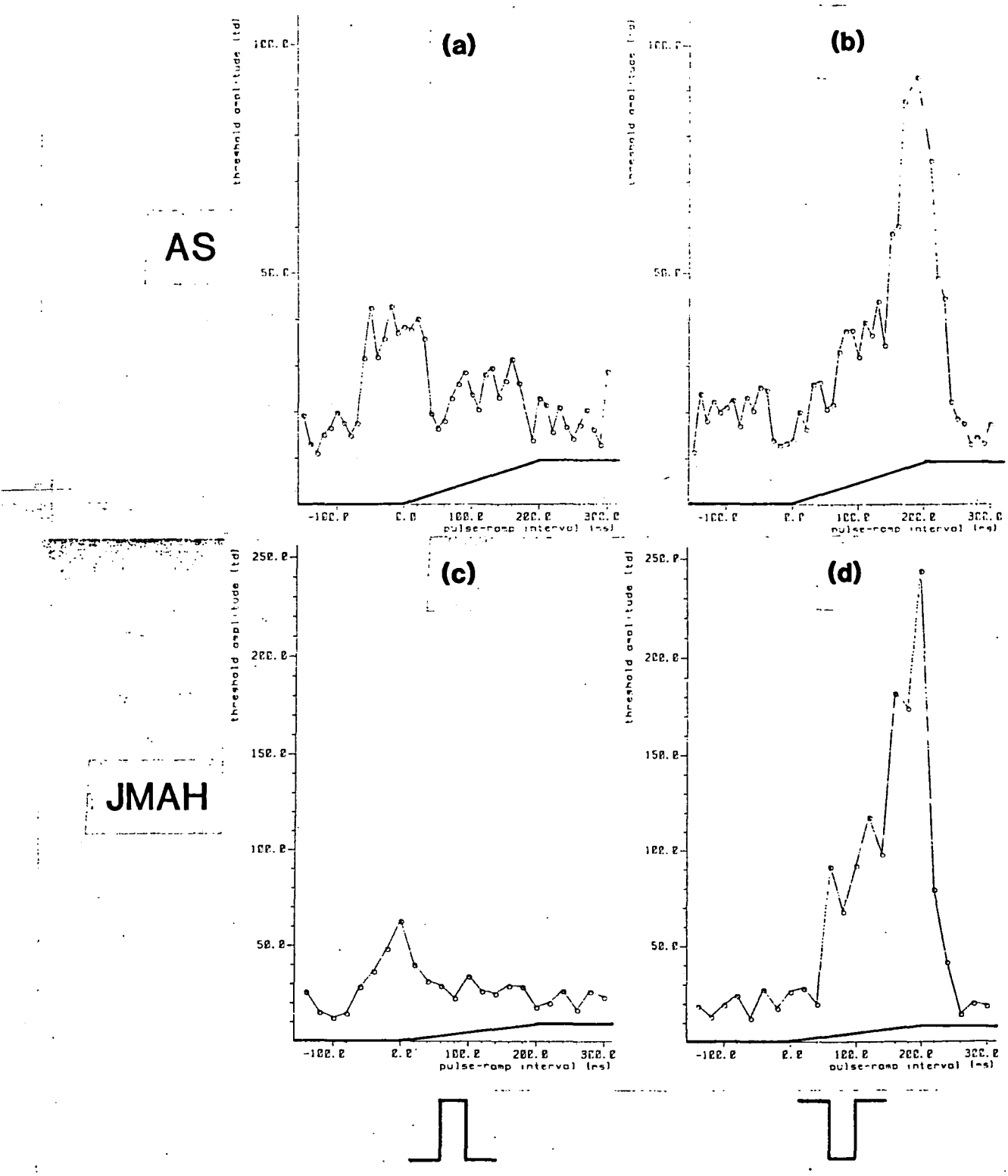

Figure 8.05 : As Figure 8.03, for the 10 td / 200 ms condition.

conditions, and is most often seen when threshold elevation is greatest. This suggests that the apparent complementarity is an artifact of the interleaving of positive and negative trials. When one of the threshold measurements was particularly difficult vigilance was increased, with a beneficial effect on the opposite threshold.

The internal response curves were derived by Equation 7.12, and are shown in Figures 8.06 to 8.08. The general form, seen in each condition, is once again biphasic, with the positive phase centred on the onset of the ramp and the negative phase centred on the offset. This contrasts with the step responses measured in Chapter 7, in which the peaks occurred at 33 ms on either side of the stimulus.

Also shown in Figures 8.06 to 8.08 are the responses to the ramps of the step - system model proposed in Chapter 7. These curves were obtained by convolving the ramp function with a DOG filter, using the time constants that gave the best fit to the step response (Figure 7.08). The positive and negative scaling factors were then independently adjusted to give the best fit. The fit is reasonable in most of the six conditions, although the obtained response appears to be more oscillatory than predicted. This is seen particularly clearly in Figure 8.06b, the response of JMAH to a 5 td / 100 ms ramp, the only condition in which the model does not provide an adequate account.

The bandpass nature of the DOG filter means that it is primarily responsive to the 2nd derivative of the signal, which varies with the gradient of the ramp. A further test of the validity of the model may thus be made by comparing the curves in Figure 8.07 (gradient = 100 $td \cdot s^{-1}$) with those in Figures 8.06 and 8.08 (50 $td \cdot s^{-1}$). When the obtained data,

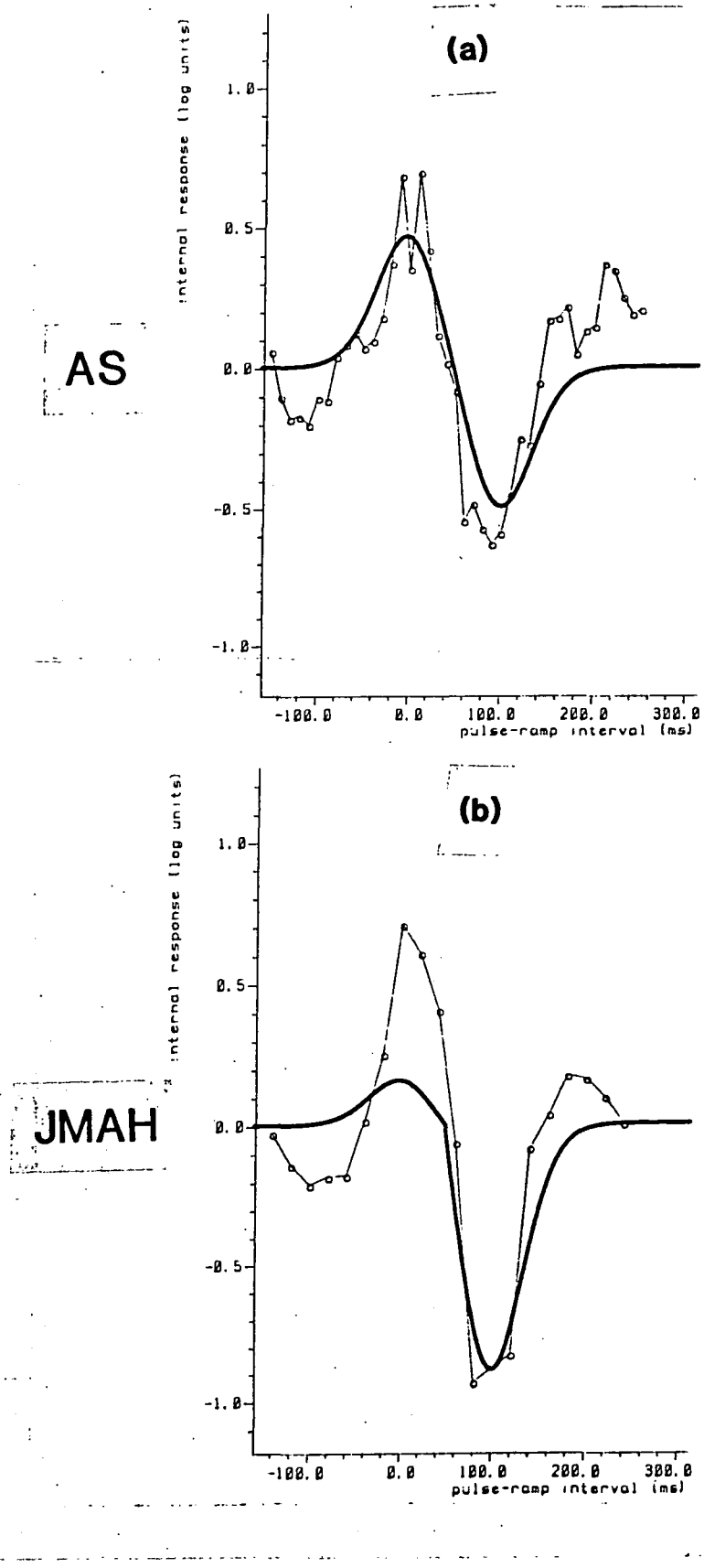

Figure 8.06 : The light lines and data points show the internal response to the 5 td / 100 ms ramp, calculated from the positive and negative pulse thresholds by Equation 7.12. The responses of the two subjects are plotted separately, although on the same scale. The heavy line shows the predicted response of the step - detection system shown in Figure 7.09. The time constants of the proposed filters are unchanged, although the scaling factors are adjusted to give the best least - squares fit to the data.

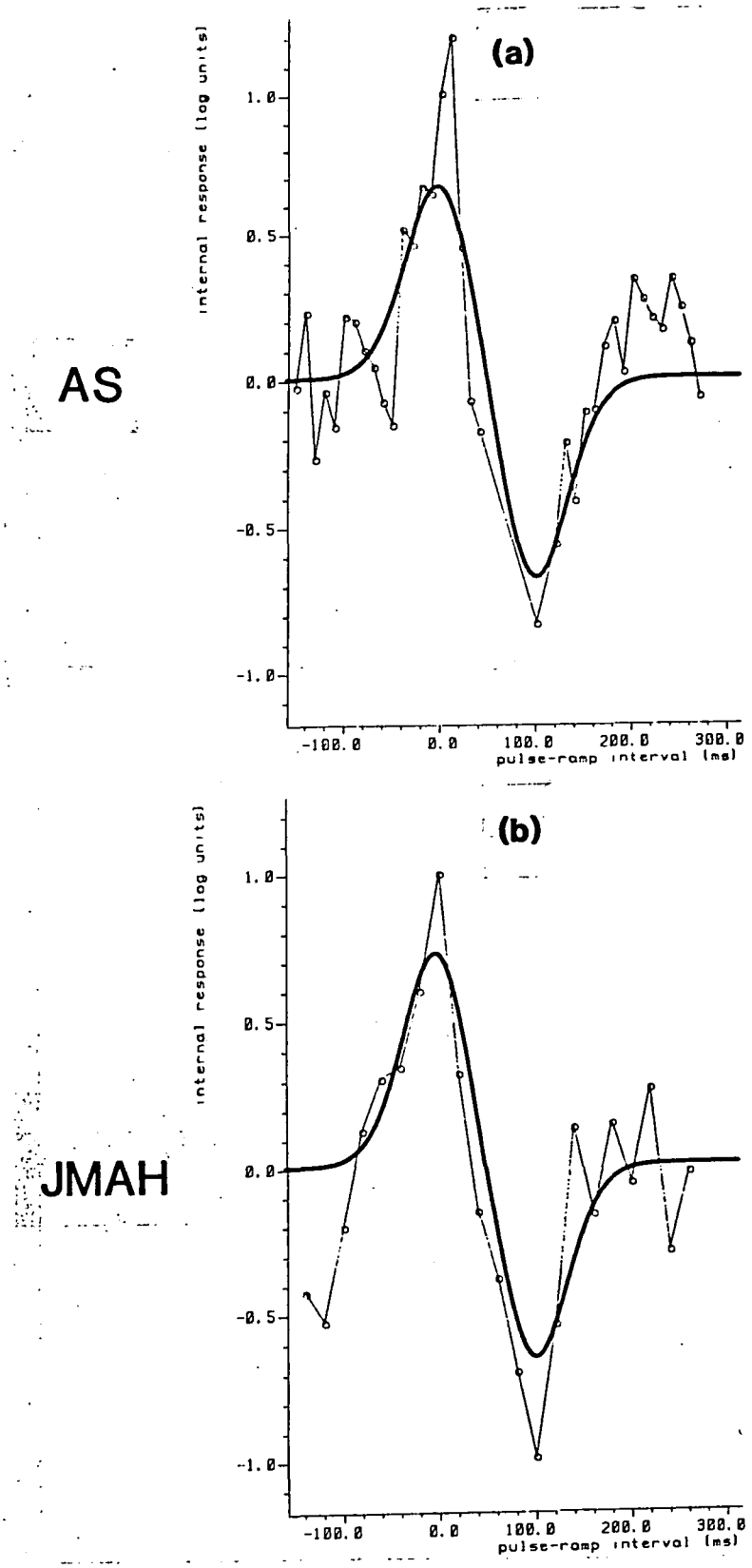

Figure 8.07 : As Figure 8.06, for the 10 td / 100 ms ramp.

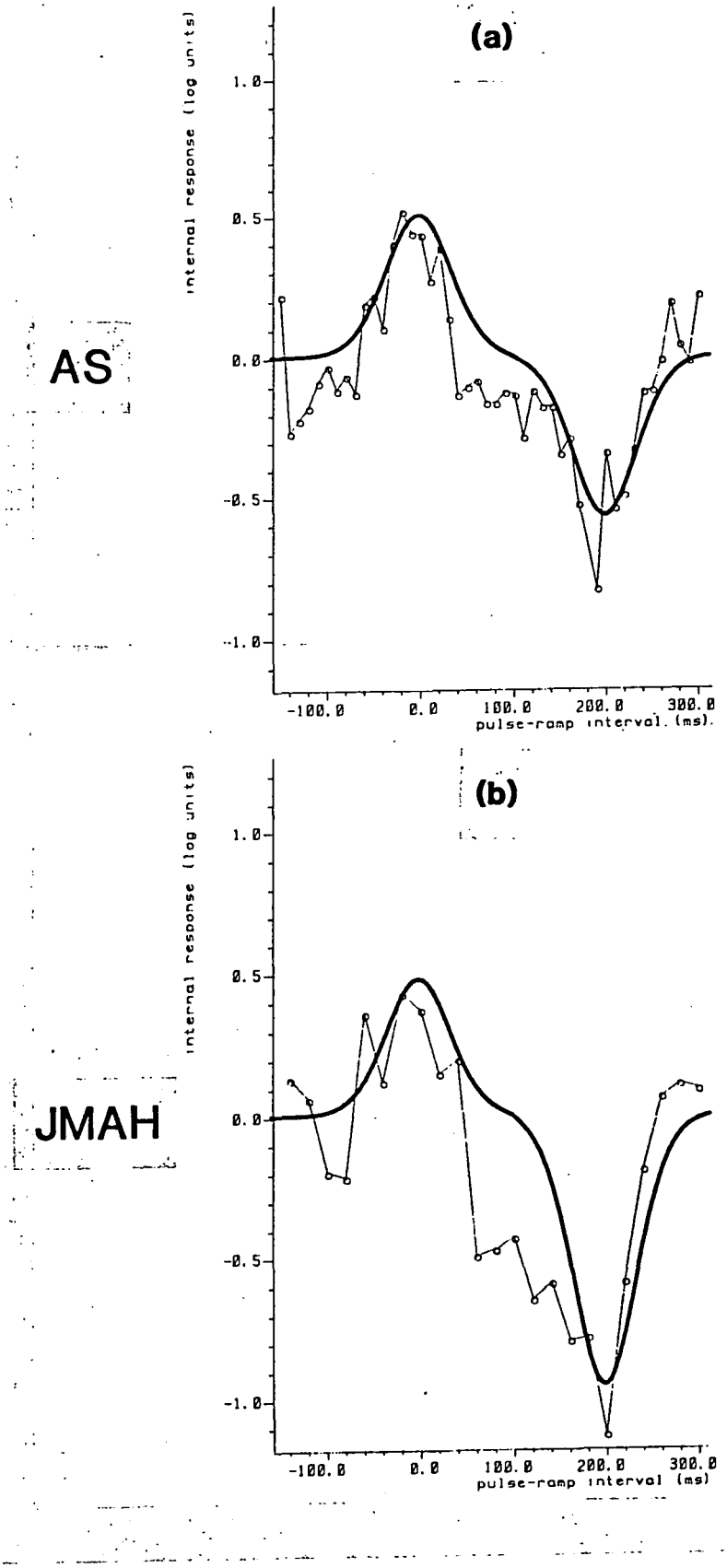

Figure 8.08 : As Figure 8.06, for the 10 td / 200 ms ramp.

rather than the fitted curves, are considered we would expect the peaks in Figure 8.06 to be 0.3 log units greater than those in the other two conditions. The positive peak follows this prediction in both subjects. The negative peak is less predictable, although the expected pattern may still be seen in the data for AS. This is most probably due to the fact that negative probe thresholds were extremely high around the ramp offset, particularly for JMAH, and hence less reliable than those for positive probes around ramp onset.

8.3 Discussion

The primary feature of the data from Experiment 8.1 is the very large increase in probe threshold occurring at the onset and offset of the stimulus ramps. Some threshold estimates were up to five or six times the maximum amplitude available from the display, leading inevitably to increased variability. This should be borne in mind when drawing conclusions from the results.

The measurement of the ramp response in this experiment was intended as a sequel to the study of steps in Chapter 7 (also Roufs and Blommaert, 1975; 1981). This was undertaken in the context of the Roufs parallel model of temporal contrast analysis, interpreted as comprising separate systems for fast and slow temporal transients. The step responses obtained in Experiment 7.2 allowed a quantitative model of the fast transient system to be described (Figure 7.09). Using the same time constants chosen to fit the step response, it seems that this model may also account for the ramp

responses of Experiment 8.1.

Figures 8.06 to 8.08 compare the obtained responses with those predicted by the step detection model. Three features of the theoretical curves may be noted:

1) The peaks of the response coincide with the ramp onsets and offsets. This is not necessarily so: as the time constant increases the peaks shift away from the centre of the ramp.

2) The model predicts a flattening of the response in the centre of the 10 td / 200 ms ramp (Figure 8.11). This is in accordance with the data of subject AS, although JMAH does not show the effect as clearly. No such flattening is either seen or predicted with the shorter duration ramps. It is likely that the appropriate time constants are different for the two subjects, and that the values derived from subject AS in Experiment 7.2 do not provide the best fit for JMAH.

3) There is a suggestion that the amplitude of the response is dependent on ramp gradient. As gradient halves from 100 to 50 $td \cdot s^{-1}$, the peak response of subject AS falls from slightly over 0.7 to 0.5 log units. Within the variability of the results at these levels, this is at least comparable with the fall of 0.3 log units which would be expected if the response varied directly with gradient.

These three pieces of evidence suggest that the step detection model provides a reasonable fit to the ramp response data. However, before

accepting the model of Figure 7.09 as a good predictor of both step and ramp responses, two further points deserve comment. Firstly, there is considerable evidence that the ramp response is more oscillatory than expected. This is particularly clearly seen in Figure 8.06b, the most notable failure of the model, where secondary lobes appear to flank the main biphasic response. Although less well - defined, this four - phase response may also be seen in the other conditions. Additional response lobes may be produced in the model by including an additional opponent pair of Gaussian filters in series with the first. Such a fundamental change to the model is not justified by the current data. Secondly, the positive and negative phases of the response appear to be more symmetrical than in the step response of Figure 7.08. Although differential scaling was applied to positive and negative responses, the scaling ratio was never greater than ± 0.13 from unity, except in Figures 8.06b and 8.08b. This suggests that differential sensitivity may not be an essential feature of the model, introduced as it was on the basis of only one measured step response. The model in Figure 7.08 may be amended so that the thresholds of the two channels are approximately equal. Positive and negative responses are thus handled by separate, though symmetrical systems.

With regard to the 'swell' channel of the Roufs model, assumed to be sensitive primarily to just such nonperiodic, nonabrupt transitions as these, the data are essentially negative. We may have expected that the ramp response would not be well-fitted by the step detection model, but that the obtained response could be used to determine the characteristics of a ramp - specific system. Instead it appears that the ramp response is fairly well predicted by the step model, specified as a band-pass filter composed of an opponent pair of low-pass filters with different cutoff frequencies. This implication of a single system for both fast and slow transients, conflicting

with the Roufs model, may be true or may be an artifact of the experimental method. The masking technique assumes that the threshold for a stimulus will be raised only by the presence of other stimuli in the same channel as itself. Threshold will be unaffected by noise, etc in other channels. The ramp response is defined by the rise in threshold of the probe stimulus, as a function of test - probe interval. Thus, by using a fast transient pulse, what these experiments may be measuring is not the complete ramp response, but only that part of it to which the fast - transient system is sensitive. This system has a graded response dependent on the 2nd derivative of luminance change. If correct, this analysis shows that the system is not restricted to abrupt transitions. However, it does not exclude the possibility of other systems sensitive to other features of slow transitions. At low rates of change, or low flicker frequencies, such systems may be more sensitive than this one, as Roufs suggests. In itself, therefore, this experiment offers evidence neither for nor against the qualitative aspects of the Roufs model.

CHAPTER 9

GENERAL DISCUSSION

9.1 Overview

The work in this thesis has been concerned with the mechanisms underlying the analysis and detection of temporal contrast. The existing literature on such mechanisms is largely restricted to descriptive models of the temporal MTF of the visual system, and is particularly lacking in the investigation of:

a) the nonlinear processing of low frequency flicker, and

b) the relationship between the analysis of periodic and nonperiodic temporal contrast.

The present work was stimulated in response to these perceived deficiencies. The development of the theory of channels in the field of spatial contrast, together with the psychophysical techniques associated with their specification, has been a major conceptual influence. Channel theory provides the framework for an explanatory model of perceptual mechanisms, by specifying the components into which an arbitrary stimulus is analysed. Such a model provides a deeper level of understanding than the descriptive models designed to account for flicker thresholds.

A perceptual channel may be regarded as an independent system, selectively sensitive to a subset of all possible stimuli. The task of the psychophysicist is to characterise this subset, which may be a stimulus

dimension (eg velocity or frequency) or a range along a dimension (eg 5 to 10 Hz). The cascaded RC filter models of deLange (1952, 1961) and Kelly (1971) are single - channel models, in which all time-varying stimuli pass through the same filter. The characteristics of these models are specified in detail, enabling accurate prediction of flicker thresholds. However, while providing a detailed quantitative analysis of flicker detection, the qualitative analysis may be over-simplified. The first three experimental chapters of this thesis reversed this imbalance, asking how flicker is detected rather than if flicker is detected.

The work of this thesis should be seen in the context of the Roufs (1974a) model of temporal contrast analysis. This model represents a significant advance on the earlier single - channel models, with its proposal that temporal contrast is processed by two parallel channels, sensitive respectively to opposite ends of the flicker frequency spectrum. Roufs termed these channels the 'swell' and 'agitation' channels, reflecting the distinct percepts associated with each. This distinction, with its implication of separate detection mechanisms at high and low frequencies, presents a serious problem for the conventional psychophysical application of linear systems analysis, which assumes that the detection threshold is independent of frequency. Roufs himself has concentrated on describing the high frequency 'agitation' channel, concluding that it may be characterised as a linear bandpass filter. My work has concentrated instead on the low frequency 'swell' system. The central argument is that this system is primarily sensitive to slow, nonperiodic luminance changes, and hence is characterised most appropriately in the time rather than the frequency domain. The two channels of the Roufs model are often referred to as the 'periodic' and 'nonperiodic' channels. However, this terminology should not be confused with the distinction between periodic and nonperiodic

contrast. Any model of the nonperiodic system must be capable of handling both slow transients (ramps) and low frequency sinewaves; similarly the periodic system is sensitive to both fast transients (steps and pulses) and high frequency flicker.

The next section of this chapter contains a review of the main experimental findings reported in Chapters 3 to 8. In Section 9.3 the theoretical implications of the findings are discussed. The model proposed in Chapters 7 and 8 is looked at more closely, and its place within a more complete model of temporal contrast analysis is explored.

9.2 Review of experimental results

9.2.1 Introduction

Each of the experimental chapters has contained a relatively detailed discussion of the results reported in that chapter, together with an indication of their relevance to the overall argument being pursued. This section is intended to clarify the logical structure of the experimental work, and to provide a summary of the main findings. Detailed reiteration of the experimental results will be omitted.

At the end of the review of flicker research in Chapter 1, the conventional quantitative - descriptive approach to the modelling of temporal contrast analysis was examined. In particular the assumption of a single channel mechanism implicit in the simple application of linear systems

analysis to the entire system was questioned. It was suggested that this detailed level of analysis is premature when the internal macro-structure of the system being measured is unknown. Accordingly, the experiments were designed firstly to establish that the temporal contrast system was a nonlinear, multiple channel system, secondly to determine the global characteristics of these channels, and finally to return to a more conventional, quantitative systems description of their operation. As will be seen, this final aim was only partially successful. The isolation of the individual channels and their response selectivity was achieved using the technique of adaptation, in the series of experiments reported in Chapters 4 and 5. Having demonstrated the existence of separate channels for fast and slow transient changes, the detailed specification was achieved by simple parametric threshold measurement, subthreshold summation, and temporal masking in Chapters 6 to 8.

9.2.2 Chapter 3

The starting point of the investigation was the hypothesis that temporal contrast is analysed in the time domain rather than the frequency domain. Prior to the adaptation experiments, therefore, Chapter 3 reported two experiments which attempted to establish this distinction by parametrically varying the time function of a flicker waveform, independently of its fundamental frequency. In Experiment 3.1 flicker sensitivity functions were measured at five adaptation levels, using a peak clipping technique in which the slope of the waveform remained constant as its amplitude was adjusted. It was found that threshold at low frequencies was dependent on L_{mean}, as is the case when slope varies with amplitude. and independent of frequency (and hence also of gradient) up to 5 Hz. While appearing to suggest that

the visual system is insensitive to the gradients in flicker, this conclusion takes no account of the fact that as amplitude of the gradients was reduced, so also was their duration. Below a certain duration ramps will be detected as steps. If the step system were more sensitive than the ramp system, this would give uniform thresholds irrespective of actual slope. The later results of Experiment 6.1, determining the critical duration for ramp discrimination, provide support for this interpretation.

The possible influence of gradient on flicker threshold was investigated more directly in Experiment 3.2, by independently varying frequency and slope in a 9 x 9 matrix of triangular waveforms. Using the clipping method of amplitude adjustment again, it was found that threshold was affected by gradient, but that the nature of the effect was far from simple. As gradient increased, the extent to which threshold varied with frequency (ie the slope of the de Lange function) changed, but in a nonmonotonic way. Such a complex interaction is an unpromising starting point for a study of the mechanisms of gradient detection. While statistically significant, this result was taken merely as evidence in support of a time domain effect, rather than as a specific and replicable gradient effect. In retrospect, the parametric study of gradient may be more reliably undertaken with single luminance ramps, as in Chapter 6. Even so the positive, if complex, effect of varying gradient was sufficient to justify further investigation into temporal profile effects in flicker detection.

9.2.3 Chapter 4.

In Chapter 4, the first of three flicker adaptation experiments looked at frequency - specificity of the threshold elevation induced by adaptation.

Although of tangential interest in its own right, this question had been studied previously by other investigators. Smith (1971) and Nilsson et al (1975) had found only relatively broadband tuning effects with sinewave adaptation, suggesting the possibility that sinewaves were producing adaptation across a range of gradient - specific channels. In Experiment 4.1, therefore, the hypothesis of frequency - specific adaptation was tested against that of gradient - specific adaptation, using sinewaves in the first case and the clipped triangular waveform in the second. The tuning curves revealed by adaptation were markedly asymmetrical, falling off more gradually below the adapting frequency than above, and the degree of asymmetry increased with decreasing frequency. However, essentially the same effects were seen with both sinewaves and triangle-waves. The lack of difference between the two waveform conditions argues against processing by an array of gradient - tuned channels. However the tuning curve asymmetry is consistent with a separate, nonspecific system sensitive to low frequency flicker. It was proposed that sinewave flicker is detected, at least in part, by a system sensitive to relatively slow luminance changes, irrespective of their periodicity. This system was termed the 'nonperiodic' system, and appeared to be a broadband mechanism sensitive to all rates of change up to an unspecified cut-off point. Above about 5 Hz, frequency - specific tuning was increasingly seen, thus it was suggested that the 'periodic' system consisted of an array of parallel frequency - tuned channels, extending down to about 5 Hz. As in the experiments in Chapter 3, it seems that the search for effects contingent on the gradient of the slope in flicker was too specific, and that more general properties of gradient detectors need to be established first. The suggestion from Experiment 4.1 that the nonperiodic system is sensitive particularly to low frequency sisnewaves led directly to the second adaptation study, Experiment 5.1.

9.2.4 Chapter 5.

Chapter 5 presented the results of two experiments which used the adaptation technique to look at 'waveform tuning' in an analogous way to the more conventional frequency tuning study. Experiment 5.1 examined the conclusions reached in Chapter 4 concerning the periodic and nonperiodic systems, to determine the functional relationship between them. Using sinewave flicker as an adjustable test stimulus, threshold elevation was measured after adaptation to sinewaves and to squarewave flicker, across a range of frequencies. At low frequencies sinewaves should be detected by the nonperiodic system, sensitive to slow transitions, but squarewaves detected by a separate system, sensitive to fast transients. As predicted, below 5 Hz sinewave threshold elevation was much greater after adaptation to sinewaves than to squarewaves. Such a result is difficult to account for in purely linear systems terms. Since the two adapting stimuli were equated for fundamental amplitude, they should have equal effects on any system dependent on frequency composition. Above about 5 Hz both squarewaves and sinewaves have essentially the same effect on sinewave sensitivity. Combining the threshold elevation curves from the two conditions allows an estimate to be made of the relative sensitivity of the sinewave specific mechanisms (Figure 5.03), showing a monotonic decrease from 1 Hz to zero at about 6 Hz. It is not possible to say whether the waveform independent effect at high frequencies is due to periodicity, or to a common effect on a nonperiodic fast transient detector. However, the results confirmed the hypothesis that at low frequencies sinewaves and squarewaves are detected by separate systems, and the assumptions underlying the adaptation technique argue that these systems are parallel and independent.

Having established this preliminary point, Experiment 5.2 used the

same technique of waveform - specific adaptation to investigate whether the slow transient system contains sub-channels selective for the polarity, or direction of luminance change. Using flicker with a sawtooth waveform, threshold elevation for flicker with a positive - going slow phase was measured after adaptation to flicker with the same and with an inverted waveform. The experiment was repeated with a negative slow - phase sawtooth. The results were unfortunately not as clear cut as expected. With the positive sawtooth, the relative sensitivity curve of the polarity - specific system showed a peak between 3 and 7 Hz, rather than the predicted monotonic decline, while the negative sawtooth showed no reliable polarity - specificity at any frequency. In retrospect, it seems likely that post-adaptation thresholds were determined not by the slow phase of the waveform but by the fast phase, a conclusion supported by subjects' reports of their observations. If true, this interpretation also implies that the fast phase is <u>not</u> detected by a polarity - specific pair of channels. We may conclude therefore that any polarity specific adaptation is due to operation of the slow phase detectors, but that these are less sensitive than the fast phase detectors (a similar conclusion was reached from the results of Experiment 3.1). Furthermore, it appears that the system is more sensitive to positive going than to negative going ramps.

At the end of this series of adaptation experiments we have a rough, qualitative model of the internal structure of the temporal contrast system. To be consistent with the experimental results, the system must have parallel channels for the detection of fast and slow luminance changes. The temporal characteristics of the systems are such that, at threshold, the crossover point occurs at about 5 Hz. The slow system appears to contain a pair of channels selectively sensitive to opposite directions of change, but is not otherwise subdivided into gradient tuned channels. In contrast, the fast

system is insensitive to polarity, but does contain subsystems that are tuned, albeit relatively broadly, to the frequency of repetition. In the range tested, ie down to 1 Hz, the fast system is more sensitive than the slow system, for a given amplitude change, and the positive slow channel is more sensitive than the negative channel.

9.2.5 Chapter 6.

Having enabled these global characteristics to be determined, the limitations of the adaptation technique, discussed at the end of Chapter 5, required that different methods be used for the detailed, quantitative description of the system. At the same time, the results so far were sufficient to show that the temporal contrast system is primarily sensitive to nonperiodic stimuli, ie luminance steps and ramps, rather than periodic flicker stimuli. The experiments in the remaining three experimental chapters were thus devoted to characterising the step and ramp systems.

The proposal of separate systems for fast and slow transients leads to the question of the perceptual boundary between the two classes of stimuli. Evidence from the adaptation experiments of the previous two chapters suggested that, with sinewave flicker input, the boundary occurred at about 5 Hz at threshold, representing a ramp duration of approximately 100 ms. However, this estimate is unsatisfactory, not only because the sinewave signal is not optimal for a ramp detector, but also because ramp gradient is uncontrolled. In Chapter 6, therefore, the discrimination threshold was measured directly, as a function of gradient. It was found that the duration for discrimination was about half that estimated from the flicker experiments at the shallowest gradients tested, tending to decrease with increasing slope.

This suggests that the ramp detection system acts as an imperfect integrator, and hence that it does not operate with a fixed temporal window. The data were then used to predict hypothetical flicker thresholds, assuming that these were based solely on ramp detection with no probability summation. When converted to notional sinewave amplitudes, the gradient range chosen lay mostly above 10 Hz. Thus, although the analysis confirmed that actual sinewave sensitivity was greater than predicted in this range, it was not possible to show that ramp sensitivity was a good predictor of flicker sensitivity below 5 Hz. However, the data were sufficient to argue against the claim of van der Wildt and Rijsdijk (1979) that ramp thresholds could predict flicker thresholds at all frequencies, by showing that their thresholds were not those of the ramp system alone.

9.2.6 Chapter 7.

Finally, in Chapters 7 and 8, three experiments were reported in which the internal response to firstly a step and then a ramp stimulus was measured directly using psychophysical probe techniques. Having identified apparently independent subsystems within the complete temporal contrast system, it was now possible to return to the concepts of systems analysis as a means of characterising these systems. From the measured step and ramp responses the transfer characteristics of the systems involved can be derived, with the expectation that two different systems will emerge.

The investigation started in Chapter 7 with two experiments to measure the response to a subthreshold luminance step. The first used a variation of the subthreshold summation technique described by Roufs and Blommaert (1975, 1981), the second a masking paradigm similar to that commonly

found in auditory psychophysics. In summation the presence of a signal is marked by a decrease in probe threshold if the two have the same sign, and an increase in threshold if the two are opposite in sign. Measuring the same signal with a pair of opposite polarity probes thus results in a pair of mirror symmetrical threshold functions. In Experiment 7.1 this complementarity was not observed, with probe thresholds increasing above but not decreasing below their baseline levels. This suggested that a further nonlinearity had been discovered, and thus that the perturbation method of Roufs and Blommaert was not appropriate to the measurement of the step response. Although the main effect of the nonlinearity is on the amplitude scaling of the measured response, the general form of the response remains valid. The symmetrical, biphasic response obtained confirmed Roufs's (1974a) conclusion that the step system acts as a linear bandpass filter.

Essentially the same step response function was obtained in Experiment 7.2, using a masking technique. In masking the subject is required to detect the probe stimulus specifically, rather than the presence of the probe and test combination. When presented together, the test stimulus acts to disrupt detection of the probe. It will thus raise probe threshold in proportion to its power in the same channel as the probe. The technique does not depend on the assumptions of linearity central to the Roufs perturbation technique, and is thus better suited to the investigation of systems containing more than one channel. The overall step response is obtained by combining the separate response curves from the two probe pulses. This curve peaks symmetrically at about 40 ms either side of the step, with the second, negative step somewhat larger. The parallels were noted between this response and that produced in the spatial domain by the edge detecting model of Marr and Hildreth (1980). The Marr and Hildreth filter may be approximated by a filter whose impulse response is the difference of two

Gaussian distributions with unequal variances. When the ratio of the variances is fixed, this model may be fitted to the data with only two parameters, a scaling factor and one standard deviation. Values for these parameters were obtained which minimised the squared deviations, and it was found that the difference of Gaussians (DOG) filter provides a reasonable fit to the measured step response. It was observed that the separate response curves from the two probes appeared to be mutually exclusive. Since the test stimulus was always a positive - going step, this suggests that polarity selectivity is taking place at the level of the internal response, ie after the initial bandpass filter stage.

9.2.7 Chapter 8.

The model derived from an analysis of the results of Experiment 7.2 can now be placed in the context of the general model of the temporal contrast system outlined above. The DOG filter and subsequent rectification processes form the filter stage of the fast transient system, which was found to be indifferent to step polarity but tuned to repetition frequency. In the final experiment, therefore, the characteristics of the slow transient system were investigated to complete the description of the model. The same masking procedure as before was used, this time with a set of three luminance ramps, varying in duration, amplitude, and gradient. The internal response showed a sharp positive peak coinciding with the onset of the ramp, and a sharp negative peak at its offset. The size of the peaks appeared to be related most closely to the gradient of the ramp, rather than to its duration or amplitude, suggesting that the system is primarily sensitive to the second derivative of the stimulus. This is a property of the system proposed by Marr and Hildreth (1980) for spatial transients and found to

account well for the step response in Chapter 7. Accordingly, the ramp response of the step detection model previously described was calculated, with no change in the parameters, and was found to give a good fit to the data. The positive and negative phases of the ramp response appeared to be approximately equal, unlike the asymmetrical step response, suggesting that the differential sensitivity built into the model may be unnecessary.

It seems unlikely that the transfer characteristics of the fast and slow transient systems are almost identical, and the adaptation experiments of Chapters 3 and 4 show that the two systems are separable. It is possible that the ramps were not long enough to be detected by the slow system, but the discrimination thresholds of Chapter 6 suggest that they were well within the senstivity range. The most plausible solution of this paradox is that Experiment 8.1 measured not the response of the slow system, but the response of the fast system to ramp stimuli. As noted above, the masking procedure measures the response to the test signal of the system sensitive to the probe, ie the fast system. While this response is interesting in itself, it does not provide any further information about the operation of the ramp system, which remains to be explored. For the moment we must conclude, along with Kelly (1961) and Roufs (1974a), that the best estimate of the transfer function of the slow system is provided by subtracting the transfer function of the fast system from that of the whole.

Experiment 8.1 completes the review of the main experimental findings of the thesis. In the next section the theoretical model proposed in Chapter 7 is examined more closely, and its place in the complete system of temporal contrast analysis is considered.

9.3 Theoretical modelling

It is now possible to use the experimental findings reviewed in the previous section to construct a theoretical model of the temporal contrast system, so as to be as consistent as possible with the observed phenomena. The overall structure of such a model has already been discussed. All that remains is to formalise the structure in a block diagram, and in particular to consider the detailed operation of the fast and slow transient systems.

At the end of Chapter 7, a filter was descibed whose output approximates the 2nd derivative of the time - varying input (Figure 7.08). The bandpass filter chosen, which was adapted from recent models of spatial contrast analysis, has an impulse response which may be considered as the difference of two Gaussian distributions with unequal standard deviations. However, this filter shape does not represent a unique, or even a best - fitting description of the measured response. A number of options exist for two features in particular of the model in Figure 7.08:

1) Structure. The filter is represented as an opponent pair of low-pass filters with different roll-off frequencies, reflecting the derivation of the impulse response. This structure was chosen for its clarity and convenience, and does not exclude the possibility of a single bandpass filter, eg one using feedback - induced resonance. The data obtained are equally consistent with either model.

2) Gaussian filter shape. Very similar results could have been obtained with an opponent pair of simple 1st order filters: the data are not sufficiently noise - free to discriminate minor differences in the

form of the response. Given that the choice is relatively unconstrained, the Gaussian filter has a number of advantages which have led to its increasing use in the modelling of complex biological systems. The large body of statistical theory, based on the Gaussian probability density function, may be used in the development of complex serial and parallel networks. The phase transfer function is identical to that of a pure time - delay system, and is independent of the gain. The gain function is exponential, and is formally equivalent to an infinite cascade of simple 1st order elements with equal time constants. In principle this limits the physical realisability of such a system, although in practice the match to a measured function is limited instead by the noise and variability in the measurement. Kelly (1972) points out that just such an exponential gain function is required by a strict interpretation of the Ferry - Porter law. Kelly (1961) has also shown that the measured flicker sensitivity function does have an accelerating slope at high frequencies, rather than converging onto a single linear asymptote. This observation provides independent evidence that the Gaussian filter, as well as being a convenient theoretical tool, may also provide a good description of the temporal contrast system, despite the inherent problems of realisability.

The earlier flicker adaptation experiments, together with the work of Roufs (1974a), suggest that the complete temporal contrast system consists of two parallel channels, sensitive respectively to fast and slow luminance changes. The model described in Figure 7.08 thus comprises the 'fast' transient system, and its place within the complete model is shown in

Figure 9.01. The designation 'fast' is not entirely accurate since, as shown in Experiment 8.1, the system is also responsive to the transition points in ramp inputs, ie those points containing energy in the middle to high frequency region. This system is responsive not only to fast transients, such as steps, pulses, and low frequency squarewaves, but also to flicker inputs, irrespective of waveform, above a certain frequency. The sinewave vs squarewave adaptation comparison of Experiment 5.1 showed that this point occurs at about .5 Hz. In Chapter 4 evidence was presented of some frequency tuning at these higher frequencies. Although the tuning effects were somewhat weak, this may well be an artifact of the relatively imprecise adaptation method. In Figure 9.01, therefore, the detector stages of the original model act as pulse encoders, the outputs of which are passed to an array of tuned filters.

The slow transient branch of the complete system remains unspecified, although some of its general properties may be described. The central requirement of the system is that it blocks all signal variations which are shorter than a certain duration, or faster than a given rate. Given an appropriate nonmonotonic phase transfer function, a 1st order filter will display rate - sensitivity. The lead-lag system is so termed because of its nonmonotonic phase characteristic, with relative phase lead below the peak and phase lag above. The step response, y(t), of such a system is given by:

$$y(t) = k(1 - x \cdot e^{-t/T}), \quad x > 0 \qquad \text{Equation 9.01}$$

where T is the time constant of the system. The peak value of the output is dependent on the slope of the input transient, thus the step response

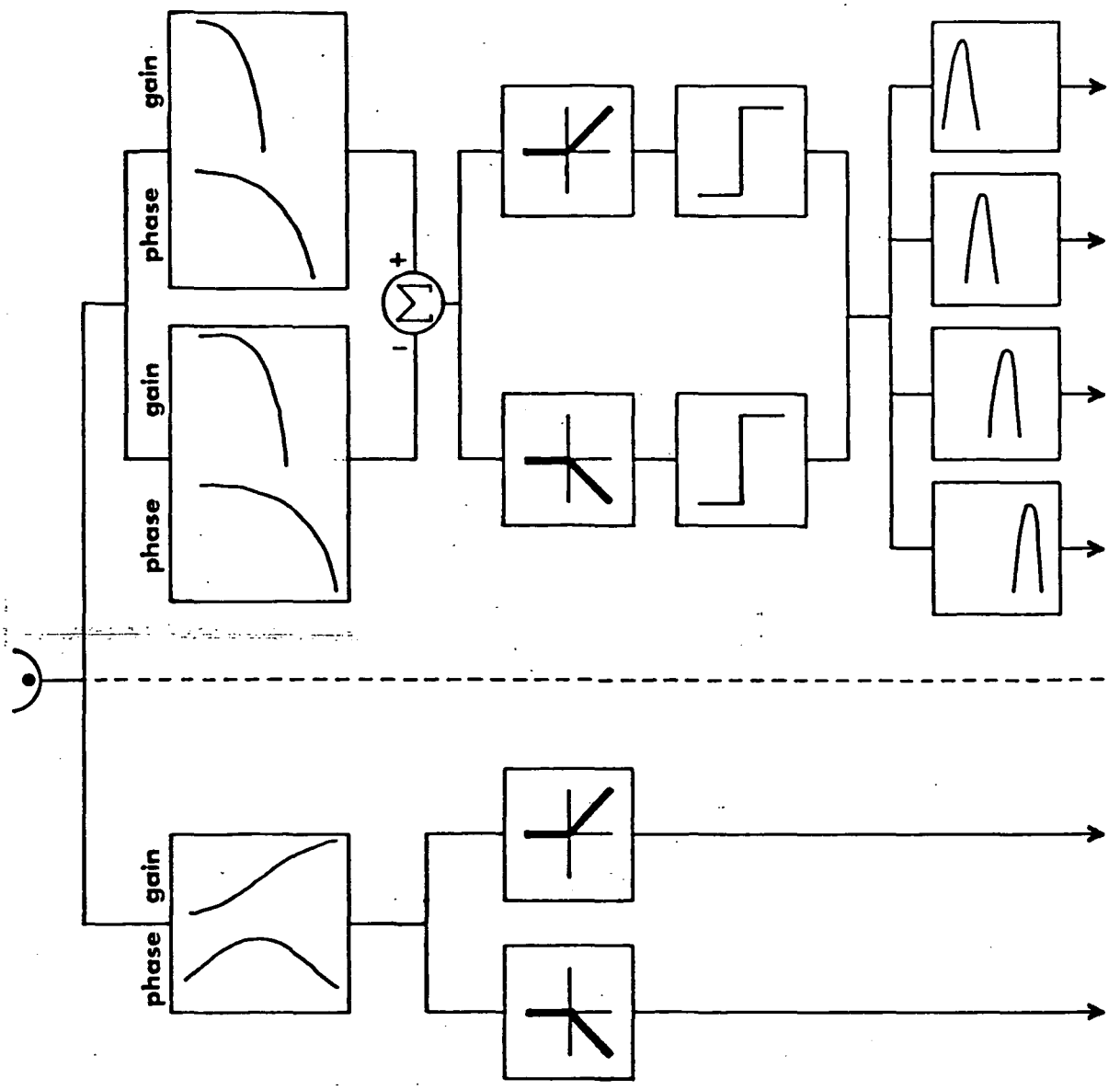

Figure 9.01 : The complete temporal contrast model. The dotted line separates the fast transient system, at the top, from the slow transient system underneath. The fast system is essentially similar to that shown in Figure 7.09, with the addition of an array of bandpass filters as a final output stage. The slow transient system consists of a rate - sensitive filter whose output undergoes half-wave rectification to give a polarity - specific response in the two output channels. The arrowed outputs form the input to the spatial integration processes of the movement detection system. See the text for further details.

represents the limiting case. As the time constant (T) increases, ie as the cut-off frequency is reduced, the step response will decrease. However, it will always be greater than the ramp response, leading to problems in designing a filter which is more sensitive to ramps than to steps. The experiments reported here provide no information about possible mechanisms for limiting the step response of a rate - sensitive system. Further modelling of the slow transient system must therefore follow more experimental studies of its operation, although the ramp discrimination data of Experiment 6.1 may give first approximations of some of the time-constants involved.

Any model of the slow transient system must include a system accounting for the polarity selectivity observed in Experiment 5.2. In Figure 9.01 this is achieved by half-wave rectification of the filter output. This unidirectional sensitivity characteristic suggests that the slow system may be described more appropriately by the application of a nonlinear, unidirectional rate - sensitive (URS) mechanism, explored extensively by Clynes (1961, 1962). Such a system displays essentially the same transient responses described above, but to inputs of only one polarity. When stimulated periodically, the output shows a DC shift, proportional to the maximal slope of the input waveform. Clynes (1962) showed how this model provides an accurate account of the pupillary reflex and of the heart-rate respiratory response. Many features of the URS model are more consistent with known biochemical and biophysical constraints than is the conventional linear description. Although the problem of limiting the response to screen out fast transients remains, this type of model would seem to be an important tool in the further investigation of the temporal dynamics of the visual system.

9.4 Epilogue

This investigation of temporal contrast grew out of an original interest in the analysis of spatiotemporal contrast, as the basis of a mechanism of movement detection. Stimulated by the work of Foster (1969, 1971), I decided to work from a model of movement analysis based on the spatial integration of information from a series of localised temporal change detectors. As Foster had already developed a model of the spatial comparison mechanisms - his horizontal (H) units - I decided to look instead at the localised vertical (V) units. An investigation of the literature on flicker detection revealed that the concepts and methods in this area had not developed to the same extent as those in the spatial domain. Indeed, the field had been largely dormant since the early 1960s, and had not benefitted from the developments of channel theory, introduced to spatial contrast via the application of systems analysis in the late 1960s. Models of flicker detection were largely restricted to detailed descriptions of threshold phenomena, rather than being concerned with the basic elements and mechanisms of analysis. An exception to this trend was the work of Roufs (1972 - 1981), which became a major influence in my thoughts on temporal contrast mechanisms.

My experimental results have shown clearly that the temporal contrast system cannot be considered as unitary, and this fact alone presents a problem for the application of systems analysis. When applied psychophysically, a central assumption for systems analysis is that threshold is independent of frequency: this can no longer be guaranteed if the system being measured consists of two or more parallel channels. However, I still believe that systems analysis is a valuable tool when applied to each of

these channels individually, and it is now a challenge to the psychophysicist to design experiments which make this possible. The investigation of the slow transient system is a particularly promising area for future research. I have described the general properties of the system, but the detailed description of its operation remains an attractive goal. In this context, the recent work on luminance gradients in the spatial domain by Campbell (Campbell, Johnstone and Ross; 1981), one of the pioneers of spatial frequency analysis, is likely to lead to important theoretical and methodological developments.

The ultimate aim of the study of temporal contrast must be its reintegration within a model of spatiotemporal, ie movement, analysis. I have not attempted to do this with my own work, as I believe that such a synthesis is still premature. However, it is a common criticism by the layman of the scientist that the isolation of a subject of study from its everyday context, necessary for its scientific investigation, often leads to work on extremely esoteric and artificial situations. At present this criticism can almost certainly be directed, with some justification, at the study of visual flicker.

APPENDIX

The following is a summary of the main notation and abbreviations used throughout the thesis. Some of the terms are explained graphically in Figure A.01.

subscript $_c$	'critical' or threshold value. For example t_c = threshold duration of a flash.
$cd \cdot m^{-2}$	candelas per square metre. The SI (Systeme Internationale) unit of luminance.
CFF	critical flicker frequency. The threshold frequency (f_c) at which flicker becomes undetectable.
f	frequency - temporal unless otherwise specified.
subscript $_f$	relating to the Fourier fundamental. Figure A.01d illustrates some uses of the term.
G	gain (of a linear system). Usually expressed as a function of frequency - G(f).
HF	high frequency.
Hz	Hertz - cycles per second. The SI unit of temporal frequency.
$\pm\Delta L$	amplitude of a luminance waveform or transient. The difference between peak and mean luminance ($L_{max} - L_{mean} = \Delta L$) - see Figure A.01b and c.
L_{mean}	time - average stimulus luminance - see Figure A.01.
L_{min}	minimum stimulus luminance.
L_{max}	maximum stimulus luminance.
LDR	light-dark ratio. A term erroneously used by Landis (1954b) as synonymous with PCF.
LF	low frequency.
m	modulation. A dimensionless measure of amplitude as a proportion of mean level, defined as $(L_{max} - L_{min}) / 2L_{mean}$.
MTF	modulation transfer function. The gain or attenuation of a signal, as a function of frequency, as it passes through a system, defined as output modulation / input modulation.
PCF	pulse to cycle fraction. The proportion of a rectangular cycle occupied by the 'on' or light phase (Figure A.01a).
t	the duration of a single flash.

td — troland - a unit of retinal illumination. Defined as the illumination produced by 1 $cd \cdot m^{-2}$ passing through a pupil of area 1 mm^2 at the nodal point of the eye. [Named in recognition of the work of L.T. Troland (1917) which established this standard; Troland himself proposed the name 'photon' for this unit, which was used until the present name was adopted in 1950.]

v — velocity (of a moving grating). Measured in terms of degrees (of visual angle) per second.

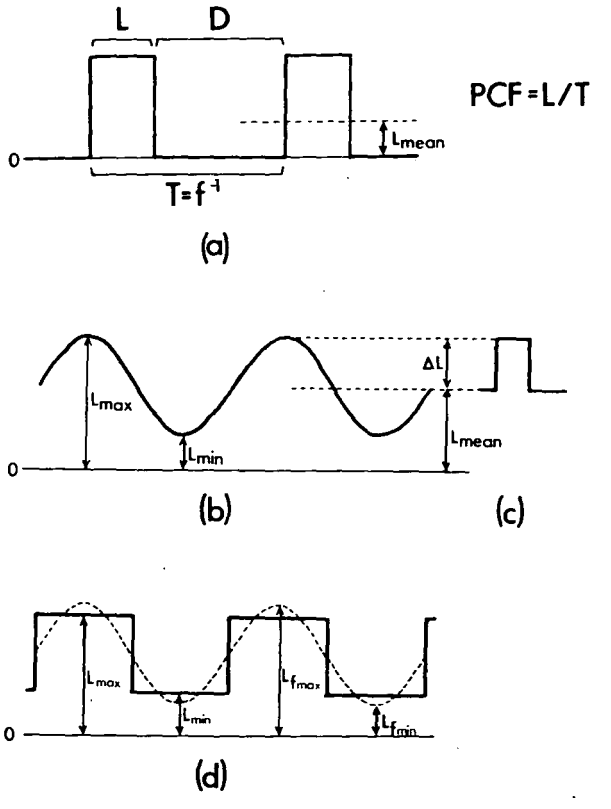

Figure A.01 : Parameters of rectangular (a) and sinewave (b) flicker and (c) impulse stimuli.

REFERENCES

Anstis SM (1967) : "Visual adaptation to gradual change of intensity." Science, 155, 710-711.

Baader EG (1891) : "Uber die Empfindlichkeit des Auges gegen Lichtwechsel." Medical Dissertation; University of Freiburg in Braisgau.

Baker HD (1953) : "Instantaneous threshold and early dark adaptation." Journal of the Optical Society of America, 43, 798-803.

Barlow HB (1965) : "Optic nerve impulses and Weber's law." Cold Spring Harbour Symposium on Quantitative Biology, 30, 539-546.

Blackwell HR (1963) : "Neural theories of simple visual discriminations." Journal of the Optical Society of America, 53, 129-160.

Blakemore CB and Campbell FW (1969) : "On the existence of neurones in the human visual system selectively sensitive to the orientation and size of retinal images." Journal of Physiology (London), 203, 237-260.

Bloch AM (1885) : "Experiences sur la vision." Compte Rendu des Seances de la Societe de Biologie, 2, 493-495.

Bode HW (1945) : Network Analysis and Feedback Amplifier Design; Van Nostrand, Amsterdam.

Bouman MA and Brink G van den (1952) : "On the integrate capacity in time and space of the human peripheral retina." Journal of the Optical Society of America, 42, 617-620.

Boynton RM and Kandel G (1957) : "On responses in the human visual system as a function of adaptation level." Journal of the Optical Society of America, 47, 275-286.

Brown JL (1965) : "Flicker and intermittent stimulation." In Graham CH (ed) : Vision and visual perception; Wiley, New York.

Campbell FW, Johnstone JR and Ross J (1981) : "An explanation for the visibility of low frequency gratings." Vision Research, 21, 723-730.

Campbell FW and Robson JG (1968) : "Application of Fourier analysis to the visibility of gratings." Journal of Physiology, 197, 551-566.

Charpentier A (1887) : "Influence de l'intensite lumineuse sur la persistance des impressions retiniennes." Compte Rendu des Seances de la Societe de Biologie, 8, 89-91.

Clynes M (1961) : "Unidirectional rate sensitivity: A biocybernetic law of reflex and humoral systems as physiologic channels of control and communication." Annals of the New York Academy of Science, 92, 946-969.

Clynes M (1962) : "The non-linear biological dynamics of unidirectional rate sensitivity illustrated by analog computer analysis, pupillary reflex to light and sound, and heart rate behaviour." Annals of the New York Academy of Science, 98, 806-845.

Cobb PW (1934) : "Some comments on the Ives theory of flicker." Journal of the Optical Society of America, 24, 91-98.

Crawford BH (1947) : "Visual adaptation in relation to brief conditioning stimuli." Proceedings of the Royal Society of London Series B, 134, 283-302.

Crozier WJ (1936) : "On the variability of critical illumination for flicker fusion and intensity discrimination." Journal of General Physiology, 19, 503-523.

Dow JS (1907) : "The speed of flicker photometers." The Electrician, 59, 255-257.

Duffieux PM (1946) : "L'integrale de Fourier et ses applications a l' optique." Besançon; privately published.

Ferry ES (1892) : "Persistence of vision." American Journal of Science, 44, 192-207.

Findlay JM (1978) : "Estimates on probability functions: a more virulent PEST." Perception and Psychophysics, 23, 181-185.

Finney DJ (1948) : Probit analysis. Cambridge University Press; Cambridge.

Foster DH (1969) : "The response of the human visual system to moving spatially - periodic patterns." Vision Research, 9, 577-590.

Foster DH (1971) : "The response of the human visual system to moving spatially - periodic patterns: further analysis." Vision Research, 11, 57-81.

Fuortes MGF and Hodgkin AL (1964) : "Changes in time scale and sensitivity in the ommatidia of Limulus." Journal of Physiology (London), 172, 239-263.

Graham CH and Kemp EH (1938) : "Brightness discrimination as a function of the duration of the increment in intensity." Journal of General Physiology, 21, 635-650.

Granit R and Davis WA (1931) : "Comparative studies on the peripheral and central retina. IV. Temporal summation of subliminal visual stimuli and the time course of the excitatory after-effect." American Journal of Physiology, 98, 644-653.

Grind WA van de, Grusser O-J and Lunkenheimer H-U (1973) : "Temporal transfer properties of the afferent visual system." In Jung R (ed) : Handbook of Sensory Physiology, vol VII/3; Springer - Verlag, Berlin.

Hanly M and Mackay DM (1979) : "Polarity - sensitive perceptual adaptation to temporal sawtooth modulation of luminance." Experimental Brain Research, 33, 37-46.

Hargroves JA and Hargroves RA (1971) : "Bibliography of work on flashing lights." Vision Research, Supplement 2, 1-111.

Hecht S and Verrijp CD (1933) : "Intermittent stimulation by light. III. The relation between intensity and critical fusion frequency for different retinal locations." Journal of General Physiology, 17, 251-265.

Herrick RM (1956) : "Foveal discrimination as a function of the duration of the decrement or increment in luminance." Journal of Comparative and Physiological Psychology, 49, 437.

Ikeda M (1965) : "Temporal summation of positive and negative flashes in the visual system." Journal of the Optical Society of America, 55, 1527-1534.

Ives (1922a) : "Critical frequency relations in scotopic vision." Journal of the Optical Society of America and Review of Scientific Instruments, 6, 254-268.

Ives (1922b) : "A theory of intermittent vision." Journal of the Optical Society of America and Review of Scientific Instruments, 6, 342-361.

Jung R (1973) : "Visual perception and neurophysiology." In Jung R (ed) : Handbook of Sensory Physiology, vol VII/3; Springer - Verlag, Berlin.

Keller M (1941) : "The relation between the critical duration and intensity in brightness discrimination." Journal of Experimental Psychology, 28, 407-418.

Kelly DH (1959) : "Effects of sharp edges in a flickering field." Journal of the Optical Society of America, 49, 730-732.

Kelly DH (1960) : "J_o stimulus patterns for visual research." Journal of the Optical Society of America, 50, 1115.

Kelly DH (1961a) : "Visual responses to time - dependent stimuli. I. Amplitude sensitivity measurements." Journal of the Optical Society of America, 51, 422-429.

Kelly DH (1961b) : "Visual responses to time - dependent stimuli. II. Single channel model of the photopic visual system." Journal of the Optical Society of America, 51, 747-754.

Kelly DH (1966) : "Frequency doubling in visual responses." Journal of the Optical Society of America, 56, 1628-1633.

Kelly DH (1971) : "Theory of flicker and transient responses. I. Uniform fields." Journal of the Optical Society of America, 61, 537-546.

Kelly DH (1972) : "Flicker." In Hurvich LM and Jameson D (eds) : Handbook of Sensory Physiology, vol VII/4; Springer - Verlag, Berlin.

Kennelly AE and Whiting SE (1907) : "The frequencies of flicker at which variations in illumination vanish." National Electric Light Association Convention, 30, 327-340.

Krauskopf J (1980) : "Discrimination and detection of changes in luminance." Vision Research, 20, 671-677.

Landis C (1954a) : "Crozier and Wolf on flicker - fusion, 1933-1944." The Journal of Psychology, 37, 3-17.

Landis C (1954b) : "Determinants of the critical flicker - fusion threshold." Physiological Reviews, 34, 259-286.

Lange H de (1952) : "Experiments on flicker and some calculations on an electrical analogue of the foveal systems." Physica, 18, 935-950.

Lange H de (1954) : "Relationship between critical flicker - frequency and a set of low - frequency characteristics of the eye." Journal of the Optical Society of America, 44, 380-389.

Lange H de (1958) : "Research into the dynamic nature of the human fovea - cortex systems with intermittent and modulated light. I. Attenuation characteristics with white and coloured light. Journal of the Optical Society of America, 48, 777-784.

Lange H de (1961) : "Eye's response at flicker fusion to square-wave modulation of a test field surrounded by a large steady field of equal mean luminance." Journal of the Optical Society of America, 51, 415-421.

Levinson E and Sekuler R (1975) : "The independence of channels in human vision selective for direction of movement." Journal of Physiology (London), 250, 347-366.

Levinson J and Harmon LD (1961) : "Studies with artificial neurons. III. Mechanism of flicker fusion." Kybernetik, 1, 107-117.

Lloyd VV and Landis C (1960) : "Role of the light-dark ratio as a determinant of the flicker - fusion threshold." Journal of the Optical Society of America, 50, 332-336.

Luckiesh M (1914) : "On the growth and decay of color sensations in flicker photometry." Physical Review, 4, 1-11.

Marimont RB (1965) : "Numerical studies of the Fuortes - Hodgkin Limulus model." Journal of Physiology (London), 179, 489-497.

Marr D and Hildreth E (1980) : "A theory of edge detection." Proceedings of the Royal Society of London Series B, 207, 187-217.

Matin L (1968) : "Critical duration, the differential luminance threshold, critical flicker frequency and visual adaptation: A theoretical treatment." Journal of the Optical Society of America, 58, 404-415.

McCann JJ, Savoy RL, Hall JA Jr and Scarpetti JJ (1974) : "Visibility of continuous luminance gradients." Vision Research, 14, 917-927.

Nes FL van, Koenderink JJ, Nas H and Bouman MA (1967) : "Spatio-temporal modulation transfer in the human eye." Journal of the Optical Society of America, 57, 1082-1088.

Nilsson TH, Richmond CF and Nelson TM (1975) : "Flicker adaptation shows evidence of many channels selectively sensitive to temporal frequency." Vision Research, 15, 621-624.

Pantle A (1971) : "Flicker adaptation. I. Effect on visual sensitivity to temporal fluctuations of light intensity." Vision Research, 11, 943-952.

Pieron H (1922) : "L'influence de l'intensite lumineuse sur la persistence retinienne apparente." Archives Physiologique, 7, 199-212.

Pieron H (1961) : "La vision en lumiere intermittente." Monographes Francaises de Psychologie, no 8. Centre National de la Recherche Scientifique, Paris. [English translation Pieron, 1965.]

Pieron H (1965) : "Vision in intermittent light." In Neff WD (ed) : Contributions to Sensory Physiology; Academic Press, New York.

Pinter RB (1966) : "Sinusoidal and delta function responses of the Limulus eye." Journal of General Physiology, 49, 565-593.

Quick RF (1974) : "A vector - magnitude model of contrast detection." Kybernetik, 16, 65-67.

Rashbass C (1970) : "The visibility of transient changes of luminance." Journal of Physiology (London), 210, 165-186.

Rashbass C (1976) : "Unification of two contrasting models of the visual increment threshold." Vision Research, 16, 1281-1283.

Robson JG (1966) : "Spatial and temporal contrast sensitivity functions of the visual system." Journal of the Optical Society of America, 56, 1141-1142.

Ross J and Johnstone JR (1980) : "Phase and detection of compound gratings." Vision Research, 20, 189-192.

Roufs JAJ (1966) : "On the relation between the threshold of short flashes, the flicker fusion frequency and the visual latency." IPO Annual Progress Report, 1, 69-77.

Roufs JAJ (1972a) : "Dynamic properties of vision. I. Experimental relationships between flicker and flash thresholds." Vision Research, 12, 261-278.

Roufs JAJ (1972b) : "Dynamic properties of vision. II. Theoretical relationships between flicker and flash thresholds." Vision Research, 12, 279-292.

Roufs JAJ (1973) : "Dynamic properties of vision. III. Twin flashes, single flashes and flicker fusion." Vision Research, 13, 309-323.

Roufs JAJ (1974a) : "Dynamic properties of vision. IV. Thresholds of decremental flashes, incremental flashes and doublets in relation to flicker fusion." Vision Research, 14, 831-851.

Roufs JAJ (1974b) : "Dynamic properties of vision. V. Perception lag and reaction time in relation to flicker and flash thresholds." Vision Research, 14, 853-869.

Roufs JAJ and Blommaert FJJ (1975) : "Pulse and step response of the visual system measured by means of a perturbation technique." IPO Annual Progress Report, 10, 60-67.

Roufs JAJ and Blommaert FJJ (1981) : "Temporal impulse and step responses of the human eye obtained psychophysically by means of a drift-correcting perturbation technique." Vision Research, 21, 1203-1221.

Roufs JAJ and Pellegrino van Stuyvenburg JA (1976) : "Gain curve of the eye to subliminal sinusoidal modulation of light." IPO Annual Progress Report, 11, 56-63.

Schade OH (1956) : "Optical and photoelectric analog of the eye." Journal of the Optical Society of America, 46, 721-739.

Segner JA (1740) : Introduction to Bielck GG : De raritate luminis. Medical doctorate thesis; Vandenhoek, Gottingen.

Smith RA (1970) : "Adaptation of visual contrast sensitivity to specific temporal frequencies." Vision Research, 10, 275-279.

Smith RA (1971) : "Studies of temporal frequency adaptation in visual contrast sensitivity." Journal of Physiology (London), 216, 531-552.

Sperling G and Sondhi MM (1968) : "Model for visual luminance discrimination and flicker detection." Journal of the Optical Society of America, 58, 1133-1145.

Stiles WS and Crawford BH (1934) : "The liminal brightness increment for white light for different conditions of the foveal and parafoveal retina." Proceedings of the Royal Society of London, Series B, 116, 55-102.

Talbot HF (1834) : "Experiments on light." Philosophical Magazine (3rd series), 5, 321-334.

Taylor MM and Creelman CD (1967) : "PEST: efficient estimates on probability functions." Journal of the Acoustical Society of America, 41, 782-787.

Troland LT (1917) : "On the measurement of visual stimulation intensities." Journal of Experimental Psychology, 2, 1-33.

Veringa F (1961) : "Enige natuurkundige aspecten van het zien van gemoduleerd licht." Doctoral dissertation, University of Amsterdam.

Veringa F (1970) : "Diffusion model of linear flicker response." Journal of the Optical Society of America, 60, 285-286.

Watson AB (1982) : "Derivation of the impulse response: comments on the method of Roufs and Blommaert". Vision Research, 22, 1335-1337.

Watt RJ and Andrews DP (1981) : "APE: adaptive probit estimation of psychometric functions". Current Psychological Reviews, 1, 205-214.

Watt RJ and Morgan MJ (1983) : "Mechanisms responsible for the assessment of visual location: theory and evidence." Vision Research, 23, 97-109.

Wildt GJ van der, Keemink CJ and Brink G van den (1976) : "Gradient detection and contrast transfer by the human eye." Vision Research, 16, 1047-1053.

Wildt GJ van der and Rijsdijk JP (1979) : "Flicker sensitivity measured with intermittent stimuli: II. Comparison between temporal gradient detection and the 'De Lange' curves." Journal of the Optical Society of America, 69, 666-669.

Wilson HR and Bergen JR (1979) : "A four mechanism model for threshold spatial vision." Vision Research, 19, 19-32.